NOTICE

AVIS

Canada

THE UNIVERSITY OF ALBERTA

THE VOLCANO-SEDIMENTARY DEPOSITS OF LA MINITA, MICHOACAN, MEXICO

BY

FELIPE ORTIGOZA CRUZ

A THESIS

SUBMITTED TO THE FACULTY OF GRADUATE STUDIES AND
RESEARCH IN PATRTIAL FULFILMENT OF THE REQUIREMENTS FOR
THE DEGREE OF
MASTER OF SCIENCE

DEPARMENT OF GEOLOGY

EDMONTON, ALBERTA

FALL 1988

THE UNIVERSITY OF ALBERTA

RELEASE FORM

NAME OF AUTHOR: FELIPE ORTIGOZA CRUZ

TITLE OF THESIS: THE VOLCANO-SEDIMENTARY DEPOSITS OF
LA MINITA, MICHOACAN, MEXICO

DEGREE: MASTER OF SCIENCE

YEAR THIS DEGREE GRANTED: FALL 1988

Felipe Ortigoza Cruz
....
(Student's signature)

Piramide de la Luna No 24 Col Avante

Coyoacan 21 D.F. MEXICO 04460

(Student's permanent address)
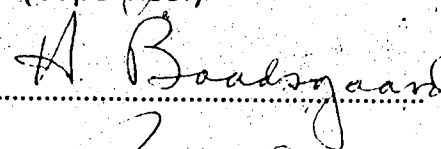
Date: *October 6, 1988*
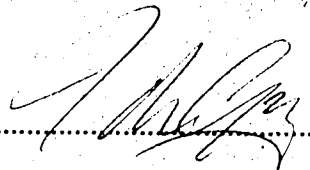
THE UNIVERSITY OF ALBERTA
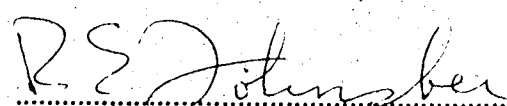
FACULTY OF GRADUATE STUDIES AND RESEARCH

The undersigned certify that they have read, and recomend to the Faculty of Graduate Studies and Research for acceptance, a thesis entitled **The Volcano-sedimentary Deposits of La Minita, Michoacán, México** submitted by **Felipe Ortigoza Cruz** in partial fulfilment of the requirements for the degree of **Master of Science.**

....
(Supervisor)

....

....

....

Date:...............................

ABSTRACT

The Albian-Cenomanian, stratabound-stratiform mineralization of La Minita, in Michoacan Province, Mexico consists of replacement bodies in reefal limestones and of exhalative, sedimentary pyritites and Fe-Mn formations. The mineralization developed within the tropical-subtropical, shallow waters of an ancient island archipelago.

Fluid inclusion and oxygen isotope data suggest that the solutions which formed the replacement bodies cooled from temperatures of about 327°C to less than 134°C, with a progressive decrease in fluid salinity from ~9.2 to 2.4 wt% NaCl. Boiling of the solutions was an important cause of mineral deposition. The intricate variance in textures exhibited by the replacement bodies probably resulted from hydraulic fracturing of systems confined by an exhalative siliceous-sinter cap. This cap would at times prevent boiling of the fluids and thus sponsored their recirculation causing replacement of paragenetically earlier mineral associations.

Sulfur- and carbon-isotope data suggest that seawater sulfate and inorganically-reduced sulfur (and/or igneous sulfur) were the main sources of sulfur in the system. Oxygen isotope data point to an extensive replacement of reefal limestones, at low water/rock ratios, during the pre-ore stage Fe-oxide mineralization and to larger water/rock ratios during sulfate-sulfide mineralization. In the latter stages of mineralization (post-ore stage) very large water rock ratios prevailed.

Sr in barites was apparently derived from two sources i.e.volcanic rocks and limestones. The volcanics had a large influence upon the Sr ratio of the fluids. The barium may thus be traced to the host trachytic-rhyolitic volcanics.

The pyritic and Fe-Mn stratiform bodies represent exhalative sediments of both proximal and distal nature.

iv

The La Minita deposits exhibit some broad similarities to classical Kuroko models, but certain features differ notably.

In general, the mineralization at La Minita was both lithologically and structurally controlled, these features providing clear exploration criteria. Isotopic information could also be used in future exploration programs.

ACKNOWLEDGMENTS

TABLE OF CONTENTS

LIST OF TABLES

Figure IV.3. Homogenization temperture of ore and post-ore stage quartz and sphalerite from Vulcano and Tabaquito.

is shown in figure IV.3. Ore stage quartz has a more restricted range of T_h than the barite. More than 75 % of the data occur in the range from 150 to 200°C, the average T_h being 188°C. The post-ore stage quartz has a somewhat lower average T_h of 169°C.

A post-ore stage quartz sample (#85) yields a wide range of T_h from 140 to 219°C, with an average of 178°C, which is close to the ore stage average for quartz. This sample shows evidence of trapping of a heterogeneous fluid; some inclusions homogenized to the gas phase at an undetermined temperature. This phenomenon was also observed in some inclusions in barite.

Sphalerite from ore and post-ore stages have distinct patterns. T_h of ore stage inclusions range from 160 to 200°C with an average of 181°C. The post-ore stage inclusions have a wider range from 90 to 150°C, however there is a prominent peak at 145°C, the average being 134°C.

In summary, the formation temperature of the ore and post-ore stage minerals is as follows:

i) ore stage, consisted of two hydrothermal events, one took place at 240°C and the other at 205 to 181°C

ii) post-ore stage, occurred at lower fluid temperatures of from 169 to 134°C.

Data Correction and Interpretation

A "pressure correction" of T_h is required when fluid inclusions were trapped above the boiling P-T conditions. Samples from Vulcano and Tabaquito show evidence of trapping of a heterogeneous fluid. It has also been commented upon that some of the inclusions in those samples homogenize to the gas phase whilst others homogenize to the liquid phase. In fact, the large spread of values for ore stage barite might be related to

the presence of inclusions which trapped a heterogeneous fluid, although secondary effects may also account for such a feature. Variable filling ratios of primary inclusions have been considered as evidence of boiling (Bodnar et al., 1985). However, in order to prove that boiling did occur, homogenization into the gas phase and into the liquid phase, by coeval inclusions, over the same range of temperatures must be obtained (Shepherd et al., 1985). The samples from Vulcano and Tabaquito do homogenize into the vapor and liquid phase, however the T_h of the gas-rich inclusions could not be checked, due to the absence of inclusions with capillary reentrants.

Independent evidence also points to trapping of the inclusions at conditions near the boiling point. At the temperatures of trapping and salinities indicated by ore stage inclusions (240 and 205 -181°C, and 6.2 wt% NaCl), boiling would take place at depths of between 350 and 80m in a system open to the surface under hydrostatic pressure, according to the boiling curves for NaCl solutions of Haas (1971).

These depths are not incompatible with the mineralizing event at La Minita. Paleontologic evidence suggests shallow depth environments of deposition of up to 55 m deep (Fabre, 1940; Bergquist et al., 1957). In addition, the fact that geothermometers independent of pressure (oxygen and sulfur isotopes) yield similar temperatures as T_h, suggests that the pressure effect is negligible. Thus, a correction for pressure is thought to be unneccesary in the case of samples from La Minita, and it is thought that the fluid was in the range of boiling conditions. Boiling of the ore solution must have been a common feature in these environments.

An interesting aspect is the lack of evidence of boiling in some of the samples. It would be expected that all of them would show this feature,

since they were formed at relatively similar depths and temperatures high enough to cause boiling. However boiling would be prevented in cases where direct action of a hydrostatic regime was prevented. This could have happened if an impermeable cap developed on the replacement bodies.

Formation of an impermeable cap is a recognized process in environments of submarine exhalative mineralization (Goldfarb *et al.*, 1983; Hekinian *et al.*, 1983; Von Damm *et al.*, 1985). Formation of this cap has been considered an essential part of massive sulfide evolution (Eldridge *et al.*, 1983; Barton, 1978). Constraining of the hydrothermal fluids by such a cap favours circulation of the fluid within the sulfide zone, establishes a higher temperature regime within the mound than in the exterior environment, and promotes replacement of early deposited phases (Goldfarb *et al.*, 1983; Lyndon, 1988). At La Minita, the presence of a jasper cap (c.f. the tetsusekiei horizon in Kuroko-type deposits) has been recognized on the Vulcano and Tabaquito replacement bodies, which might have prevented boiling by confining the system. In addition, the extensive replacement shown in these localities is in agreement with pervasive circulation of the fluids within the ore zone. The fact that the jasper is brecciated and that mixture of textures occurs within the bodies must have resulted from hydraulic fracturing during release of pressure and boiling.

D) Conclusions

The sulfate-sulfide minealization of the Vulcano and Tabaquito replacement bodies were formed by a hydrothermal system which cooled from a maximum temperture of approximately 310°C to less than 120°C. There were three main thermal events at 240°C, 205 - 181°C, and 169 - 134°C, the first two representing the ore stage. Minor amounts of CO_2 were present during the highest temperature-formation of the ore stage minerals. This might reflect the contribution of CO_2 to the system by dissolution of calcite-aragonite during the replacement processes. Boiling of the hydrothermal fluid was a not uncommon situation, although it was prevented at times due to the formation of an impermeable jasper cap over the mineralized bodies. Replacement during confining of the hydrothermal fluid was enhanced, which combined with brecciation of the ores produced a mixture of textures within the orebody.

Fluid salinities had an average value between 9.2 and 6.2 wt% NaCl, the highest salinities having been acquired at the highest temperatures when CO_2 was present in the system. The post-ore stage fluids were much more dilute (2.4 wt% NaCl). Thus, salinities of the fluid at La Minita were close to the range of Kuroko-type fluids, however the presence of more saline fluids and of a wider range of salinities at La Minita, suggests that the fluids were more similar to those which produced epithermal deposits (Roedder, 1984).

V. STABLE ISOTOPES (OXYGEN, SULFUR, AND CARBON)

A) Introduction

Stable isotopes of low mass have been widely utilized in the study of ore deposits. Their application has been twofold in that they have proven useful both in geothermometry and in petrogenetic investigations. They provide geothermometers which are independent of pressure (Clayton, 1981; O'Neil, 1987). Thus, in some instances, they may yield more reliable temperatures than fluid inclusions, whose properties are somewhat influenced by pressure. In petrogenesis they help place constraints upon the origin of both the source of certain elements and of the ore fluid. In addition, since isotopic fractionation, especially of sulfur and carbon isotopes, is largely dependant upon redox reactions involving the isotopic species (Ohmoto, 1986), the physico-chemistry of the environment plays a major role in controlling the isotope partitioning. Conversely, by means of the measured fractionation between substances, it is possible to make inferences concerning the conditions of the depositional environment.

In this study stable isotopes of *oxygen, sulfur,* and *carbon* were studied in order to critically examine the data obtained from the fluid inclusion study and to gain a clear insight into the origins of the mineralization.

B) Methods and Results

Samples from Vulcano, Tabaquito, and Ojo de Agua were studied. These included representatives of the three mineralizing stages and of different zones in each locality. Mineral grains which were large enough to be

59

resolved under a stereoscopic microscope were hand-picked. Fine-grained samples were crushed and the different phases separated by mechanical means using heavy liquids and a magnetic separator. Mineral concentrates were checked for purity under the petrographic microscope, the impure samples being discarded. Whenever possible, mineral pairs were preferentially separated for the isotopic study.

Oxygen in magnetite and quartz was extracted by the means of the BrF_5 technique of Clayton and Mayeda (1963). Oxygen in barite was extracted using the graphite reduction method (Longinelli and Craig (1967)) corrected by Sakai and Krouse (1971) for memory effects. Oxygen and carbon from carbonates were extracted by reaction with 100 % phosphoric acid at 25°C (McCrea, 1950) for one hour in the case of calcite, and for 7 days in the case of dolomite. Sulfur from sulfides and barite was extracted by reaction with $V_2O_5+SiO_2$ at 1000°C; any evolved SO_3 was converted to SO_2 by reaction with metallic copper (Ueda and Krouse, 1986).

Stable isotope concentrations are expressed as delta (δ) in units of per mil. δ is defined as:

$$\delta R = [(R_{mineral}/R_{standard}) - 1] \times 10^3$$

where R is the ratio of the heavy isotope to the light isotope, and the standard varies according to the element in question. For oxygen the standard is SMOW, which has a value of $^{18}O/^{16}O = 20.052 \times 10^{-4}$ (Baertschi, 1976). Carbon is referred to the PDB standard whose $^{13}C/^{12}C$ ratio is 1123.75×10^{-5} (Craig, 1957). Sulfur isotope abundances are measured relative to the Cañon Diablo Troilite (CDT), in which $^{34}S/^{32}S = 449.94 \times 10^{-4}$ (Thode et al. 1961).

The analytical error involved in isotopic measurements of each

element was generally ±0.2 ‰, the reproducibility showing a similar range of ± 0.2 ‰. In the case of sulfur repeat runs one sample gave poor reproducibility (e.g. 2.3 ‰) which is likely due to contamination of the sample. All the results are presented in tables II (oxygen in magnetite and quartz), III (oxygen and carbon in carbonates), and IV (oxygen and sulfur in sulfates and sulfur in sulfides).

Quartz showed a consistent ^{18}O-enrichment, in accordance with experimental and theoretical information (O'Neil, 1986). $\delta^{18}O$ for this mineral ranges from +15 to +27.8 ‰, the largest ^{18}O-enrichment being exhibited by the lowest-temperature quartz.

Magnetite showed, as expected, the least ^{18}O-enrichment of all the phases analyzed. It also showed a more restricted range of variation than quartz, from -1.6 to +8.3 ‰.

Calcite is also largely enriched in ^{18}O. Although both fresh and recrystallized limestone were analyzed, $\delta^{18}O$ only varied between the narrow range from +17.1 to +24 ‰. Two dolomites (31-9* and 31-7*) showed a consistent ^{18}O enrichment with respect to their associated calcite, as predicted by experimental information (Northrup and Clayton, 1966; Mattheus and Katz, 1970). On the other hand, carbon isotope abundances in calcite and dolomite were indistinguishable. The $\delta^{13}C$ range for both minerals was from -3 to +3.3 ‰.

Oxygen isotope abundances in barite were remarkably uniform. The $\delta^{18}O$ ranged from +9 to +14.4 ‰ having an average of +11.2 ‰. Samples from Tabaquito and Ojo de Agua had a more restricted range from +9 to +11 ‰, whereas those from Vulcano range from +10 to +14 ‰. Far more sulfur isotope data were obtained for this mineral. They are graphically presented in figure V.1. Most of the $\delta^{34}S$ values for barite cluster in a narrow range

TABLE II. δ^{18}O OF MAGNETITE AND QUARTZ FROM VULCANO AND TABAQUITO

SAMPLE	MINERAL	LOCALITY	∂18O	DESCRIPTION
31-7	MAGNETITE	VULCANO	1.3	very fine-grained, intermixed with calcite-dolomite; alteration of limestone
31-9	MAGNETITE	"	5.8	" " " " " " " "
74	MAGNETITE	"	-1.3	cellular network of fine-grained magnetite intermixed with barite
78C	MAGNETITE	"	3.1	fine-grained, massive magnetite enclose by tabular barite and anhedral chalcopyrite
78D	MAGNETITE	"	8.3	massive magnetite apparently replacing patches of milky quartz
	QUARTZ	"	16.2	
DD 92-1	MAGNETITE	"	6	fine-grained magnetite-quartz aggregate; replaces colloforme hematite
	QUARTZ	"	25	
85	MAGNETITE	"	-0.6	irregular patches and veinlets of magnetite replace limestone; occurs intermixed with quartz which replaces, preferentially, fossil shels
	QUARTZ	"	27.8	
19	MAGNETITE	TABAQUITO	-1.6	saccharoidal intergrowth of magnetite and quartz; fossil relicts are present.
	QUARTZ	"	15	
11B	QUARTZ	"	20.8	fine-grained, replaces barite
27	MAGNETITE	"	-4.2	" " " " "
	QUARTZ	"	15.6	
35	MAGNETITE	"	5.9	veryfine-grained; occurs intermixed with barite and minor sulfides

TABLE III. $\delta^{18}O$ - $\delta^{13}C$ OF CARBONATES FROM LA MINITA, MICHOACAN

SAMPLE	δ18O	δ13C	LOCALITY	DESCRIPTION
56B	24	3.3	Vulcano	olistostrome within tuffaceous matrix
59A	23.3	1.7	"	" " " " "
78'	19.4	2	"	recrystallized limestone, overlies the ore body
80G	19	.4	"	coarse-grained calcite hosting pyrite veins
85	22.9	.5	"	fossiliferous limestone; replaced by quartz-magnetite
31-7	19.1	1.6	"	recrystallized, mt-replaced, fossiliferous limestone
31-7*	21.7	1.7	"	" " " " " "
31-9	18.4	0.4	"	" " " " " "
31-9*	25.1	0.1	"	" " " " " "
17B	22.4	2.2	Tabaquito	recrystallized limestone; replaced by magnetite-barite
38	19.7	-3.1		fresh limestone; upper unit
44	17.1	-0.1	Ojo de Agua	limestone altered to hematite-barite
89	17.6	-1.1	Sapo Negro	bedded, fresh limestone
*dolomite				

TABLE IV. $\delta^{34}S$ AND $\delta^{18}O$ OF SAMPLES FROM LA MINITA, MICHOACÁN

SAMPLE	∂34S	∂18O	MINERAL	LOCALITY	DESCRIPTION
11B	14.7	10	barite	Tabaquito	fine-grained, in replacement body
11C	0.6	- - -	sphalerite	"	subhedral, hosted by barite-quartz
11C	2.2	- - -	chalcopyrite	"	fine-grained, disseminated
11D	14.7	9.7	barite	"	laths in replacement body, along banDs
11D	0.4	- - -	sphalerite	"	coarse-grained, forms irregular bands
11F	15.7	- - -	barite	"	fine-grained disseminations
11F	0.4	- - -	sphalerite	"	" " " "
11F	3.6	- - -	galena	"	euhedral, fine-grained disseminated
11G	15.6	- - -	barite	"	fine-grained laths replaced by quartz
11G	1.1	- - -	sphalerite	"	fine-grained, replaced by quartz
11I	16.8	9.4	barite	"	coarse-grained vein in replacement body
12	16.6	10	barite	"	" " " " " "
14A	17	10.1	barite	"	coarse grained vein in jasper
18A	14.8	10.9	barite	"	coarse grained laths replacing limestone
18B*	14.9	10.3	barite	"	" " " " "
32C	15.6	9	barite	"	vein in tuff
34*	14.7	10.4	barite	"	fine-grained in replacement body (limestone)
35	16.3	10.5	barite	"	" " " "
107	16.1	11.2	barite	"	coarse-grained vein in replacement body
t 11 7	15	10.8	barite	"	fine-grained, in silicified tuff
31-6	14.6	11.4	barite	Vulcano	coarse-grained in replacement body
31-6	1.8	- - -	sphalerite	"	fine-grained, replaced by quartz
31-6	0.8	- - -	chalcopyrite	"	" " " "
33-2*	-14.4	- - -	pyrite	"	cubes in veins which transect barite
33-3	15.6	- - -	barite	"	coarse-grained laths enclosed by sulfides
33-3	-13.5	- - -	sphalerite	"	coarse-grained crystals in contact with barite
33-3	-13.8	- - -	pyrite	"	fine-grained cubes interlocked with sphalerite
33-5*	13.6	13.9	barite	"	coarse-grained, replaces jasper
33-5	-13.2	- - -	sphalerite	"	idiomorphic, in contact with barite and pyrite
33-5*	-9.7	- - -	pyrite	"	veins transecting barite-quartz body
33-7	16.8	10	barite	"	laths largely replaced by quartz
33-7*	1.3	- - -	sphalerite	"	fine-grained crystals replaced by quartz
33-8	16	- - -	barite	"	coarse-grained laths in contact with Fe-oxides
58A	14.5	10.5	barite	"	coarse-grained, forming concretions in tuff
58B	14.8	- - -	barite	"	coarse-grained, replacing jasper
58B	1	- - -	sphalerite	"	coarse-grained, partly replaced by barite
61	15.6	14.4	barite	"	coarse-grained replacing fossil (rudist) in tuff
62B	15.6	11.5	barite	"	coarse-grained, replacing limestone
63A	14.7	- - -	barite	"	coarse-grained, replacing chloritized tuff
67B	16.3	- - -	barite	"	coarse-grained, replacing chloritized tuff
67C	16.4	11.3	barite	"	coarse-grained laths and plates in tuff
67C	3.5	- - -	sphalerite	"	fine-grained; occurs between barite-laths
68A	15.2	12	barite	"	coarse-grained, replacing chloritized tuff
73	14.5	11.4	barite	"	fine- to coarse-grained bands
73	3.2	- - -	sphalerite	"	fine- to medium-grained bands

74	14.5	12	barite	"	coarse-grained, intermixed with magnetite
75B*	15.7	10.2	barite	"	sheared laths within brecciated volcanics
75B	2.8	- - -	sphalerite	"	fine-grained; occurs between barite laths
77A	15.7	13.4	barite	"	coarse-grained sheared crystals replacing tuff
77A	3.2	- - -	sphalerite	"	fine-grained, occurs along barite margins
77B	2	- - -	sphalerite	"	fine-grained, interlocked crystals
78C	15	10.5	barite	"	medium-grained; occurs in silicified limestone
78C**	0	- - -	chalcopyrite	"	fine-grained, clustered around barite zones
79B	16.8	13.1	barite	"	fine-grained, occurs near pyrite rich zone
80C	14.4	- - -	barite	"	coarse-grained veins in jasper limestone zone
80D	-8.1	- - -	pyrite	"	fine-grained, in massive, exhalative body
80F	-10.6	- - -	pyrite	"	" " " "
80F	-8.7	- - -	pyrite	"	" " " "
80H	-2.6	- - -	pyrite	'	fine-grained, replaced by post-ore stage sph.
80H	-4.7	- - -	sphalerite	'	coarse-grained replacing massive-pyrite body
82	15.5	12.1	barite	"	coarse-grained, in replaced limestone
86D	7.1	- - -	galena	"	fine-grained veins in silicified tuff
112-3	13.7	12.4	barite	"	veins hosted by chloritized + silicified tuff
113-1	11.8	12.7	barite	"	medium-grained in replaced limestone(?)
113-2	15.1	12.6	barite	"	coarse-grained veins hosted by altered tuff
114-D	0.9	- - -	pyrite	"	thin layer in black calcareous shale
114-D	10.7	- - -	pyrite	'	" " " "
114-I	12.7	- - -	pyrite	'	" " " "
45	16.3	10.5	barite	Ojo de Agua	coarse-grained laths in massive limestone
46	17	- - -	barite	"	laths replacing limestone
47	17.2	11	barite .	"	laths; coexist with hematite veins in limestone
*Average					
of 2 data					
**Average					
of 6 data					

from +14 to +18 ‰ (average +15.4 ‰), despite the fact that barites from different bodies and distinct mineralizing stages were analyzed. In contrast, the sulfides have much lower $\delta^{34}S$ values and a wider spread. The different sulfate-sulfide occurrences are characterized on the basis of their $\delta^{34}S$ values in figure V.1. The replacement bodies of Vulcano and Tabaquito show a similar distribution of $\delta^{34}S$ of sulfides, ranging from 0 to +3.6 ‰, however at the center of the Vulcano deposit pyrite and sphalerite exhibit large negative values (from -9.7 to -14.4 ‰ and from -13.2 to -13.8 ‰ respectively). The body of massive pyrite at Vulcano is characterized by negative $\delta^{34}S$ values ranging from -10.6 to -2.6 ‰; it should be noted that the highest $\delta^{34}S$ value was obtained from a sample of massive pyrite in contact with post-ore stage sphalerite veinlets ($\delta^{34}S_{sph}$ = -4.7 ‰). Pyrite layers of the shale-limestone (upper) unit at Vulcano, which are not related to the mineralizing events, have positive $\delta^{34}S$ values ranging from +0.9 to +12.7 ‰.

The barite occurrences at Vulcano, Tabaquito and Ojo de Agua show slightly different $\delta^{34}S$ values. For each locality the average value is: Vulcano $\delta^{34}S$ = +15.2 ‰, Tabaquito $\delta^{34}S$ = +15.5 ‰ and Ojo de Agua $\delta^{34}S$ = +16.8 ‰. The differences, although small, might be real since the geology of the three localities is somewhat different.

Replacement bodies at Vulcano and Tabaquilo and barite at Ojo de Agua

Pyritic ore at Vulcano

Pyrite layers within black shales (sedimentary unit) at Vulcano

$\delta^{34}S$ ‰

galena
sphalerite
pyrite
chalcopyrite
barite
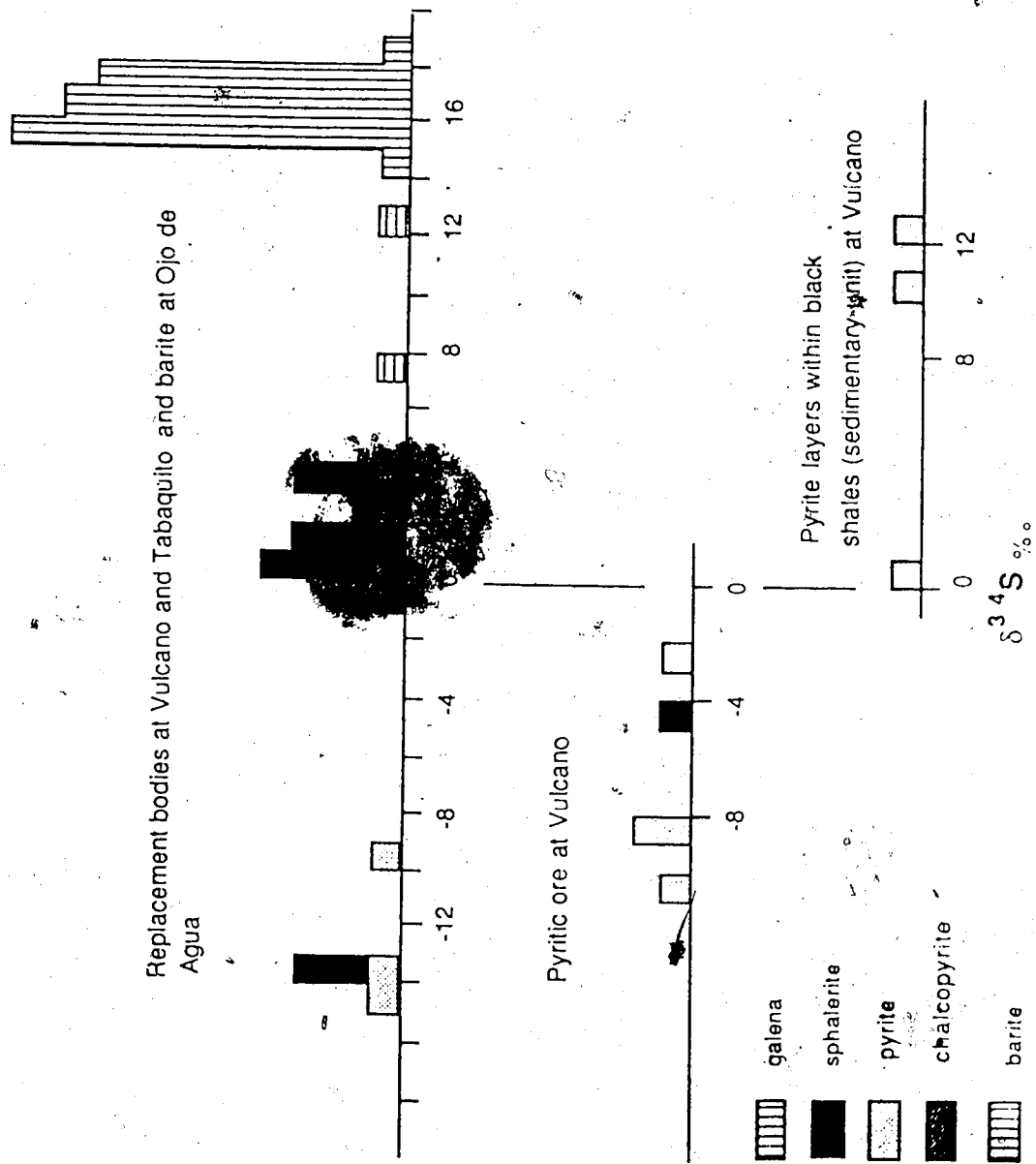
Figure V.1. Distribution of $\delta^{34}S$ values for the analyzed samples from La Minita, Michoacan

LIST OF FIGURES

LIST OF PLATES

xiv

I. INTRODUCTION

A) Setting and Geology: General

The La Minita mining district occurs in the northwestern sector of the Michoacan Province, near the Michoacan-Colima-Jalisco provincial boundary. Its central geographic coordinates are Lat. 18° 52' 06" N and Long 103° 17' 06" E (figure I.1). There are two main access-routes to La Minita. The most convenient begins at Manzanillo City which has an international airport. From Manzanillo, the highway MEX 110 leads to Pihuamo village, through Colima City; 12 km before this village the 58 km long, unpaved road to La Minita starts. A less convenient way to reach La Minita is through Guadalajara City. This city also has an international airport and is connected to Pihuamo by highway, but is located farther away than Manzanillo.

La Minita occurs within a Late Jurassic-Cretaceous island arc belt. At La Minita, a series of stratiform-stratabound Fe-Ba-Zn-Pb-Ag deposits lie within a Mid-Cretaceous vulcano-sedimentary unit of island arc type. The mineralization is of two types, namely: (i) epigenetic, and (ii) syngenetic. The former developed by the replacement of biohermal, fringing reefs, while the latter by underwater hot-spring deposition onto nearby seafloor. Thus, La Minita represents a very shallow-depth environment of deposition developed during the evolution of an island arc archipelago.

1
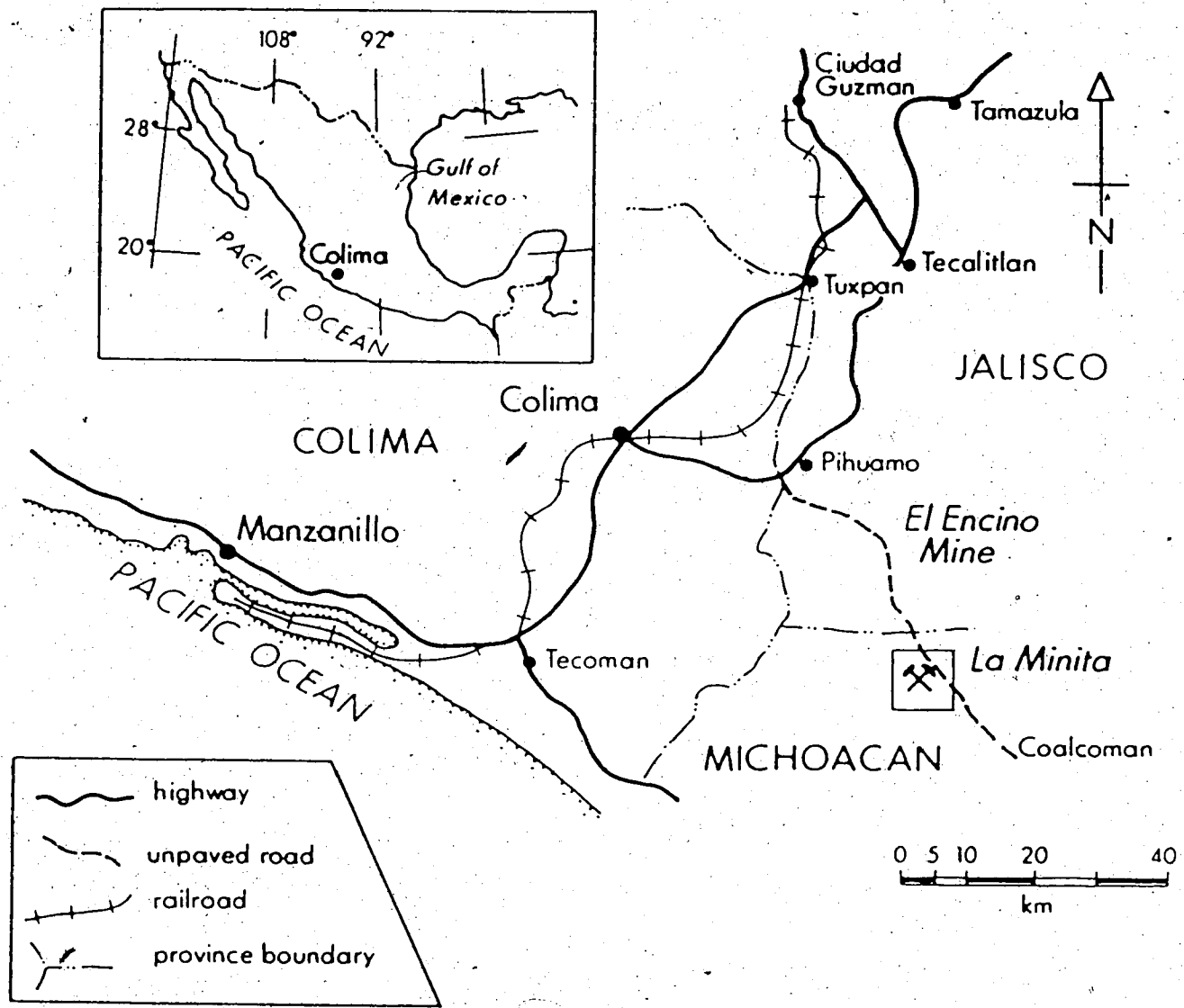
Figure I.1. Location of the La Minita district

B) Physiography and Climate

The La Minita district is located within the so-called Sierra Madre del Sur (Southern Sierra Madre) physiographic province defined by Raiz (1964). This province parallels the west coast of southern Mexico, and extends from Jalisco Province to Oaxaca Province. It is distinguished by its mountainous morphology developed on rock sequences that span from Late-Precambrian (in Oaxaca) to Tertiary. In the Sierra Madre del Sur a series of NW-SE trending compressive structures (anticlines, synclines and thrusts) have controlled the development of closely-spaced ranges and valleys, which are usually characterized by steep slopes. This array is frequently disrupted by the presence of plutonic intrusives. The rugged topography of the sierra reflects its intricate terrane assemblage.

At La Minita, the most rugged areas correspond to volcanic rock units, while the rolling zones to sedimentary-volcanosedimentary units. The highest peaks, made up of submarine volcanics, reach up to 1800 m.a.s.l. and exhibit cliffs and sharp valleys of steep gradients and dendritic patterns. The low areas, usually 700 m.a.s.l., show a smoother topography of wide hills and valleys that cut into less resistant sedimentary and pyroclastic sequences. Reef patches generally stand out of the enclosing pyroclastics, and a poorly-defined karstic relief has developed on them.

The intense weathering and erosion at La Minita reflects the severe weather. This region is characterized by a warm-subhumid climate, with an average annual temperature > 22°C and an average annual rainfall of between 950 and 1215 mm (CETENAL-Instituto de Geografia, 1970).

C) **History of Mining Activity**

There is very little published information on the mining activity of the district. Although Fe and base-metal exploration has been carried out for several decades in the region by federal and by private companies, there is no report that predates those of Compañía Peñoles. Small-scale mineral extraction had been going on before this company started its investigation of the ores (Gaytan et al., 1979).

In 1976 Compañía Peñoles began an intensive exploration program of the La Minita's mineralization. By 1979 a mineralized body with more than 6×10^6 tonnes grading 48.0 % barite, 4.0 % Zn, 0.33 % Pb and 78 g/t Ag had been outlined. A mill and benefication plant were built for production at an estimated rate of 600,000 tonnes/year.

The decline of the price of barite and silver has been an important factor in the decrease of the ore-reserves. The inventory of reserves as of October, 1986 indicated that the orebody consisted of over 2.7×10^6 tonnes of mineral grading 34.9 % barite, 4.48 % Zn, 0.34 % Pb and 58 g/t Ag (Alonso and Jimenez, 1986). At that time the expected life of the mine was 5 years, and exploration of the nearby mineralized zones (Tabaquito, Ojo de Agua, and La Cuchilla) was intensified in order to increase the reserves and extend the life-time of the mining district.

D) **Present State of Knowledge**

The investigation of the La Minita mineralization was reported by Gaytan et al. (1979). The district was defined to occur within an Albian-Cenomanian

volcanosedimentary terrane, which was properly related to the development of the Early Cretaceous island arc of southwestern Mexico. The main ore occurrence, named Vulcano, consists of oxides-sulfates-sulfides. These occur at the base of a reef limestone and present a vertical zoning, with sulfates-sulfides at the bottom and oxides at the top. Sedimentary, colloform and replacement textures were described as occurring intermingled in the ore zone, which was ascribed to underwater mass movements.

The deposit was classified as volcanosedimentary and compared with the Kuroko type, the Vulcano deposit being older and associated with reefal limestone. On the basis of paleontologic evidence, it was supposed that the ores were deposited on the seafloor at very low temperatures (0 - 20°C) and very shallow depths (< 50m). In this model it was proposed that subsequent burial of the zone and reactivation of the hydrothemal system made possible the recrystallization of the barite and the replacement of the reef limestone. Further, it was inferred that the Vulcano deposit formed in a submarine caldera, where frequent vertical movements took place.

Additionally, less detailed descriptions of other nearby occurrences (Tabaquito, Sapo Negro, La Cuchilla) have been made by geologists of Compañia Peñoles. In all of them the authors have concluded that the mineralization is volcanosedimentary and that it occurs at a similar stratigraphic level as Vulcano.

E) Purpose of the Study

The only previous study of the La Minita's mineralization was done by Compañía Peñoles. In it, detailed mapping and a petrographic-mineragraphic

investigation was carried out which led to the delineation of an economic deposit. However many details concerning the origin of the mineralization were not clarified and some interpretations (e.g. formation temperatures) were based upon inferences and upon comparisons with classic Kuroko models.

In this study an actualized review of the La Minita's mineralization has been undertaken, with the following objectives:

(i)   to determine the formation temperature of the mineral deposits.

(ii)   to characterize the ore fluids.

(iii)   to determine the source of sulfur and of the ore metals

(iv)   to define the mechanisms of ore-formation.

(v)   to evaluate the similarities and differences between La Minita's deposits and the Kuroko deposits.

(vi)   to define future exploration criteria for this kind of deposit.

In order to fulfill these objectives the study was divided as follows: i) field stage, which consisted of 30 days of field work; ii) lab stage, which included preparation of samples and petrographic study of ores and enclosing lithologies, preparation of samples and fluid inclusion study, and analyses of S, O, C, Sr, Rb and Pb isotopes of various ore materials and their enclosing lithologies.

This study is thus intended to give a fresh insight into the nature of the Cretaceous island arc mineralization of southwestern Mexico, and to contribute to the creation of a modern database on Mexican ore deposits, where isotopic techniques should be increasingly utilized.

II. REGIONAL GEOLOGY

The Sierra Madre del Sur is a region of complicated geological relationships. This, augmented by the inaccessible topography, has hampered the accurate identification and mapping of rock units and, thus, the precise application of stratigraphic criteria.

In the past, regional correlations have proven unsuccessful due to the intricate terrane assemblage of juxtaposed lithologies which show rapid facies changes and inhomogeneous deformational styles.

Perhaps the best approach to the solution of these difficulties has been set forth by Ortega-Gutierrez (1981) and by Campa and Coney(1983), with their application of the concept of tectonostratigraphic terranes. Each tectonostratigraphic terrane is characterized by coherent rock assemblages and deformation, which suggests a uniform origin. In most cases it appears that the basement of each of the terranes is distinct and has played an important role in the development of the terrane itself.

According to Campa and Coney (1983), the southwestern sector of Mexico is characterized by an heterogeneous assemblage of Jurassic-Cretaceous volcanosedimentary terranes (Guerrero and Juarez) and of older metamorphic terranes (Oaxaca, Xolapa, Mixteca) (see figure II.1). The old terranes whose age is Precambrian (Oaxaca) and Paleozoic (Mixteca) are restricted to a narrow area, and seem to have evolved independently and to have been welded together during the collision of North and South America (308 M.a., Keppie, 1977). All the aforementioned terranes were apparently accreted to North America during Late Mesozoic to Early Tertiary times (Campa and Coney, 1983).

Tertiary - Quaternary Cover

G Guerrero Terrane
A Alisitos
J Juarez
M Maya
MI Mixteca
O Oaxaca
XO Xolapa
V Vizcaino
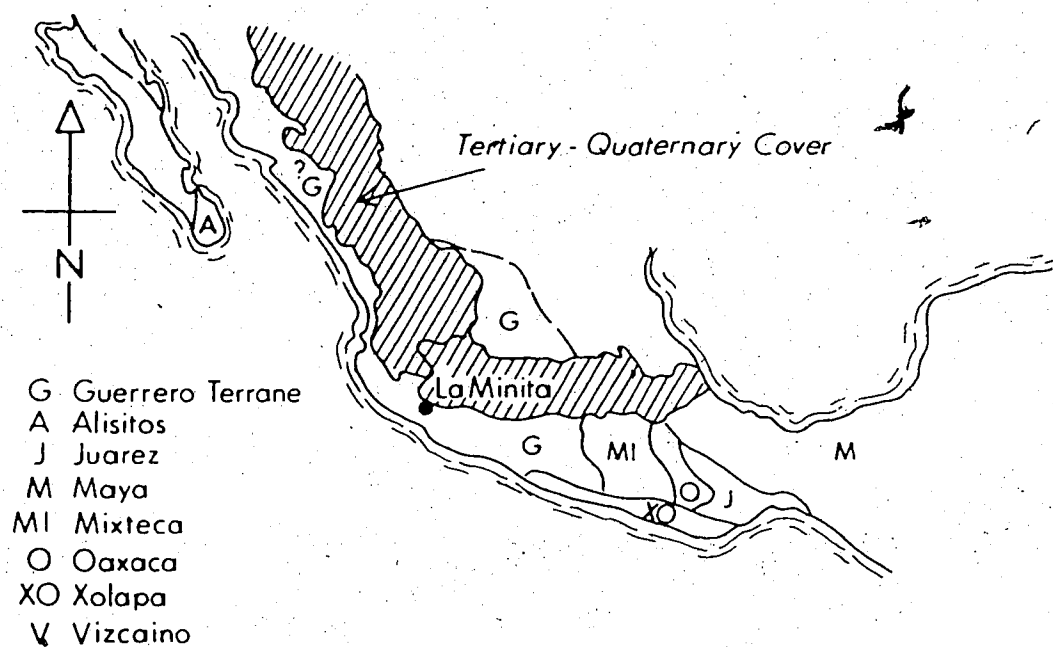
Figure II.1. Tectonostratigraphic terranes of Southwestern Mexico (adapted from Campa and Coney, 1983).

A) Stratigraphy of the Guerero Terrane

The Guerrero terrane, within which the La Minita mineral deposits occur, extends along the west coast of Mexico, up to Sinaloa Province. Off the coast of Sinaloa, the Alisitos terrane, which extends along Baja California, is apparently correlative with the Guerrero terrane.

The Guerrero terrane constitutes an accreted ancient island arc, which has been generally related to the Cretaceous subduction of the Pacific Plate, off the western coast of Mexico (Campa and Ramirez, 1979; Vidal et al., 1980; Coney, 1983; Urrutia, 1981). The absence of a crystalline basement below this terrane has been considered as an indication of the generation of this terrane either upon young continental or upon oceanic crust (Moran, 1986; Urrutia 1981). The Guerrero terrane has been further divided into 3 sub-terranes of similar stratigraphy but of contrasting structure, namely: the Zihuatanejo, the Huetamo, and the Teloloapan sub-terranes (Campa and Coney, 1983).

The Zihuatanejo Sub-terrane

The Zihuatanejo sub-terrane, which includes the La Minita district, consists of a thick sequence of andesitic volcanics intercalated with reef limestone and some shale-sandstone interbeds (more than 3000 m of this unit were recovered from the Jalisco 1 drill-core (Lopez Ramos, 1981)). The existence of evaporitic strata intercalated with these limestones, and of local clastic shallow-water sediments with dinosaur footprints, has been described elsewhere (Lopez Ramos, 1981; Ferrusquia et al., 1978). The upper part of this sequence grades into a clastic unit. According to the paleontologic evidence, this volcanosedimentary assemblage was formed in Late Jurassic-Middle Cretaceous time, although there is a predominance of Albian-Cenomanian

sequences. Folding and faulting have affected this sub-terrane, but no metamorphism has been imprinted.

The Huetamo Sub-terrane

The Huetamo sub-terrane consists of Upper Jurassic volcaniclastic sediments overlain by a Neocomian sandstone-shale sequence which grades into an Albian unit of limestone, tuff and redbeds. Late-Cretaceous redbeds and ignimbrites form the upper member of the sequence. Tight, upright folds and an absence of obvious metamorphism characterize this terrane.

The Teloloapan Sub-terrane

The Teloloapan sub-terrane consists of a low-grade metamorphic sequence. It contains intensely deformed, andesitic lavas and volcaniclastic material interbedded with shale, sandstone and limestone of Late-Jurassic to Early Cretaceous age (Campa, 1978; Campa and Coney, 1983).

In both the Zihuatanejo and the Huetamo sub-terranes, the lithologic facies define a series of topographic highs with shallow- to deep-basins. The presence of patch reefs within volcanic-pyroclastic sequences, very common in the La Minita-Coalcoman area, suggests seamount-like enviroments with fringing atolls. Shallow-water and transitional environments also suggest the existence of an ancient archipelago

The presence of the metamorphosed Teloloapan sub-terrane in between the apparently unmetamorphosed Zihuatanejo and Huetamo sub-terranes, all three being of similar age, has constituted an enigma. Campa (1978) suggested that these sub-terranes were tectonically juxtaposed, and that the outcrops of the Teloloapan terrane represent the upper block of a nappe, for in some

instances they have been found overlying unmetamorphosed sequences. The presence of these terranes of similar age but of contrasting deformation, could be explained by stacking of trust belts during the process of accretion, similar to the origin of the accretionary belts of Japan and of the western coast of North America.

B) The Sierra Madre Metalliferous Domain

From a metallogenic viewpoint, the Southern Sierra Madre has experienced two principal epochs. In the area of the Guerrero terrane, these are associated with distinct magmatic events.

Upper Jurassic-Middle Cretaceous Epoch

The first epoch was related to an island arc volcanism of predominantly mafic composition. Zn, Pb, Ba, Cu, Ag, and Au constitute the most important ore metals, which were commonly emplaced as volcanosedimentary deposits and as hydrothermal veins. It has been pointed out that all the massive sulfides of southwestern Mexico were formed during this epoch (Campa and Coney, ibid); thus, they are concentrated within the Guerrero and Juarez terranes. Rarely, ultramafic intrusions carrying Fe-Cr-rich assemblages were tectonically emplaced within the island arc complex (Delgado and Morales, 1984).

Late Cretaceous-Tertiary Epoch

The second metallogenic epoch was associated with a phase of plutonic activity of calc-alkaline affinity. During this epoch, Fe-skarns and Cu-porphyries were widely developed along subparallel zones trending NW-SE. The copper porphyries correspond to the possible meridional extension of the

Cordilleran Copper Porphyry Belt (Damon *et al.*, 1983; Stillitoe, 1975). This belt is well exposed in northwestern Mexico, but its southern extension is not clearly defined. Most of the porphyry copper deposits were emplaced during the period 75 to 50 Ma ago, synchronous with the Laramide Orogeny, although those of the southern portion of the belt appear to have formed ~15 M.a. after.

According to Damon *et al.* (1983), the occurrence of copper porphyries appears not to be related to the terrane intruded. On the basis of isotopic information they concluded, in contrast, that these deposits are closely related to an easterly migrating magmatic arc originating in the mantle. The copper was derived from a mantle source and some lithophile elements associated with the mineralization were acquired by assimilation of crustal materials.

On the other hand, the vast majority of the important Ag-Au and Pb-Zn mineral occurrences of Mexico, which formed during this epoch, show a clear affinity to the terrane distribution. Thus a clear influence of the "basement" is recognized, since these deposits were generally produced after the accretion of terranes to North America. For instance, Ag-Au mineralization is preferentially concentrated in regions with Mesozoic vulcanosedimentary basement (Guerrero and Juarez terranes) whilst Pb-Zn mineralization occurs preferentially in regions floored by Precambrian basement (Campa and Coney, 1983).

C) Petrogenesis

It is worth noting that initial Sr ratios of all the Laramidic and younger plutons of the meridional portion of the Guerrero terrane are rather low (0.7041 to 0.7055). Damon *et al.* (1983) interpreted these ratios as being evidence

of negligible crustal contamination of mantle-generated magmas. In addition, the lack of crystalline basement in the region of the Guerrero terrane suggests that the Late Jurassic-Middle Cretaceous magmatic rocks could not have been derived from melting of continental material; that is, they represent rocks produced by primary magmas as well. Should this be the case, assimilation of these older magmatic rocks would not affect, significantly, the initial Sr ratios of the Laramide plutons. A low initial Sr ratio at La Minita obtained by the present author (0.7049±2) support this statement. Therefore, this reasoning fits reasonably well the hypothesis that the southern Guerrero terrane did not evolve on ancient continental crust.

In contrast, evidence of crustal contamination is present in the Laramidic plutons of the septentrional sector of the Gerrero terrane. They exhibit the influence of the North-American basement as high initial Sr ratios, probably acquired by assimilation of old crustal material.

It can be concluded, therefore, that the vulcanosedimentary mineralization of the Guerrero terrane sets an example of the mineralization generated in a primary terrane. It must represent the mineralization associated with the initial stages of continental crust-formation.

III. LOCAL GEOLOGY

The la Minita district typifies the volcanosedimentary mineralization of the Guerrero terrane. As was pointed out earlier, this type of mineralization is restricted to the Late Jurassic-Early Cretaceous island arc of southwestern Mexico. At La Minita shallow water environments around volcanic islets favored the formation of fringing reefs which were frequently draped by volcanic eruptions of pyroclastic material.

A) Lithologic Setting

At La Minita three principal lithologic units may be recognized. The lower unit is of predominatly mafic, volcanic character. The middle unit includes volcanic (lava flows and pyroclastics) and sedimentary components of intermediate to felsic composition. The upper unit consists of an uncomformably-deposited turbiditic sequence.

In the following sections reference is made to several localities within the district, namely: Vulcano[1]; Tabaquito[2]; Ojo de Agua[3]; Sapo Negro[4]. These are shown in the map of figure III.1. The description of units is based upon the petrographic study by the author of over 140 thin sections, and complements that of Gaytan *et al.* (1979).

---

[1] Vulcano = Volcano
[2] Tabaquito = Little Tobacco
[3] Ojo de Agua = Spring
[4] Sapo Negro = Black Toad

1 4
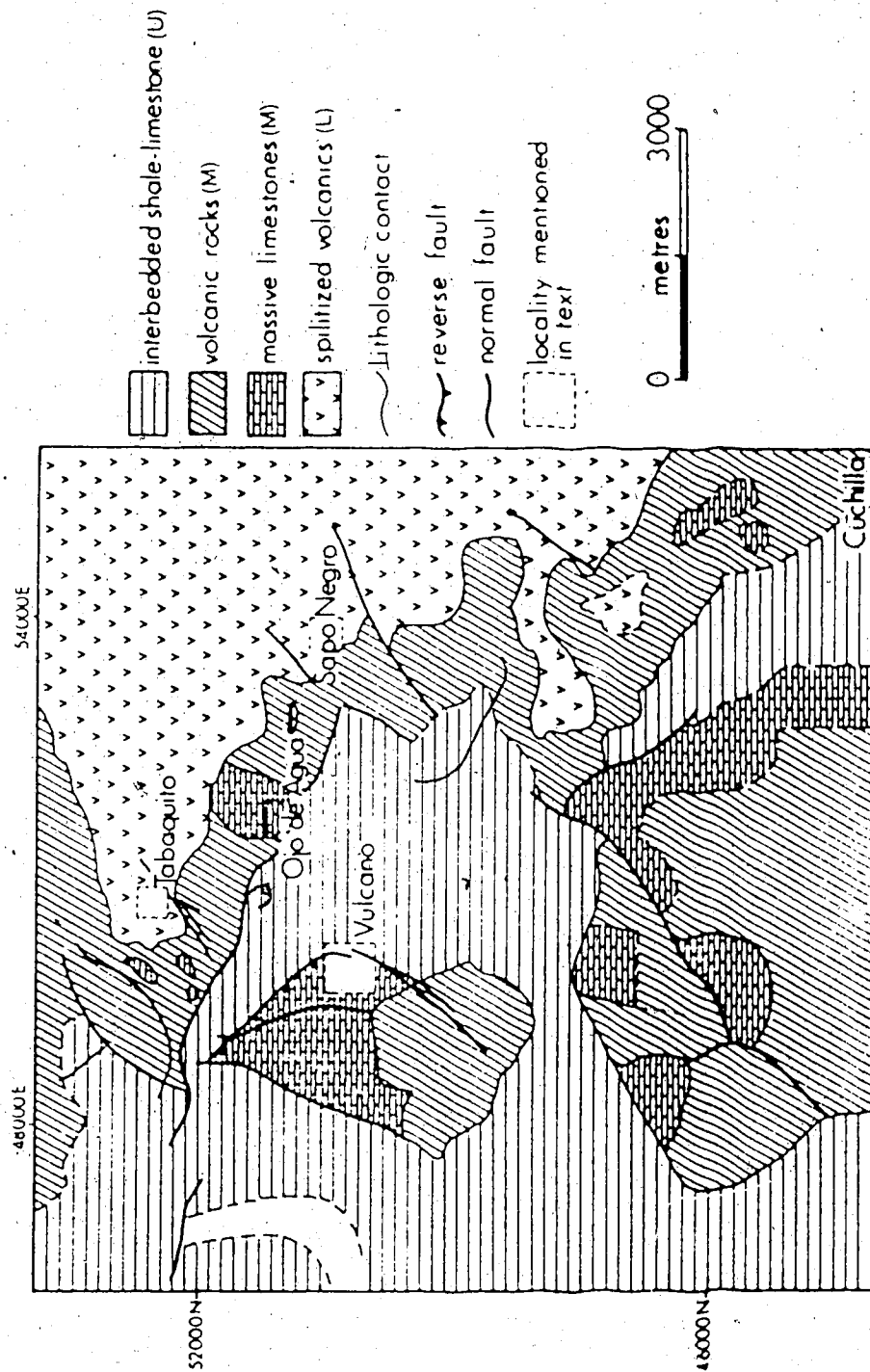
Figure III.1. Geology of the La Minita district. (L) = Lower unit; (M) = Middle unit; (U) = Upper unit (adapted from Compañía Peñoles, 1987).

Lower Unit (Volcanic)

This unit occurs at the lowest stratigraphic level in the district, although topographically it may be found forming the highest peaks. Its main outcrops are located in the northern and eastern sectors and it probably floors the rest of the region

Massive lava flows and proximal pyroclastic beds are the sole components. The lavas are porphyritic, autoclastic andesites and aphanitic basalts. In the andesites, the only surviving essential component is oligoclase, which frequently is altered to epidote (pistachite) and calcite. These phenocrysts are set in matrix of chlorite-albite-calcite-hematite commonly showing relict glassy structure. The basalts show a trachytic texture of andesine-oligoclase microlites. As it is the case with the andesites, the basalts show a typical spilitic alteration to chlorite-calcite-hematite, in addition to tremolite-actinolite, clinozoisite, zeolites, and melilite (or vesuvianite?). These basalts occur intercalated with bedded, micritic limestone at the Sapo Negro locality. The presence of melilite has been long known to occur where basaltic dikes or lavas were emplaced in contact with carbonate rocks. The altered andesite-basalt association corresponds to the greenstones described elsewhere as spilitic. Although the origin of spilites (and related keratophyres) was a contentious issue for some time (Amstutz, 1968; Amstutz and Patwardhan, 1974; Vallance, 1974), it is now generally accepted that they are produced during submarine alteration of basalts-andesites (and associated rocks) by addition of Na+ at varying P_{CO_2} (Condie et al, 1977; Moody, 1979; Best, 1982; Hyndman, 1985).

Similarly, the pyroclastic members are of andesitic composition and show a chloritic alteration as well. They are volcanic breccias and lappilli tuffs, and occur in massive structures. It is clear that they represent the proximal facies

of explosive eruptions. In fact, the whole unit defines a submarine volcanic center, probably a seamount within an island arc.

Middle Unit. (Volcanosedimentry)

This unit consits of pyroclastics, volcaniclastic sediments, and patch reefs. It occurs at Vulcano, Tabaquito, and Ojo de Agua and is characterized by a more felsic composition of the volcanic material.

The pyroclastics are mainly ash fall tuffs and sporadic ash flow tuffs. They consist of trachytic lapilli and altered ash. Aligned sanidine microlites set in a glassy matrix are widely represented in the lithic fraction of the tuffs. There are also lithic fragments which are totally devitrified. In fact, very rarely has the glass been preserved, being largely altered to an association of chlorite, quartz, and sericite.

Lavas are far less common in this unit. They are aphanitic and porphyritic rocks highly altered to chlorite-quartz, where sericitized sanidines are the only remaining phenocrysts. Some rocks show prominent glassy relict textures, with chlorite flakes aligned along the contour of perlitic structures. Gaytan *et al.* (1979) have described the wide occurrence of fluidal, vitric rhyolitic components and of "small intrusives" within this unit.

The volcaniclastic sediments of this unit consist of re-worked volcanic material. These are sandstones and conglomeratic sandstone made up of round, elongated clasts of trachytic and aphanitic texture. Graded bedding may be present. These rocks are suggestive of near-shore erosion of the volcanic rocks described above.

Clearly the volcanic and volcaniclastic rocks have been affected by hydrothermal alteration. In addition to the wide occurrence of chlorite, quartz, and sericite, barite laths and hematite veinlets have often replaced the rock.

Likewise, secondary fresh K-feldspar occurs in some instances, although it is more restricted.

Biohermal patches of fossiliferous limestone are intercalated with this volcanic sequence. The outcrops of this member are concentrated along a belt which extends NW-SE through the studied area (figure III.1). At the Tabaquito occurrence, the limestone is more than 40 m thick. It contains a large number of fossils, among which the caprinulid rudists are the most common. Gradation from fresh limestone into a zone of magnetite-quartz and then into the ore body can be clearly traced. On the whole, it appears that these reefs developed fringing the volcanic islet defined by the lower unit.

The main exposure of reef limestone occurs in the center of the district, adjacent to the Vulcano orebody. Here, it consists of more than 150 m of biohermal reef limestone bearing gastropods and pelecypods. Among the pelecypods, Caprinuloidea sp. and Coalcomana ramosa are the most common rudists, which are typical of Cretaceous carbonate sequences of Mexico, specifically the Albian-Cenomanian (Palmer, 1928; MacGillavry, 1932; Dechaseaux and Perkins, 1969; Harris and Hodson, 1922; Pantoja and Estrada, 1986). It has been postulated that rudists were organisms which tolerated energetic, shallow-water, warm marine environments (Böse and Cavins, 1927; Cox, 1933; Enos, 1974; Palmer, 1928; Mulleried, 1934), which is in agreement with the facies apparently defined by the middle unit.

This reefal body comprises at least two growth stages, as suggested by the presence of a disconformity marked by an horizon of shaley material and dissolution cavities in the lower member. This particular bioherm did not grow fringing a volcanic island, but rather above a shallow shelf covering an eroded (?) volcanic pile. The dissolution cavities suggest a short period of emergence or uplift.

Most of the biohermal reefs of the district, show extensive evidence of coeval reef growth and barite-sulfide/magnetite-hematite mineralization. Barite and hematite-magnetite commonly alter the limestone, and it is not uncommon to find fossils finely replaced by quartz, magnetite or by barite. In fact this kind of alteration is an important indicator of mineralization in the district, the main occurrences having originated by replacement of the reef itself (at Vulcano and Tabaquito).

The aforementioned alteration also occurs in marginal zones of the reef as veinlets, with rare recrystallization of the enclosing limestone. Replacement of fossils and veinlet development could have clearly been the result of hydrothermal activity developed in the reef environment. The fact that organisms flourished in the area might well be related to the presence of exhalative hot-springs in the vicinity of the reef. Such hot-springs would deliver nutrients required for the support of large thermophilic communities. Further evidence of the coeval development of the biohermal reefs and exhalative sites comes from the common occurrence, at a similar stratigraphic level, of syngenetic pyritic bodies and bedded iron formations which probably formed in off-reef, fault controlled basins.

Laterally, the main reef body at Vulcano thins out, giving way to tuffs and volcaniclastic sediments. The presence of olistostromes within a shaley-tuffaceous matrix suggests mass movement, probably triggered by volcanic seismic activity. In other cases, slump folds within iron formations (at El Sapo Negro) also suggest disruption of the seabed.

On the basis of the previous information, a paleogeographic reconstruction suggests the existence of a shallow marine, sub-tropical or tropical environment. This existed around volcanic islets, with submarine hot-springs issuing waters during hiati between eruptive cycles. Also, during

these hiati reef forming biota flourished on and around the islets. Evidence from the Vulcano and Ojo de Agua sectors indicates that pyroclastic flows commonly buried the reefs. The presence of well-preserved rudists within ash-fall tuffs is a common feature that has been also noticed in the Huetamo and El Encino Mine regions (Pantoja,1959; Pantoja and Estrada, 1986).

Upper Unit (Sedimentary)

In contrast to the dominantly volcanic character of the two previous units, the upper unit is solely of sedimentary nature. The base of the unit consists of turbiditic strata of sandstone-shale and limestone. Towards the top, it is composed of a black shale-limestone sequence with frequent thin pyritic layers. This unit was uncomformably deposited on the middle unit. At Vulcano it lies on a kaolinized-chloritized tuff which in turn overlies the main reef. No basal conglomerate has been observed at the unconformity level, however the lack of alteration and of volcanic material on the upper unit suggests a sharp change in the tectonic/volcanic regime of the region.

This unit seems to have been deposited on a faulted terrain, within small graben-like basins of variable depth (Gaytan et al., 1979).

Correlation and Age

The Albian-Cenomanian is a period widely represented in southwestern Mexico. In the Guerrero terrane and its surroundings, sequences of this age have been described elsewhere (The Morelos Formation (Pantoja, 1959; Fries, 1960; and the like); The El Pochote Formation (Campa, 1978); The Vallecitos Formation and The El Encino Formation (Pantoja and Estrada, 1986) etc.).

Apart from dating by the means of fossils, there are but a few examples of the absolute dating of the volcanic-sedimentary complex. Czerna et al. (1978)

reported a Rb-Sr age of 311±30 M.a. for the volcanic sequence west of Zihuatanejo. Gastil *et al* (1979) determined a 114 M.a. age for the volcanics of Puerto Vallarta. Delgado and Morales reported a 96 M.a. K-Ar age for the ultramafic complex of El Tamarindo, Guerrero, which is suspected to be genetically related to the Guerrero terrane. Finally, Pantoja and Estrda (1986) reported a 93 M.a. (method was not indicated) age for the volcanosedimentary sequence at El Ecino Mine.

At La Minita, the Rb-Sr study carried out during this investigation, yielded a pseudo-isochron. The age calculated by means of this line is 100 M.a. and the initial Sr ratio 0.7049. This age and the initial ratio appear reasonable for the island arc volcanism of the region. The paleontologic evidence agrees with such an age, for the Albian-Cenomanian boundary has been placed at 97.5 M.a. (Harland *et al.*, 1982). However the pseudo-isochron renders some degree of uncertainty due to the lack of precision. This aspect will be discussed in the Sr isotope section (chapter VI).

B) Structural Geology

The structural features of the La Minita district were developed during two main deformational stages. The first one was probably initiated even before the deposition of the ores, whilst the second one formed after depositon of the upper lithologic unit.

First Deformational Stage

This is manifested as prominent normal faults of NE-SW trend. Evidence of the existence of these faults prior to the mineralization is found at Vulcano (see figure III.3). In this locality a normal fault with NE55SW orientation transects the replacement and pyritic bodies (which will be fully described in the Deposit Descriptions section), and has raised the underlying volcanics. A minimum 50 m throw is deduced from the reconstruction of the lower part of the replacement body. The significant observation is that this fault does not affect the upper lithologic unit, and therefore it existed prior to the sedimentation of this unit. There are, on the other hand, other normal faults which clearly affect the upper unit.

The faults of this deformational stage might have provided a vent for fluid circulation and deposition of the ores, as suggested by Gaytan *et al.* (1979).

Second Deformational Stage

This stage was of compressive nature and developed after deposition of all the lithologic units. Depending upon the strength of the rock, different deformational styles were imprinted. Thus, two regimes are distinguished namely: a ductile and a brittle phase.

Ductile deformation is exhibited by the upper unit. A general NW-SE orientation for the strike of the sratification is apparent, although it is disrupted at Vulcano where, in the southern sector, it trends NE-SW. The upper unit displays tight, inclined anticlines and synclines whose axes parallel the general stike. The folds have a short wavelength (in the order of meters) and and larger amplitude (meters to tens of meters) in the northern area close to the Vulcano deposit. Farther away, the folding becomes more gentle. For instance, at Tabaquito no folding is apparent and, rather, the stratification dips 30-50° SW; in the southern sector of Vulcano it dips 20-40° SE.

Brittle deformation is manifested in the reef limestone and in the volcanics. The most dramatic example is exhibited by the reef at Vulcano, in which a prominent joint system has developed. The joints are closely spaced at ~1m intervals, have a predominant NE15SW orientation, and dip W at 84°-86° (see figure III.2).

In the Vulcano sector there is a prominent reverse fault which has brought into contact the middle and upper units (see figure III.3). It also appears to separate the northern block with NW-SE strikes from the southern block with NE-SW strikes. Its average orientation is NW35°SE, 55°SW, and the southern block is the hanging wall. Due to the faulting the reef limestone has overriden onto the upper unit, which has adopted the orientation of the fault and may appear turned-over and more intensely folded in this zone, as was mentioned previously.

The reverse fault must be responsible for the different orientation of the upper unit in the hanging and footwalls. A counter-clockwise rotation of the overriding block would explain such a feature.

The last brittle deformation manifests itself as NE20°-50°SW-trending normal faults. These faults are diagonal to the normal fault of the first

deformational stage at Vulcano, perpendicular to the general strike of the upper unit, and roughly parallel to the joint system of the reef limestone. These faults affected all the units of the district, and were probably controlled by deeper discontinuities reactivated after the culmination of the second deformational stage.

On the whole, the deformation exhibited at La Minita affords a localized example of the regional deformation of SW Mexico. Similar NW-SE trending folds and quasi-perpendicularly oriented systems of fractures and faults have been described and mapped elsewhere (Pantoja, 1959; Pantoja and Estrada, 1986; Campa, 1978; etc.).
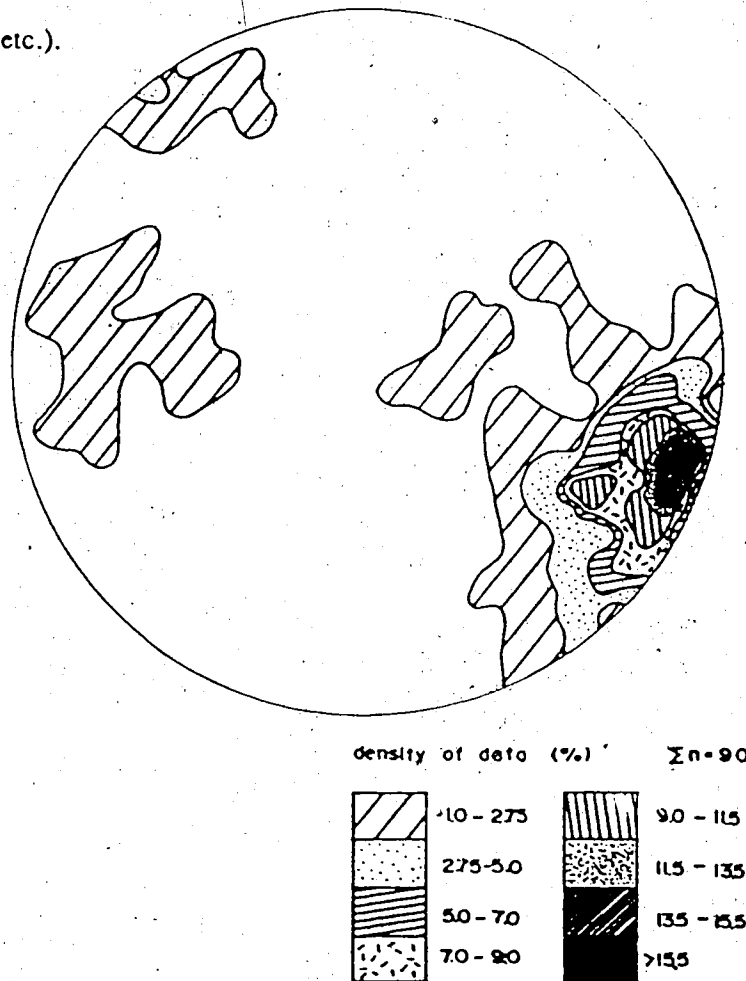
Figure III.2. Contoured and shaded equal-area projection of the poles of joints in reef limestone at Vulcano.

C) Deposit Descriptions

Mineralization in the La Minita district is apparently dominated by iron oxides, but in some instances these are outweighed by sulfate-base-metal sulfide mineralization. The principal mineral ocurrences are found at Vulcano, Tabaquito, Sapo Negro and Ojo de Agua (see figure III.1). The mineralization is of two principal varieties, namely: (i) epigenetic, stratabound mineralization which consists of iron oxides, barite and Zn-Pb sulfides and replaces, mostly, carbonate horizons (at Vulcano, Tabaquito and probably Ojo de Agua); (ii) syngenetic-exhalative, stratiform mineralization in the form of massive, bedded pyritites (at Vulcano) and iron formations (at Vulcano, Tabaquito and Sapo Negro).

Syngenetic and epigenetic mineralization often occur in the same area. This led Gaytan et al. (1979) to invoke early syngenetic deposition followed by recrystallization and replacement of the primary mineralization, during later resurgence of hydrothermal activity.

Taking into consideration both types of mineralization, a general mineral zonation can be defined at Vulcano and Tabaquito. In these localities barite and Zn-Pb sulfide mineralization is bordered by iron-manganese mineralization in the form of veins and stratiform deposits. Another example of zonation exists in the replacement body at Vulcano. Here, the zinc content decreases towards the top, while that of barite and silver increases in the same direction (Gaytan et al., 1979).

The Vulcano Orebody

A recent investigation of this orebody, after extraction of the central mineralized zone had exposed the interior of the body, has permitted the identification of three kinds of mineralization, namely: (i) iron oxide-barite-Zn-Pb-sulfide carbonate replacement mineralization; (ii) massive, internally-bedded pyrite mineralization; (iii) stratiform jasper-hematite mineralization. The map of figure III.3 may be consulted to more easily visualize the geologic relations at this locality.

(i) Iron oxide-barite-Zn-Pb sulfide replacement mineralization

The main replacement body occurs at the center of the mine and extends radially outwards, following a domal structure (Gaytan et al., 1979). It consists of irregular hematite, magnetite, pyrite, and sphalerite zones, principally in the lower part of the body. Hematite-magnetite are intermingled and the latter may replace the former. Most of the orebody contains radial intergrowths of fine-grained barite with disseminated sphalerite, pyrite, galena and tetrahedrite (freibergite). The top of the body is rich in jasper which occurs intermixed with brecciated limestone; this zone grades upwards into recrystallized limestone and finally into fresh limestone. Gaytan et al. (ibid) recognized the presence of sphalerite with colloform banding, which is often broken probably as a result of submarine slumps.

The whole body is transected by barite-quartz-pyrite veins. Sporadic occurrences of limestone remnants and of replaced fossils within the ore zone strongly suggest an epigenetic origin for this body.
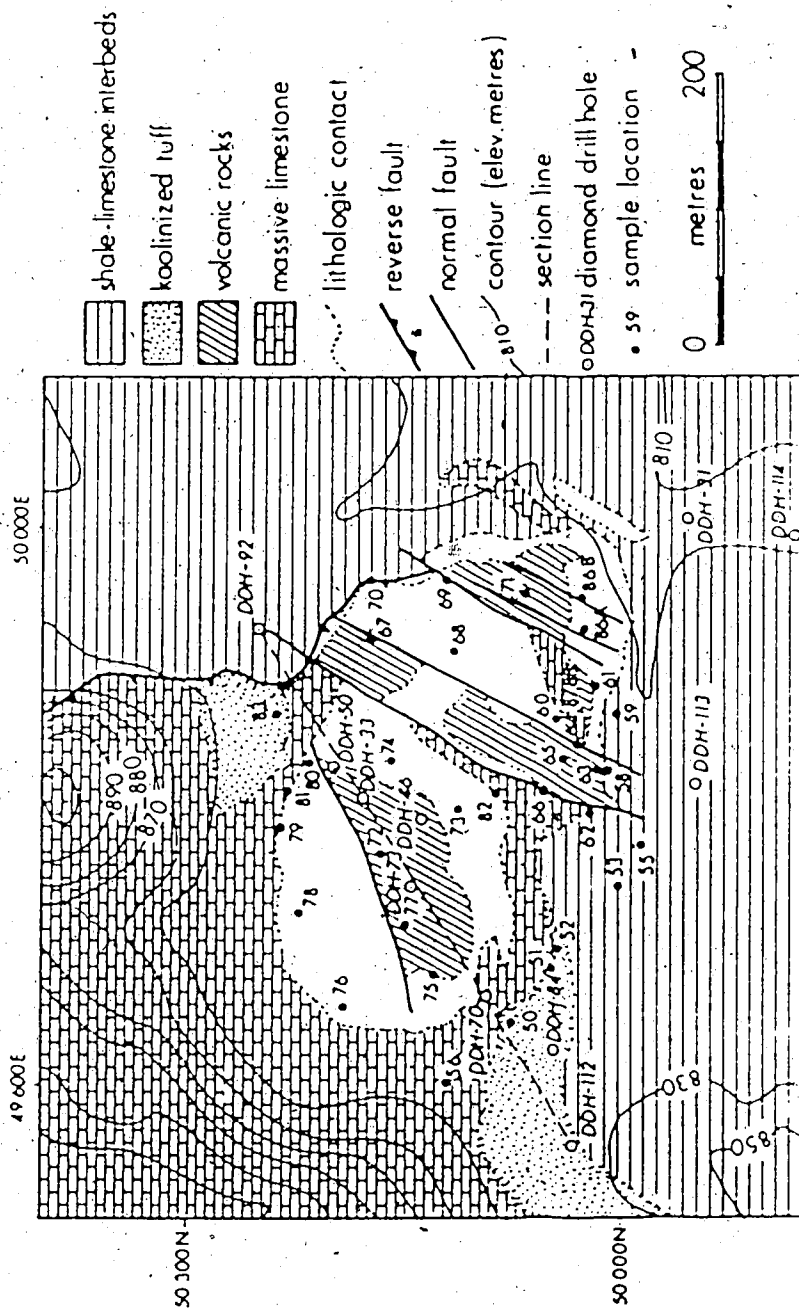
Figure III.3. Geology of the Vulcano locality. The replacement body corresponds to the white zones (adapted from Compañía Peñoles, 1987).

At depth, there are two limestone-magnetite beds, only detected in the deepest drill-holes, whose thickness reaches up to 20 m. Fine-grained magnetite, hematite, and jasper are ubiquitously present with minor associated sulfides (sphalerite, pyrite and chalcopyrite). Recrystallized calcite and some dolomite are thoroughly mixed with these minerals. Veins and irregular replacement have largely affected the limestone.

However, some samples still contain fossil shells despite the intense alteration. These strata are enclosed by dominantly trachytic-andesitic pyroclastics which are highly choritized-silicified. Disseminated sphalerite-barite, and galena veins are found in the volcanics.

At the southtwestern sector of the pit there is a zone of reefal limestone largely silicified and replaced by magnetite. Here almost all of the fossils, mainly caprinulid rudists, are finely replaced by quartz and magnetite. Similarly, irregular magnetite-quartz veinlets extensively transect the rock, however no appreciable recrystallization of the limestone remnants occurs. This seems to suggest that the alteration of the limestone took place at low temperature, along the most permeable zones, perhaps, during the diagenetic stage.

On the whole, it appears that initial iron-silica mineralization was followed by barite-sulfides-magnetite-quartz mineralization and finally by minor barite-pyrite-sphalerite

(II) Massive-pyrite mineralization

Massive, internally-bedded pyrite of syngenetic exhalative origin occurs in the northeast sector of the pit (sample location point #80). This ~5x10 m body is intensely shattered and occurs at a sheared zone of the fault of the first

deformational stage. Gradded beding, pseudo-layering, and framboidal textures are present and witness the exhalative-sedimentary nature of this body. In addition, there are pieces of crust up to a few centimeters long and two to three milimeters wide (and smaller), made up of pyrite-marcasite with minor sphalerite and barite (see plate 1). These probably constituted parts of exhalative chimneys (as those described at the East Pacific Rise (Haymon and Kastner, 1981; Styrt et al., 1981) and in Papua New Guinea (Both et al., 1986)) or of the outer shell of the pyritic body.

On the whole, this body consists of fine-grained pyrite with minor sphalerite-barite and traces of galena. There is also coarse barite and sphalerite which cross-cut, and contain left overs of (island and continents textures) the previous association (see plate 2).

Laterally the pyritic body grades into a zone of pyrite-marcasite-barite-calcite with minor sphalerite. The whole body is overlain by massive limestone and seems to be a lateral extension of the replacement body.

Thus, it would appear that there was a structural control for the deposition of this sulfide body. Ore-solutions discharging into the sea affected the patterns of carbonate sedimentation, which became dominant after the waning of the hydrothermal activity.

(iii). Stratiform iron mineralization

Stratiform iron-silica mineralization occurs at the southeastern sector of the mine (sample location points 61 and 88). It consists of at least two internally layered strata of jasper-hematite, enclosed within pyroclastic rocks. The unsorted, massive structure of the underlying pyroclastic member, which may constitute an ignimbritic unit, points to a shallow environment of deposition. Chloritization and baritization of the enclosing tuffs is extensive.
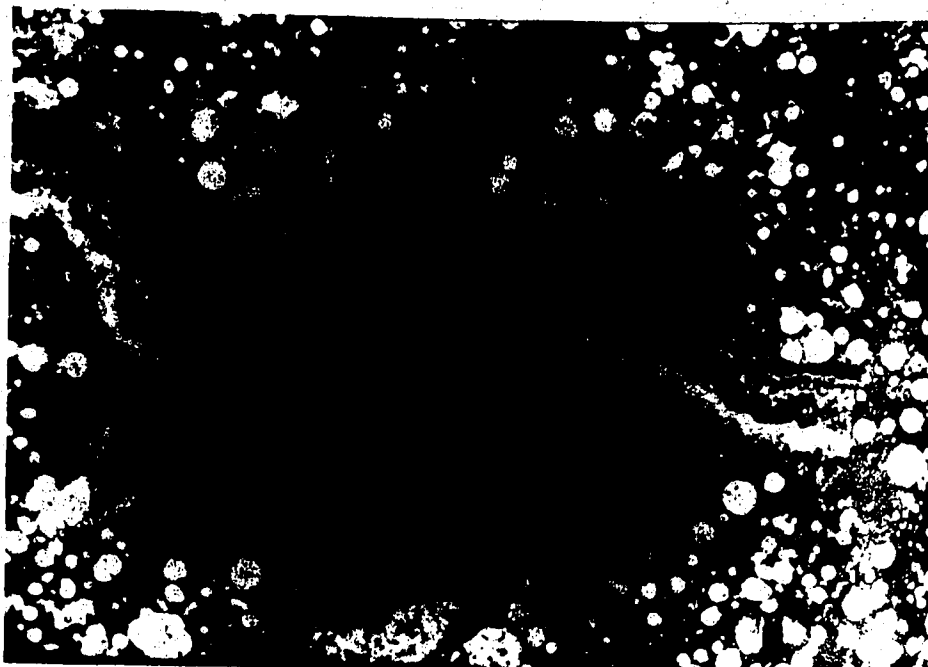
Plate 1. Sample 80D: pyrite-marcsite crust set in a matrix of framboidal pyrite with barite and minor sphalerite. Reflected light.
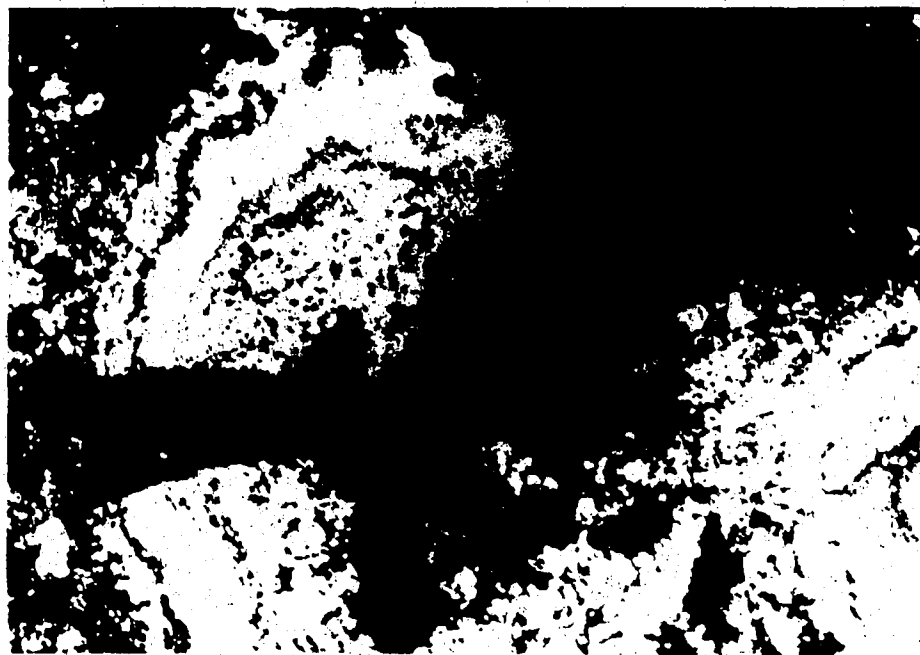
Plate 2. Sample 79A: Sphalerite transecting and replacing py-marcasite. Barite (the black mineral) may replace all the minerals above mentioned. Reflected light

Fossils replaced by barite may be found in the tuffs underneath the ferriferous layers. Additionally, olistostromes of limestone within the tuffs are, as well, highly-altered to jasper and barite, and late barite-sphalerite associations.

It is thus apparent that epigenetic and syngenetic ores were formed almost synchronously at Vulcano. The former resulted from replacement of reef limestone by sulfate-sulfide-iron oxide mineralization, while the latter formed by precipitation onto the seafloor of proximal pyritic and "more distal" jasper-hematite beds.

The Tabaquito Deposit

On the whole, the mineralized zone at Tabaquito is stratabound and hosted by the volcano-sedimentary sequence. The proportion of limestone is much less than in Vulcano, however the mineralization is again clearly spatially associated with this rock-type. The main ore zone is massive and consists of an association of barite-quartz and minor sulfides and sulfosalts (sphalerite, chalcopyrite, galena and proustite). Although the present continuity of the body has been disrupted by a series of normal faults, it seems that its lateral equivalent is a massive biohermal limestone which is almost totally replaced by magnetite and bears silicified-baritized fossils. Farther away the magnetite content decreases and the limestone becomes extensively replaced by barite laths; this zone grades into an unaltered limestone. Covering the main replacement body, there is an irregular mass of subtly-layered jasper a few meters in diameter, which is transected by barite veinlets.

The main body is generally fine-grained. It consists of a crystalline association of radial barite and euhedral, often doubly-terminated quartz which commonly replaces barite. Occasionally, irregular zones of coarse barite are present. The sulfide content of this body is very low, locally reaching a maximum of 10 %. Sphalerite and galena are generally associated with the most silicified zones and are often replaced by quartz. Coarse-barite veins and hematite-quartz veins frequently transect the body. In a few cases remnants of highly sericitized K-feldspar are recognizable in its upper part. Similarly, occasional circular – structures within the ore-zone are present and could represent totally-replaced fossils.

The mineralized body is underlain by chloritized-silicified-baritized, andesitic to trachytic volcanics. It is overlain by a less-altered volcanic-volcaniclastic sequence. Laterally the volcanics are kaolinized and transected by black veins of pyrolusite-braunite; in a general sense, this type of alteration rims the main mineralized zone.

The effects of the alteration and weathering have been extreme. Patches of fossiliferous limestone, which occur eastwards of the mineralized zone already described, have been totally weathered to an earthy, friable material, where silicified-limonitized fossils (similar to those described for Vulcano) are the only residua.

In short, as it is the case with Vulcano, Tabaquito presents evidence of a sequential development of initial iron mineralizing, followed by barite-sulfide mineralization. The stratabound nature of the body and some relict textures again point to a selective replacement of limestones and of associated volcanic rocks. Further introduction of barite-quartz and hematite through veins affected not only the main body, but the base of the overlying lithologies as

well. In contrast, the jasper body seems to have been deposited in an aqueous environment, prior to the last mineralizing event.

The Sapo Negro Deposit

At this locality a series of Mn-Fe-rich strata (Fe-formation) are enclosed by a volcanic unit which grades upwards into a layered sequence of carbonates (see figure III.4). These strata extend over an area ~200x100m and are 10 cm to ~1.0 m thick. The Mn and Fe contents of the richest stratum are 27 % and 14 % respectively (Castillo-Madrid, 1986). Two sequences can be distinguished, separated by a horizon of kaolinized tuff. The upper member consists of two strata composed of layered jasper, hematite and Mn-bearing brownish beds, separated by a thin layer of brownish-pinkish (montmorillonitic) tuff. The lower member consists of four strata of shaley material, rich in Mn oxides (psilomelane-jacobsite) and hematite, with almost negligible jasper. Internal folding due to seismically induced (?) gravitational slides are common in this lower member.

Covering this iron formation is a unit of spilitized, spheroidal basalt which grades into layered carbonates. There are two spilitized flows, the thickest lying directly upon the iron formation. The other two are intercalated with layered carbonates which contain jasper at the bottom of the sequence. The limestone is very fine-grained (micritic) and contains poorly preserved microfossils, probably Calcispherulae.

The Sapo Negro deposit probably corresponds to the jasperoid formations of the volcanogenic formation of greenstone type defined by Shatskiy (1966).

Legend:
- shale
- limestone
- Mn-shale
- argilitized tuff
- jasper
- spilite
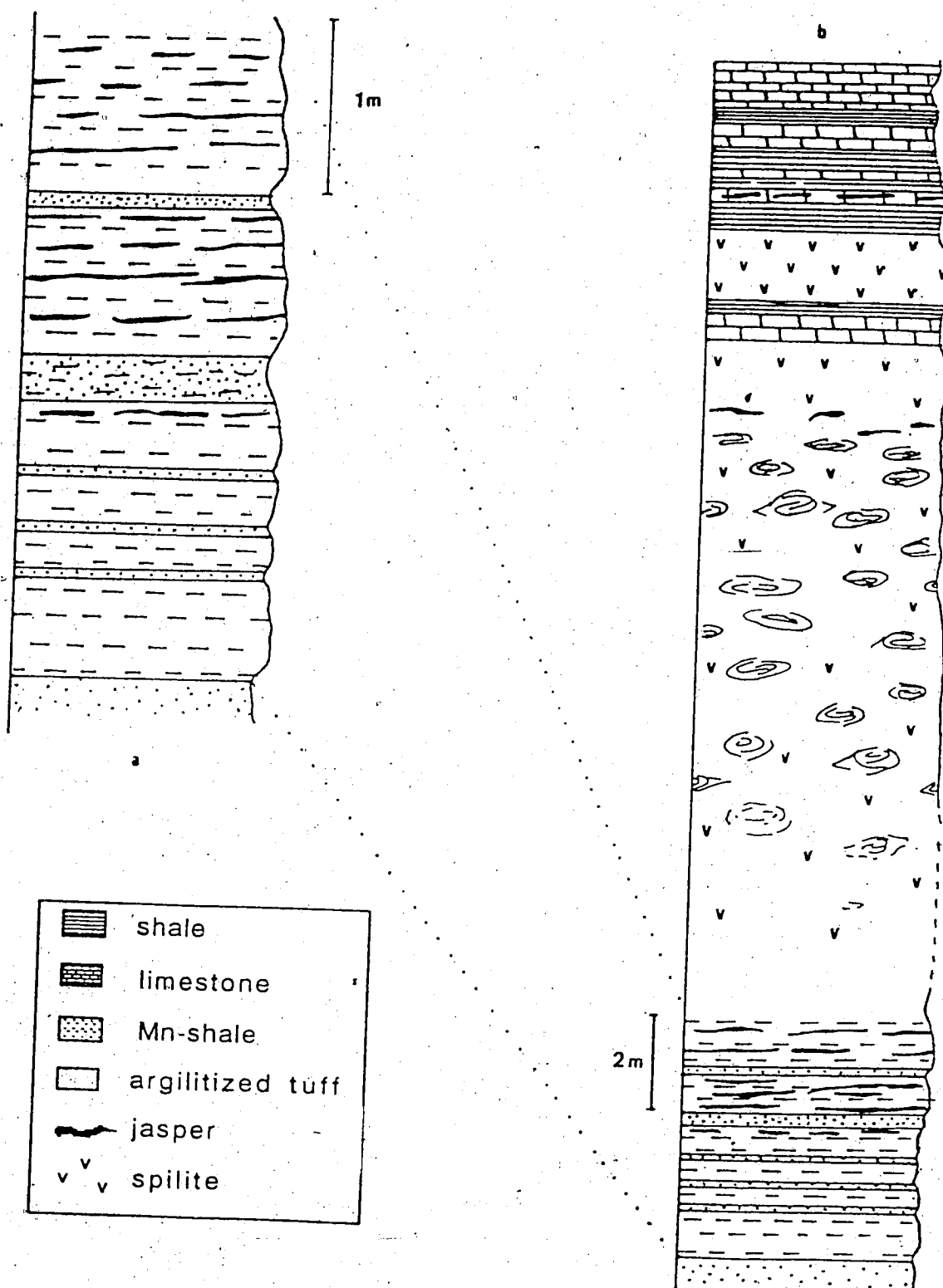
Figure III.4. (a) Stratiform Mn-Fe-rich beds comforming the Sapo Negro deposit. (b) Column observed at the Sapo Negro locality, with the iron formation at the bottom of the sequence.

The Ojo de Agua Mineral Occurrence

At this locality, barite and Fe-Mn oxides replace a biohermal mound of massive limestone. Barite laths occur disseminated and less frequently, concentrated along irregular zones. In some cases, fossils are replaced by barite and by recrystallized calcite. Hematite generally occurs along irregular veinlets containing ankerite-siderite and calcite associations. Mn oxides alter the rock mainly along irregular zones of the micritic matrix which hosts the fossils.

In contrast to the other areas, the alteration of the limestone is mild at Ojo de Agua. Although there are zones where hematite-silica veinlets are plentiful, no major occurrence of mineralization has been yet found. However, geophysical evidence indicates the presence of a magnetite body at depth.

D) Paragenetic Sequence

An idealized order of mineral deposition deduced for the Vulcano and Tabaquito replacement bodies is presented in figure III.5. Since both deposits display similar, common features, the observations made for both them have been integrated. The three stages portrayed in the diagram are based upon the relative time of formation with respect to the main ore.

Pre-ore Stage

Iron oxides and quartz were predominantly deposited in this stage. Minor amounts of barite-pyrite were also deposited; in fact, a few grains of pyrite occur dispersed in jasper-hematite. In a few cases the hematite exhibits colloform banding and is replaced by specular hematite and by granular magnetite. The hematite is altered to magnetite, which according to Ramdohr (1980) implies the transformation of hematite under higher temperature or under more reducing conditions. The magnetite bodies which underlie the replacement body at Vulcano, and the lateral iron-oxide zone of the same body and that of Tabaquito were formed during this stage.

Ore Stage

This stage witnessed the major deposition of barite-sphalerite. Barite was commonly deposited intergrown with sphalerite. They may alternate in bands suggesting, likewise, alternating deposition. These minerals represent, apparently, coeval assemblages for no replacement among them was clearly observed. Sphalerite and galena-chalcopyrite are extremely rare associations, however sphalerite seems to have formed after the other two for it encloses

	Pre-ore stage	Ore stage	Post-ore stage
jasper	— — — —	— — —	—
hematite	——	— —	
magnetite	——	— — —	—
barite	— —	——————	—
pyrite	—	— — —	
sphalerite	—	—	—
galena		—	
chalcopyrite		—	
tetrahedrite		—	
proustite		—	
quartz	—— —	— —	
calcite		— —	

Figure III.5. Paragenetic sequence of the Vulcano and Tabaquito orebodies.

them both. Finally, there was a late stage of chalcopyrite deposition where it replaces sphalerite along cleavage planes and irregular zones.

Barite-sulfide mineral deposition during this stage may account for more than 90 % of the sulfide mineralization.

Post-ore Stage

Hematite, barite, sphalerite, quartz, and pyrite were deposited during this stage. The occurrence of the minerals of this stage is far more restricted. They were deposited along veins and veinlets, and coarse-grained crystals were formed (barite up to 5 cm long; sphalerite up to 1 cm across). B and sphalerite of this stage affected not just the replacement body, but the pyritic body of Vulcano as well. This seems to indicate that the pyritic body was formed coeval to the replacement body.

Quartz-pyrite veins affected the lower part of the replacement body at Vulcano. Here a clear replacement of the ore-stage barite-sulfides association took place. In Tabaquito the ore stage assemblage was affected along irregular zones by euhedral-subhedral, saccharoidal quartz.

It is impossible to discern the span of time which elapsed between depositional stages. Nonetheless, all the stages appear to represent a more or less continuous spectrum of mineral depositon under variable oxidizing conditions: oxidizing conditions prevailing at the beginning and reducing conditions later. This depositional sequence will be addresed in a subsequent section.

E) Hydrothermal Alteration

Hydrothermal alteration at La Minita is intense. It is however restricted to the the lower unit and most of the middle unit. The mineralogy of the alteration will be described only for the volcanic rocks, which show the greatest modification of their original mineralogy. The carbonate rocks have been thoroughly mineralized and/or recrystallized, with minor formation of dolomite and siderite as alteration products.

Alteration Exhibited by Andesites-Basalts

This alteration has been already commented upon, and generalized as spilitization. In all respects, the spilitization of the andesites and basalts corresponds to a propylitic alteration. Chlorite (penninite) + epidote + tremolite-actinolite + calcite + hematite form the main mineral association. Minor clinozoisite + zeolite + melilite is recognized in the basaltic members.

The origin of propylitic associations has been demonstrably ascribed to addition of CO_2 to basaltic rocks (Rose and Burt, 1979; Gilbert and Park, 1986). Though epidote and calcite may exist under a wide range of CO_2 pressures, the presence of zeolite and clinozoisite is indicative of a more restricted range. The zeolite-clinozoisite association stability field has been determined at CO_2 pressures < 0.01-0.03 % (Kerrick, 1974; Thompson, 1971).

Alteration of Felsic Members

The more felsic rocks exhibit an alteration assemblage consisting of sericite + quartz + chlorite + barite. Minor phases include K-feldspar (adularia) and calcite. Sericite replaces not only sanidine phenocrists, but also

plagioclase and the matrix of the rocks as well. Quartz is the most widespread mineral of this alteration; it occurs as crypto-microcrystalline aggregates in association with sericite or individually in the matrix of the rock and veinlets. Chlorite occurs in the originally vitric matrix of some of the rocks, as altered glass shards and as flakes along concentric, perlitic cracks. Barite occurs as crystal laths which replace the matrix of the rock, and may contain inclusions of quartz and chlorite. Secondary K-feldspar is very rarely seen; it may be found near sericitized sanidine as a clear, inclusion-free, subhedral mineral. Calcite is found along veinlets in some rocks.

This alteration association is suggestive of hydrolysis-type reactions (Rose and Burt, 1979). The presence of secondary K-feldspar points to an increase in the a_{K^+}/a_{H^+} ratio and/or in the temperature. The calculated a_{K^+}/a_{H^+} for the range 600° to < 100°C is 10^2 - 10^5 (Montoya and Hemley, 1975). This information points to a variable mobility of K^+ and H^+ which will be considered for thermochemical calculations in chapter V.

To conclude, the type of alteration developed was chiefly controlled by the chemistry of the rock, with some influence by the hydrothermal fluid and the thermodynamic environment. Propylitic alteration was developed in the mafic members, whilst sericitic alteration affected the more felsic units. These alteration types are compatible and represent similar ranges of temperature and pressure.

IV. FLUID INCLUSION INVESTIGATION

A) Background Information

Fluid inclusions represent fluids trapped in minerals during or subsequent to their crystallization. Thus these fluids may provide an insight into the properties of the parent fluid, and of late fluids. In the most general case, fluid inclusions provide information on the chemistry of the fluid, provided that it can be analysed. There are, however, some arguments against the validity of fluid inclusions as representative of ore solutions, since the very process of mineral formation impoverishes the solution in certain components. Nonetheless, fluid inclusions have been long used to give an estimate of the amount of dissolved material in ore solutions. Most fluid inclusions are saline brines ranging in NaCl content from 0.1 to 50 % (Roedder, 1984).

By far the most useful technique of fluid inclusion analysis, though difficult to properly apply, involves the determination of the volumetric properties of the fluid. Two of the main properties analyzed in this technique are: melting temperature (T_m) and homogenization temperature (T_h).

Melting Temperature.

Under cooling the fluid inclusions solidify. Warming causes melting of the ice at a specific temperature. This is known as the melting temperature. It can be used to calculate the amount of salts dissolved in the fluid, since depression of the melting temperature of ice is a function of its salinity.

41

The presence of ions other than Na^+ and Cl^- (e.g. K^+, Ca^+, Mg^{++}, etc) has been recognized. Nonetheless it has been proven that the properties of the brine are predicted within ± 1 % by a solution with an equivalent NaCl content (Potter *et al.*, 1978), at least for solutions with < 17 % wt NaCl. Fluid inclusions may contain, in addition, CO_2, N_2, hydrocarbons, and other gases, which complicate the behavior of the inclusion under cooling, and allowance for this must be made.

Homogenization Temperature.

Under favorable conditions, fluid inclusions nucleate a bubble during cooling, due to differences in thermal contraction between the fluid and the host mineral (Roedder, 1984)). Heating of the inclusion produces the reverse effect (vacuole disappearance); the temperature at which this phase change takes place is the temperature of homogenization. This temperature is considered to be the lower limit for the formation of the mineral. Decrepitation of the inclusion after continuous heating provides an upper temperature limit for formation/entrapment.

A series of assumptions, precisely stated and discussed by Roedder (1979), have to be made if fluid inclusion data are to be used in any thermochemical study. They are:

1.- The fluid trapped was a single, homogeneous phase.

2.- No volumetric changes have occurred after sealing of the cavity.

3.- The inclusions remain closed systems after sealing.

4.- The pressure of trapping is known or is insignificant.

5.- The origin of the inclusion is known.

Paragenesis of Fluid Inclusions and Their Recognition

Three types of inclusions may be recognized on the basis of their sequence of formation relative to the host mineral, namely *primary*, *secondary* and *pseudo-secondary*. Only primary and pseudo-secondary inclusions provide information on the nature of the parent fluid; secondary inclusions characterize late fluids.

Primary inclusions form with the mineral during its initial growth. They are generally relatively large and occur isolated or forming planar arrays along former crystal surfaces.

Secondary inclusions form during healing of post-crystallization fractures within the mineral. They occur as curved planar sets that cross-cut the crystal and transgress crystal boundaries.

Pseudosecondary inclusions represent an intermediate case between the former two. They originate by healing of fractures produced in the crystal before crystallization has been completed. They occur in similar way to secondaries, however do not cross beyond crystal boundaries and terminate sudenly within the crystal.

A comprehensive list of criteria for distinguishing between the three types of inclusions has been set forth by Roedder (1979).

B) Fluid Inclusions in Samples from La Minita

No appreciable difference was detected between fluid inclusions from Vulcano and Tabaquito, and thus their description will be done in unison. Only samples from the replacement bodies contained inclusions suitable for this study. Due to the presence of multiple generations of secondary fluid inclusions, only primary and pseudo-secondary inclusions were studied.

Barite, quartz, and sphalerite contained the best inclusions. In all cases the fluid inclusions consisted of one or two fluids, namely liquid and/or gas. The general situation is the coexistence of liquid and vapor in the same inclusion, with vapor content in the range from 5 to 20 % volume at room temperatures. No CO_2 was visually detected.

Barite.

This mineral contains by far the largest number of inclusions. However the great majority are secondary. In addition, evidence of dissolution, healing, and necking is extensive, thus making the study of inclusions in this mineral rather difficult. Nonetheless it was found that apparently well-preserved primary inclusions still occur.

Some of the primary inclusions are vapor rich. Additionally, variable filling ratios (i.e. volume of gas/total volume) are commonplace. This may constitute evidence of trapping of a non-homogeneous fluid, for leaking or any other secondary process was disregarded as the cause of such a feature.

Quartz

Quartz was found to be a very useful because discrimination between

primary and secondary inclusions was much more simple than for barite. Healing and necking-down appeared negligible in this mineral. The vast majority of primary inclusions occur in the central part of the crystals and have similar filling ratios. Only one sample (#85) was found to contain primary-pseudosecondary fluid inclusions with a variable gas content of up to 80 % volume. As it is the case with some samples of barite, this quartz sample must have trapped a heterogeneous fluid.

Sphalerite

Due to the low transparency of most sphalerites, only few grains were suitable for study. This problem is particularly important in sphalerites of the ore stage, which are generally affected by alteration to chalcopyrite. A more limited number of inclusions are present in this mineral and many of them show evidence of necking; thus, the proportion of primary-pseudosecondary inclusions is rather small. Sphalerite from the post-ore stage was more adequate for the study, and appears to characterize the fluid of this depositonal stage quite well.

On the whole, despite the fact that fluid inclusions in barite, quartz, and sphalerite from two depositional stages were studied, mostly simple liquid-vapor compose all of the primary-pseudosecondary inclusions. In addition, some inclusions in barite and quartz contain a large proportion of gas, which cannot be ascribed to leaking but rather to trapping of a heterogeneous fluid.

C) Fluid Inclusion Geothermometry

Method and Results

Twenty samples were selected but only fourteen were suitable for the study. Rock slabs 1 mm thick or less were polished on both sides. After petrographic description and identification of suitable inclusions, crushing was performed followed by thermometric determinations.

Thermometric measurement were performed on a CHAIXMECA VT2-120 heating-cooling stage. Heating is produced by a resistance heater within the stage. Cooling is accomplished by circulating nitrogen-cooled nitrogen gas through the sample stage. The stage was calibrated using the melting points of solid compounds, and it was found that the accuracy varied between ±1°C over the range from 0 - 300°C. Repeat runs were performed in the same inclusion which gave reproducibilities of ± 1°C. Calibration of the stage at temperatures below 0°C was not performed. Instead, the calibration by Fluet (1986) on the same stage was adopted. At temperatures below zero degrees the correction is ~0.6°C; this has been applied to the appropriate data in table I.

Only primary and pseudosecondary inclusions were chosen for analysis. Additionally, in order to avoid study of fluids originally heterogeneous during trapping, only those inclusions which showed similar filling ratios in the same grain were selected. Thus, hereafter the term "fluid inclusion" will imply a primary-pseudosecondary inclusion, unless otherwise noted.

TABLE I. SUMMARY OF FLUID INCLUSION DATA

SAMPLE	SIZE (μm)	% VAPOR	Th °C +	Tm °C +	% NaCl +
11C					
QUARTZ (P)	13 - 5	8	145 - 178.5	- - - - - - - - - -	- - - - - - - - - -
			159.1 (13)		
11H					
BARITE * (O)	28 - 13	15 - 8	140 - 257	-7.8 -2.3	11.5 - 3.8
			215 (8)	-6.4 (7)	9.7
BARITE (O)	20 -10	15 - 10	160 - 203	-8.7 -2.8	12.5 - 4.6
			192 (13)	-6.4 (9)	9.7
QUARTZ (O)	41 - 9	10 - 6	139 - 276	-7.4 -2.2	11.0 - 3.7
			183 (53)	-3.2 (18)	5.2
SPHALERITE (P)	22 - 13	20	135-149	-1.4 0	2.4 - 0
			142.6 (20)	-0.7 (20)	1.2
11I					
BARITE (O)	30 - 9	10 - 8	205 - 212	- - - - - - - - - -	- - - - - - - - - -
			209 (3)		
32C					
BARITE (O)	15 - 10	10	160 - 229	-3.9 -3.4	6.3 - 5.5
			196 (21)	-3.6 (13)	5.8
T-11-7					
QUARTZ (P)	12 - 7	5	138 - 177	- - - - - - - - - -	- - - - - - - - - -
			163.9 (8)		
DD-31-1					
QUARTZ (O)	11 - 7	8	154 - 239	- - - - - - - - - -	- - - - - - - - - -
			212.5 (5)		
DD-31-6					
BARITE * (O)	19 - 6	10 - 5	204 - 278	-6.4 -3.4	9.7 - 4.0
			254 (7)	-4.8 (5)	7.6
BARITE (O)	25 - 10	15 - 8	171 - 309	-3.2 -2.4	5.2 - 4.0
			229 (25)	-2.8 (2)	4.6
QUARTZ (O)	26 - 7	8 - 4	166 - 202	- - - - - - - - - -	- - - - - - - - - -
			187 (10)		
DD-33-7					
BARITE (O)	20 - 9	5 - 8	179 - 294	-4.8 -1.4	7.6 - 2.4
			224.9 (4)	-3.2 (4)	5.2
QUARTZ (O)	16 - 8	5	159 - 204	-5.3	8.3
			184.8 (8)		
SPHALERITE (O)	28 - 11	10	164 - 193	-4.2 -3.6	6.7 - 5.8
			181.4	-3.8 (3)	6.1

58D					
SPHALERITE (P)	20 - 15	15	93 - 149.4	-0.9 0	1.6 - 0
			124 (19)	-0.3 (6)	0.5
71					
BARITE (P)	10 - 6	10 -	96 - 155	- - - - - -	- - - - - - -
			(12)		
71A					
BARITE * (O)	15 - 12 +	15 - 5	139.5 - 300	-8.9	12.8 - 2.1
			243.6 (12)	-5.6 (5)	8.7
75B					
BARITE (O)	19 - 10	8	150 - 229	- - - - - - -	- - - - - - -
			190.6 (20)		
85					
QUARTZ (P)	26 - 7	10	140 - 219	-4.4 -1.4	7.0 - 2.4
			178.4 (21)	-3.8 (9)	6.1
DD-113-2					
BARITE (P)	38 - 15	5	122 - 212	- - - - - - -	- - - - - - -
			154.6 (13)		
(O) Ore stage					
(P) Post-ore stage					
* CO2-bearing inclusions					
+ Range and average of values					
( ) Number of inclusions					

Crushing

Crushing experiments revealed the presence of a compressed uncondensable phase in some inclusions. This phase occurs in some samples of ore stage barite (11H, 31-6, 71A) and quartz (11H). It appeared that barite contained a larger proportion of this phase in comparison with quartz. Inclusions of this type in barite expanded up to 100 times the initial volume after fracturing of the mineral. It is suspected that CO_2 forms the uncondensable phase; since no liquid CO_2 occurs, the vapor pressure of this gas must be well below 63 atmospheres (Roedder, 1971).

The fact that inclusions which contain such a noncondensable phase did not freeze completely above -58 to -60°C during freezing experiments (the other inclusions normally being frozen at -40°C), also suggests the presence of CO_2. However, no reorganization of the inclusion was observed during warming at the T_m of CO_2 (-56.6°C).

Another gas detected in the barite is H_2S. This was only found out in post-ore stage barite (113-2) by means of its characteristic odor upon crushing.

Freezing experiments

It was found that inclusions > 10 µm produced an identifiable phase change during cooling. The inclusions were initially rapidly cooled until they appeared totally frozen. Subsequent heating was effected by warming the inclusion at 0.3 to 0.5 °C/minute, within 10°C of the melting point, until all solids had melted.

The T_m has been used to to calculate the salinity of the fluid. It is known that the degree of freezing point depression is a function of the salinity.

The equation advanced by Potter *et al.* (1974) relates salinity and T_m as follows :

$$NaCl\ wt\%\ equivalent = 1.76958T_m - 4.2384 \times 10^{-2}T_m^2 + 5.2778 \times 10^{-4}T_m^3\ (\pm 0.028)$$

Neither hydrohalite nor gas hydrates were detected. Presence of these solids would make the application of the former equation invalid. Thus it is considered that T_m yields an accurate estimate of the fluid salinity. Table I contains the NaCl wt% equivalent calculated for several samples. It should be noted that samples with suspected CO_2 contents have the lower T_m and thus yield the higher apparent salinities.

The presence of solutes in a brine have an additive effect on the degree of depression of the freezing point (Roedder, 1984). Thus the occurrence of CO_2 must provide some contribution to T_m. Inclusions with a CO_2 content of up to 1 wt% produce a depression in T_m of -0.6°C (Higgins, 1980). On the other hand, inclusions which contain liquid CO_2 at room temperatures may contain up to 7.6 wt% CO_2; this amount of CO_2 can account for a -3.6°C depresion of T_m.

The samples from La Minita do not contain liquid CO_2. The actual amount of this gas was not possible to determine, and an arbitrary 1wt% will be asumed[5]. A proper correction to allow for the presence of this gas has been applied to the CO_2-bearing inclusion data in table I.

Figure IV.1 presents an histogram of all T_m from ore and post-ore stage fluid inclusions. A distinct distribution for T_m from each stage is clearly delineated. Ore stage inclusions have T_m between -8.9 and -1.2°C with -4.4°C

---

[5] In fact, 1 wt% would represent a rather high upper limit, because, as noted in the alteration section, the propylitic alteration constrains the CO_2 content of the fluid to 0.01-0.03 wt%.
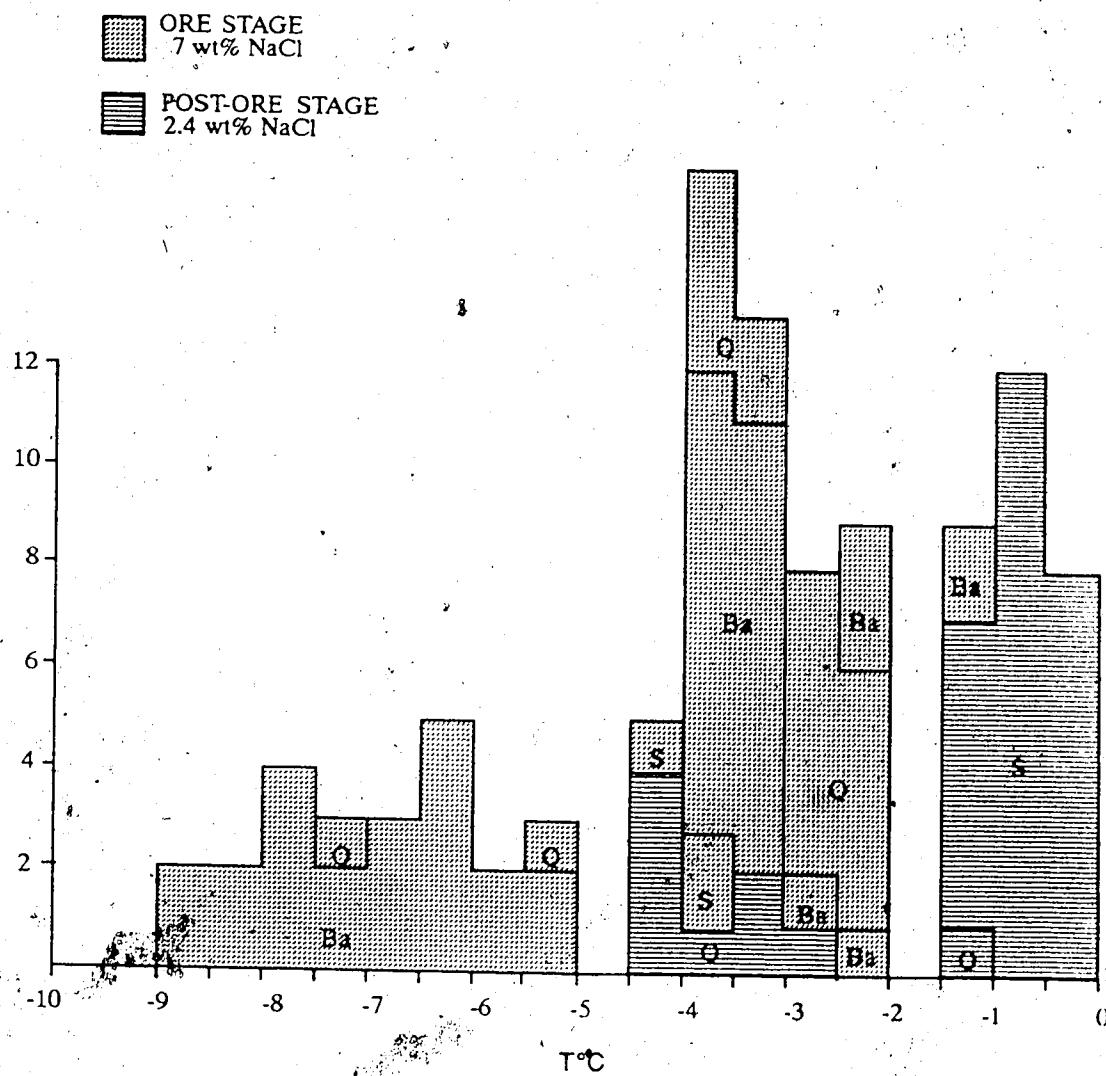
Figure IV.1. Melting temperatures of ore and post-ore stage inclusions in barite (Ba), quartz (Q), and sphalerite (S) from Vulcano and Tabaquito.

in average, which corresponds to 12.8, 2.1, and 7.8 wt% NaCl respectively. In more detail, although not shown in this figure, CO_2-bearing inclusions have an average T_m of -6°C and salinity of 9.2 wt% NaCl, whilst the rest of the ore stage inclusions yield an average salinity of 6.2 wt% NaCl. Post-ore stage inclusions have lower salinities in the range from 0 to 7 wt% NaCl with an average of 2.4 wt% NaCl.

To conclude, the ore stage fluids were clearly saline (~6.2 wt% NaCl), with the CO_2-bearing fluids being the most saline ones (~9.2 wt% NaCl). The post-ore stage fluids were considerably more dilute (~2.4 wt% NaCl).

Heating experiments

Many more T_h data than T_m data were obtained. This is because homogenization of the inclusion upon heating was easier to observe and inclusions as small as 5 μm could be studied. The summary of T_h data is presented in table I and the respective histograms in figure IV.2 and IV.3. These data are not corrected for pressure.

The histogram of figure IV.2. shows the T_h data for ore and post-ore stage barites. It can be seen that ore stage barite exhibits two populations with peak values at 255°C and 205°C. Although petrographically it was impossible to tell these populations apart, the diagram strongly suggests two ranges of temperatures of trapping. The high temperature population is characterized by a consistent concentration of data from CO_2-bearing inclusions. If these inclusions only are considered, an average T_h of 240°C is obtained. The principal trapping event took place in the range of 220 to 160 °C with an average T_h of 205°C. The post-ore stage barite has a rather low average T_h of 140°C.

The T_h distribution of both ore and post-ore stage quartz and sphalerite
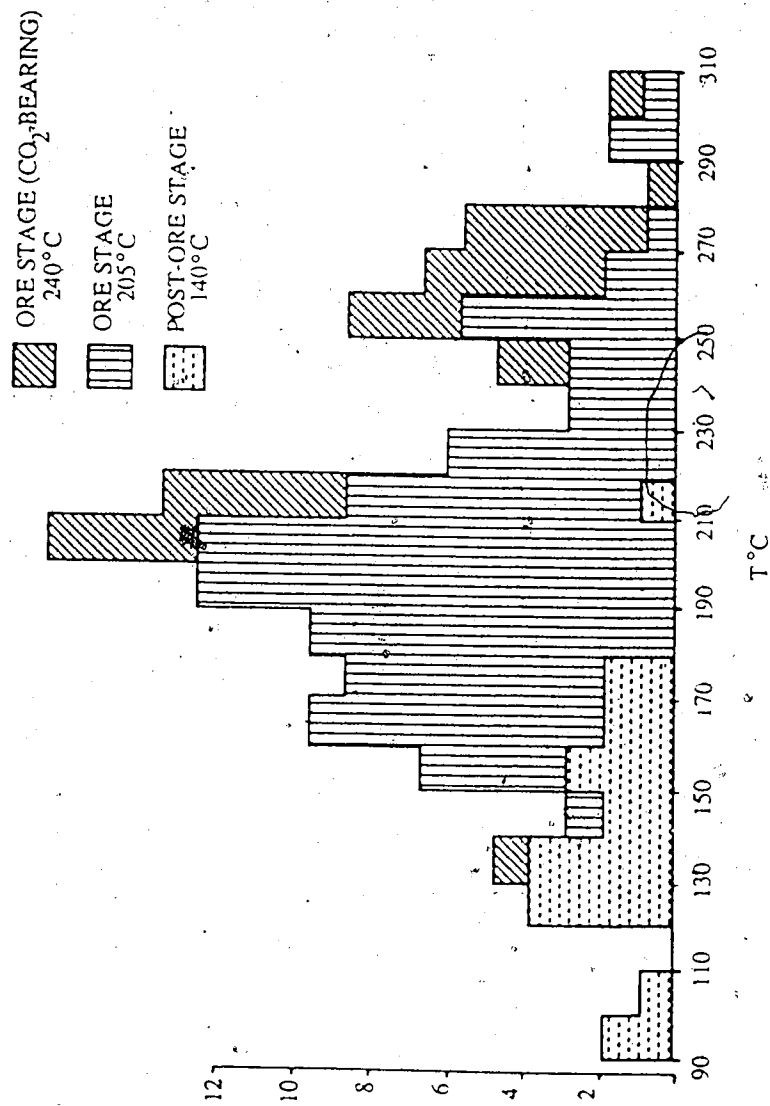
Figure IV.2. Homogenization temperatures of inclusions in barites from Vulcano and Tabaquito

C) Stable Isotope Geothermometry

Fractionation of O and S isotopes has been frequently used for determinations of the temperature of formation of ore deposits. This is because of the common occurrence of oxide- and sulfide-minerals in these environments. Additionally, these types of minerals furnish the best geothermometers, since the fractionation factor between some mineral pairs is highly sensitive to temperature, the fractionation of oxygen and sulfur isotopes in nature is large in comparison to the analytical error, and the modification of their initial isotope composition is negligible in low temperature environments (O'Neil, 1987; Longstaffe, 1987).

Nonetheless, the application of stable isotopes presents two major limitations. Firstly, attainment of equilibrium is one of the most important conditions for the valid application of isotopic geothermometric methods. For instance, at 200°C, complete oxygen isotope exchange between quartz and water produces an ^{18}O enrichment in the mineral of 12 %o In contrast, if say only 90% exchange occurs ^{18}O enrichment will only be 11.25 %o, and the calculated temperature 230°C. Thus an error of 30°C is involved in the inferred temperature. Secondly, experimental difficulties have resulted in disagreement among the fundamental fractionation factors obtained in different laboratories utilizing different techniques. This results in different calculated temperatures, depending upon the fractionation factor chosen. Even so, bearing these limitations in mind, valuable geologic information may still be obtained.

Oxygen Isotope Geothermometer

Table V shows the temperatures calculated with the oxygen isotope

TABLE V. OXYGEN ISOTOPE TEMPERATURES

SAMPLE	LOCALITY	MINERAL	∂18O	Δ∂18O	TEMPERATURE
DD 31-9 (PR)	VULCANO	MAGNETITE	5.8		
		CALCITE	18.4	12.6	327±10
DD 31-7 (PR)	"	MAGNETITE	1.3		
		CALCITE	19.1	17.8	226±5
FO 74 (O)	"	MAGNETITE	-1.3		
		BARITE	12	13.3	241±7
FO 78D (PR)	"	MAGNETITE	8.3		
		QUARTZ	16.2	7.9	526±20
FO 78C (PR)	"	MAGNETITE	3.1		
		BARITE	10.5	7.4	365±15
DD 92-1 (PR)	"	MAGNETITE	6		234±5
		QUARTZ	25	19	233 **
FO 85 (P)		MAGNETITE	-0.6		
		QUARTZ	27.8	28.4	100°
		CALCITE	22.9	27.1	100°
FO 19 (O)	TABAQUITO	MAGNETITE	-1.6		271±7
		QUARTZ	15	16.6	272 **
FO 27 (O)	"	MAGNETITE	-4.2		224±5
		QUARTZ	15.6	19.8	233 **
FO 35 (O)	"	MAGNETITE	5.9	4.6	489±44
		BARITE	10.5		
Notes:					
(PR) pre-ore stage, (O) ore stage, (P) post-ore stage					
* magnetite-water fractionation curve of Becker (1971)					
** magnetite-water fractionation of Blatner et al. (1983)					

Temperature Equations:
quartz-magnetite

$$T(°K) = 2.19 \times 10^3/(\Delta-0.39)^{0.5}$$

calcite-magnetite

$$T(°K) = 2.06 \times 10^3/(\Delta-0.81)^{0.5}$$

barite-magnetite

$$T(°K) = 2.12 \times 10^3/(\Delta-3.60)^{0.5}$$

equations obtained from magnetite-water fractionation (500-800°C) of Bottinga and Javoy (1973) and Javoy (1977); quartz-water fractionation (250-500°C) of Matsuhisa et al. (1979); barite-water fractionation (110-350°C) of Kusakabe and Robinson (1977); calcite-water fractionation (0-500°C) of O'Neil et al. (1969).

values of mineral pairs from Vulcano and Tabaquito. Only, those pairs involving apparently coeval minerals have been included. Equations for calculating the temperatures of mineral pairs were derived by combining the proper mineral-water fractionation equations. These temperature equations are listed at the bottom of the table. In addition, the error in the calculated temperature is included; this corresponds to the analytical error and to the error in the equation of fractionation. In the case of magnetite-mineral pairs the error contributed by the magnetite-water fractionation curve at $T < 500°C$ is unknown; thus the calculated temperature error is smaller than the actual error.

Magnetite-quartz and magnetite-calcite afford the most sensitive geothermometers. It appears that the precision in the calculated temperatures is drastically reduced below 200°C, due to the presence of a minimum in the magnetite-water fractionation and of a cross-over in the same pair and in the calcite-water pair (Blatner *et al.*, 1983; O'Neil *et al.*, 1969). Application of the magnetite-quartz geothermometer to low temperature assemblages has been a major problem, as noted in investigations of iron formations (Perry *et al.*, 1973; Blatner *et al.*, 1983; Hoefs *et al.*, 1987). This limitation has to do with the slow rate of isotopic exchange and the consequent uncertainty in the experimental fractionation factor.

As commented upon in the paragenetic discussion, at Vulcano and Tabaquito, oxide mineralization was dominant during the pre-ore stage. The pre-ore stage samples from these localities yielded oxygen isotope temperatures above 200°C, in the range from 226 to 526°C. Samples 35, 78C and 78D yielded the highest temperatures, and seem to represent disequilibrium associations. Nevertheless, combination of $\delta^{18}O$ of barite

from sample 78C with that of quartz from sample 78D yields T=270°C, which is similar to those temperatures calculated using other mineral pairs. Although the barite and quartz do not occur in contact, they are closely located and belong to the pre-ore stage; thus, they might have been deposited in equilibrium with a similar parent fluid.

Samples 31-7 and 31-9 are petrographically almost identical and come from the same drill-core (20m of separation). In these samples introduction of fine-grained magnetite into the limestone was accompanied by recrystallization of the carbonate. However their calculated temperatures (226 and 327°C respectively) differ by over 100 °C. Thus it appears that equilibrium was not attained and/or that these samples were actually formed at different temperatures.

On the other hand, samples 19 and 27 are also closely located to each appear to have formed under rather similar conditions. These sample consist of a saccharoidal mixture of quartz and magnetite which replaced a fossiliferous limestone. Quartz generally replaced the fossils, whilst magnetite replaced the enclosing matrix. The temperatures calculated for these samples are somewhat different (224 and 272°C). Probably they represent near-equilibrium associations.

Sample 92-1 shows an early episode of colloform hematite deposition. This was followed by magnetite-quartz replacement of the hematite; the magnetite-quartz association seems to be compatible since no mutual replacement is displayed. Additionally, the temperature yielded by this pair is similar to that of other pre-ore stage pairs (239°C), which may again represent near equilibrium conditions.

The magnetite-quartz of sample #85, a post-ore example, gives an isotopic temperature of ~100°C. Although this temperature is ~70°C lower

than the average of T_h of fluid inclusions from the same quartz sample, it suggests a waning of the thermal event during the post-ore stage. Even more, the fact that the temperature calculated using the calcite-magnetite pair is almost identical to the quartz-magnetite temperature suggests near-equilibrium for those two pairs. Calculation of these temperatures was performed by combining the magnetite-water curve of Becker (1971) with the proper equations for quartz-water and calcite-water referred to in table V. Becker's curve seems to be more adequate at temperatures below 175°C than Blatner's (Blatner *et al.*, 1983) which, for sample #85, yields worse results (i.e. rather low temperature). Thus it appears that Blatner's curve is more useful in the range 175 to 300°C, where the minimum in the magnetite-water fractionation occurs.

In conclusion, despite the large error produced both by experimental uncertainty and by questionable degrees of oxygen-isotope equilibration in La Minita's samples, an apparent temperature range is inferred. Pre-ore stage deposition possibly took place at temperatures in the range from 327 to 224°C; thus some degree of temperature-overlap between the pre-ore and the ore stage occurred. Probably this supports the idea of a continuous mineral deposition from stage to stage. Post-ore stage isotopic temperatures are below the average of fluid inclusion temperatures. This reflects the more difficult approach to equilibrium at low temperatures.

Sulfur Isotope Geothermometer

Barite-sphalerite is the most common ore-stage mineral association at La Minita. Pyrite and sphalerite coexist rarely and the coexistence of these sulfides with galena is even more rare. Table VI summarizes the $\Delta \delta^{34}S$ values and the apparent temperatures calculated for different ore stage

TABLE VI. SULFUR ISOTOPE TEMPERATURE CALCULATED FOR MINERAL PAIRS
FROM VULCANO AND TABAQUITO

SAMPLE	LOCALITY	MINERAL PAIR	Δ∂	T °C
11D	TABAQUITO	barite-sphalerite	14.3	470±36
11F	"	"	15.3	445±33
11G	"	"	14.5	465±35
58B	VULCANO	"	13.8	483±38
67C	"	"	12.9	509±42
73	"	"	11.3	563±51
75B	"	"	12.9	509±42
77A	"	"	12.5	522±44
78C	"	barite-chalcopyrite	15	463±31
33-3	"	barite-sphalerite	29.1	200±8
33-5	"	"	26.8	225±9
33-7	"	"	15.5	441±31
33-3	"	barite-pyrite	29.4	173±6
33-5	"	"	23.3	245±9
33-5	"	pyrite-sphalerite	3.4	25±31
80H	"		2.1	106±49

Temperature equations:

barite-sphalerite $\quad T(°K) = [7.9 \pm 0.05 \times 10^6/(\Delta \pm 1)]^{1/2}$ $\quad$ T > 400°C

$\quad T(°K) = [5.16 \pm 0.05 \times 10^6/(\Delta - 6 \pm 0.5)]^{1/2}$ T < 400°C

barite-pyrite $\quad T(°K) = 2.16 \times 10^3/(\Delta - 6 \pm 0.5)^{1/2}$ $\quad$ T < 350°C

barite-chalcopyrite $\quad T(°K) = 2.85 \times 10^3/(\Delta \pm 1)^{1/2}$ $\quad$ T > 400°C

pyrite-sphalerite $\quad T(°K) = 0.55 \pm 0.04 \times 10^3/\Delta^{1/2}$

obtained from the summary of Ohmoto and Rye (1979)

mineral pairs, according to the summary of Ohmoto and Rye (1979). The calculated temperatures in excess of 400°C (in almost all pairs) are unrealistically high for the mineralization temperatures at La Minita. T_h of fluid inclusions in barite gave average temperatures from 240 to 180°C. Only the barite-sphalerite and barite-pyrite pairs of samples 33-3 and 33-5 produce similar temperatures (~173°C - 245°C). In contrast, two pyrite-sphalerite pairs, including one from sample 33-5 gave isotopic temperatures that are too low. Thus, the sulfur-bearing minerals generally do not appear to have been formed in isotopic equilibrium.

It is well known that sulfate-sulfide associations generally do not reach equilibrium at temperatures below 300°C (Ohmoto and Rye, 1979; Zhang,1986; Ohmoto, 1986.). Ohmoto and Lasaga (1982) have shown that at high temperature and low pH, 90 % equilibration between aqueous sulfates and sulfides is reached in a matter of hours. However, at low temperatures (<150°C) and an alkaline pH (~9) equilibration would not be attained even for sulfate-sulfide mineral pairs of the oldest terrestrial rock. Similarly, the source of $SO_4^=$ and H_2S may influence the attainment of equilibrium i.e. $SO_4^=$ and H_2S which are delivered to the mineralizing site by discrete solutions would not produce mineral associations in isotopic equilibrium.

The coexistence of successively deposited ore stage minerals has been already commented upon. It becomes clear, then, that paragenetically late and early-mineral associations result in an apparently isotopically disequilibrated association. However, it does seem that localized near-equilibrium conditions were actually attained in the replacement body at Vulcano. This is deduced from barite-sphalerite and barite-pyrite mineral pairs of samples 33-3 and 33-5 (and from the negative $\delta^{34}S$ of pyrite of sample 33-2), whose isotopically calculated temperatures are in close

agreement with the range derived from T_h of fluid inclusions. The fact that the pyrite-sphalerite pair of these samples is of no use as a geothermometer must be due to incomplete equilibration, to subsequent modification of the isotopic composition, and to its low sensitivity (i.e. for small changes in $\Delta\delta^{34}S$, large temperature changes are derived). In the subsequent sections it will be assumed that fractionation factors between the barite-sphalerite pair and the barite-pyrite pair of these two samples may indicate equilibrium conditions.

To summarize, since La Minita's deposits were formed at low temperature, the stable isotope geothermometers are of limited reliability. It is apparent that the oxygen isotope geothermometer may provide more reasonable temperatures. The sulfur isotope geothermometer, on the other hand, is generally of little use, for the largest isotopic fractionation occurs between mineral pairs (sulfates-sulfides) which rarely form equilibrium associations.

D) Stable Isotope Petrogenesis

In this section a characterization of the sources of carbon and sulfur, of the hydrothermal environment, and of the ore fluid is pursued. Thus isotopic data will now be combined with geologic information. Since limestone is the host lithology of the replacement bodies, this discussion commences with a consideration of C and O of the carbonates.

Source of Carbon

Carbonates of marine origin have a restricted $\delta^{13}C$ - $\delta^{18}O$ range of

values. Keith and Weber (1964) obtained a $\delta^{13}C$ average of -0.13±2.61 ‰ and $\delta^{18}O$ of 25±3.7 ‰ for marine limestone. In figure V.2, the isotopic abundances of carbon and oxygen of La Minita's samples is compared with the marine limestone field of Keith and Weber (*ibid*). It is obvious from the diagram that the carbon isotopic composition of La Minita's samples is identical to that of the marine limestone; however, the oxygen isotopic composition is shifted towards lower values. This shift is more apparent in the recrystallized samples, although there are few data to make a generalization out of this behavior.

According to Ohmoto and Rye (1979) there are three principal sources of carbon in hydrothermal systems, namely an igneous source, organic matter, and limestone. The $\delta^{13}C$ of the first source may vary between a wide range of positive and negative values. Nonetheless, is likely that mantle-derived carbon has a narrower range of -5±ʒ as determined for carbonatites (Denis and Gold, 1973). Igneous rocks derived from melting of crustal material may have a wide range of $\delta^{13}C$ variation of reduced and oxidized components; however, the average value could lie close to -5 ‰ (Ohmoto and Rye, 1979). Nonetheless, the $\delta^{13}C$ of CO_2 contributed to the hydrothermal system by an igneous source is determined by the temperature, by the $\delta^{13}C$ of the source, and by the CO_2/CH_4 ratio. Thus carbonates could aquire a variable amounts of ^{13}C.

Organic carbon is characterized by large negative $\delta^{13}C$ values, due to the predominance of reduced carbon species. CO_2 derived from this source will acquire values < -10 ‰ in hydrothermal systems (Ohmoto and Rye, 1979); thus carbonates exhibiting ^{13}C-depletion will be produced in these systems.

Limestone-derived CO_2 generates solutions with $\delta^{13}C_{CO2}$ of ~ 0 ‰

Figure V.2. Carbon and oxygen isotope compositions of La Minita's fresh and altered limestone. The square represents the marine limestone field of Keith and Weber (1964). All the samples plot near this field, although the altered limestone tends to be shifted towards lower $\delta^{18}O$ values.
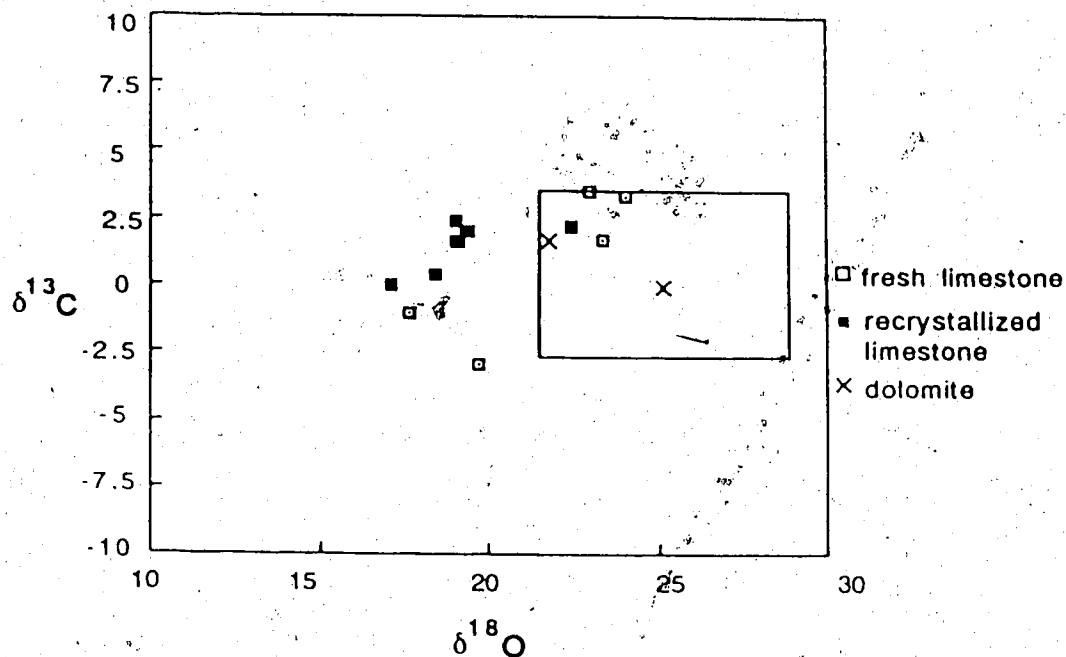
during dissolution reactions, while decarbonation reactions may produce ^{13}C-enriched solutions.

On the basis of the previous information, it is clear that the $\delta^{13}C$ composition of the recrystallized carbonates of La Minita is compatible with local derivation of the carbon, from the host limestone itself. Neither magmatic nor organic carbon appears to have been contributed to the system, especially organically derived carbon which would have produced negative $\delta^{13}C$ values in the carbonates. Production of ^{13}C-depleted carbonates by bacterially released CO_2 has been documented elsewhere (Keith and Weber, 1964; Ross and Oana, 1961). This is of relevance in the case of the La Minita mineralization. Organic processes were apparently not involved during the mineralizing events. This statement sets the background for the discussion of the origin of the sulfur in these deposits.

Source of Sulfur

Although a mineralized body may inherit the $\delta^{34}S$ of its sulfur-source, its final $\delta^{34}S$ is usually different from that of its provenance. This is mainly due to the influence of the physico-chemical environment upon the concentration of various sulfur species and upon the isotopic partitioning among them. Depending upon the degree of equilibration, the $\delta^{34}S$ of the sulfur-bearing minerals will thus reflect both the provenance of the sulfur and the environment of deposition.

An evaluation of the variables affecting the $\delta^{34}S$ values of barite and of sulfides sheds some light upon the origin of the mineralization at La Minita. Figure V.3 illustrates the behavior of the $\delta^{34}S$ of the barite-sphalerite pairs. Regardless of the mineralizing stage, barite exhibits a nearly constant $\delta^{34}S$, whilst the $\delta^{34}S$ of the sulfides ranges from +3.6 to
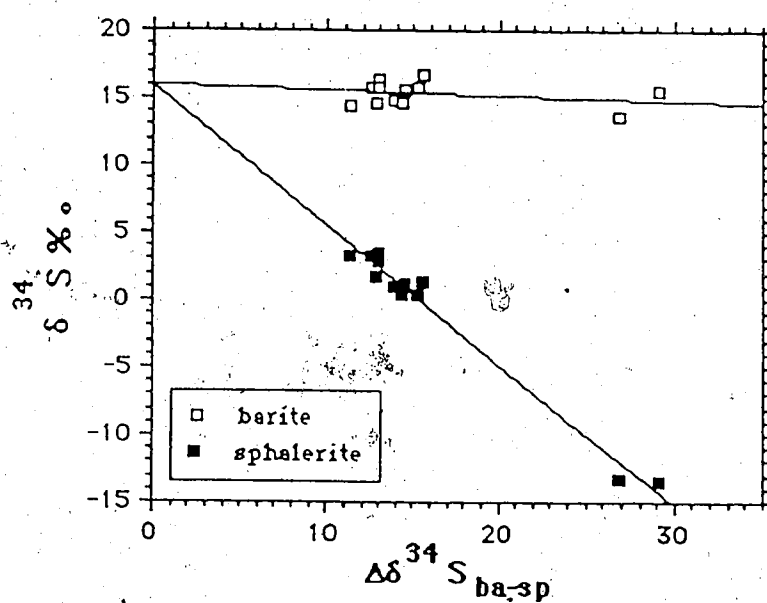
Figure V.3. Correlation between δ and $\Delta\delta^{34}S$ in barite and sphalerite from Vulcano and Tabaquito.

-13.5 ‰. The calculated curves that best fit the two sets of data points intersect the $\delta^{34}S$ axis at +15.8 ‰, which is very close to the average for barites. Although this diagram portrays an induced correlation between $\delta^{34}S$ of sulfates and sulfides, it is thus apparent that $SO_4^=$ must have constituted the dominant sulfur species in the hydrothermal system at La Minita. Shelton and Rye (1982) pointed out some of the ambiguities in interpreting the $\delta^{34}S$ versus $\Delta\delta^{34}S$ plot.

In the case of the dominant disequilibrium conditions at La Minita, the $\delta^{34}S$ of barite and of sulfides may be directly related to the source of sulfur. According to Ohmoto (1986), the $\delta^{34}S$ of minerals precipitating under disequilibrium conditions is very close to that of the $SO_4^=$ and H_2S of the ore solution and of the source region. For barite the average $\delta^{34}S$ is +15.4 ‰, which is whithin the accepted range of Cretaceous seawater sulfate (Nielsen, 1979; Claypool et al., 1980). Therefore, the marine origin of the barite's sulfate becomes self-evident. In the case of the majority of the sulfides from the replacement bodies at Vulcano and Tabaquito, the $\delta^{34}S$ values range from 0 to 3.6 ‰ with one value at +7 ‰. These values are suggestive of an igneous source and/or of inorganically-reduced sulphur by reaction of seawater sulfates with igneous rocks at 300 to 500°C (Ohmoto et al., 1976). The predominance of submarine-volcanic rocks at La Minita is compatible with either of these two sources. Such an interpretation has been generally applied to the classic Kuroko district mineralization and to the sulfide deposits of the East Pacific Rise (Ohmoto and Rye, 1979; Styrt et al., 1981).

Clearly, the previous conclusion does not explain the negative $\delta^{34}S$ of the pyritic body and of some sulfides at the center of the replacement body at Vulcano. This body of massive pyrite is characterized by $\delta^{34}S$ values

ranging from -10.5 to -2.6 ‰; the presence of coarse sphalerite (late stage) veinlets whose $\delta^{34}S = -4.7$ ‰ might indicate that heavier sulfur, from late fluids, interacted with the pyritic body. Bacterial reduction of marine sulfate in an open, system with an infinite supply of $SO_4^{=}$, could well explain such a negative range of values. Isotopic fractionation during bacterial reduction of marine sulfate may produce $\Delta_{H2S-SO4} \sim -25$ ‰, although in natural systems this value is frequently larger (Nielsen, 1979; Rye and Ohmoto, 1979). The maximum $\Delta_{pyrite-SO4}$ of the pyritic ore (assuming $SO_4^{=}$ of Cretaceous seawater ~16 ‰) is -26.5 ‰, which would be within the anticipated fractionation range produced by bacterial reduction. Coomer and Robinson (1976) have interpreted the sulfur isotope data of the Silvermines deposits, Ireland, (which exhibit a similar distribution to La Minita's sulfides) as indicative of both inorganically derived sulfur and sulfur derived from bacterial reduction. The same reasoning could be applied to the mineralization of La Minita, however it appears that the conditions required for bacterial reduction of marine sulfate were not met at the time of mineralization.

Although the $\Delta\delta^{34}S_{pyrite-seawater-SO4}$ of the pyritic ore falls between the fractionation range achieved by bacterial $SO_4^{=}$ reduction, the geological evidence does not support such a biologic reducing mechanism at La Minita. No organic-rich sediments deposited in an euxinic environment are directly associated with the mineralized horizon. The pyritic body is underlain by altered volcanics and limestone, is laterally bounded by the replacement body, and is covered by massive limestone. These lithologies are not particularly indicative of the possible preservation of organic matter, which would favor the development of bacterial activity in the depositional environment. Even more, the

oxidizing character of the environment has been already stressed, and additionally the carbon isotope information does not support the process of organic reduction at La Minita. This is in agreement with the presence of reefal colonies which would require of well-oxygenated enviroments in which organic compounds are not preserved. In the light of this evidence, a different source of sulfur must be sought.

The temporal and spatial relationships between the pyritic and the replacement bodies imply certain genetic relations. It is likely that the ore solutions which produced the replacement body had exhaled metals to the seafloor where the pyritic ore formed. The average $\delta^{34}S$ of this ore (-9.1 %o) and that of some pyrites of the replacement body (-12.6 %o in average) are notably similar. Thus, the possibility should be considered that the pyritic body was derived from exhalative ore solutions whose $\delta^{34}S_{H2S}$ was similar to that of the samples with negative $\delta^{34}S$ of the replacement body. Cooling of the ore solution would precipitate pyrite rapidly, as the fluid was exhaled onto the seafloor, such that little exchange between the sulfur of the ore solution and that of the seawater would occur. This could prevent a drastic increase of the $\delta^{34}S$ value of the exhaled pyrite. Modelling of the processes that occur during mixing of hydrothermal solutions with sea water has shown that mixture of 90 % hydrothermal fluid with 10 % seawater can produce nearly complete sulfide deposition (Drummond and Ohmoto, 1980); thus the isotopic composition of the sulfides cannot be largely modified during the mixing process. Framboidal pyrite comprising the pyritic ore suggests the process of rapid deposition.

Hydrothermal Environment

In order to illustrate how the ^{34}S-depleted sulfides were generated, it

should be remembered that the some sulfate-sulfide pairs at the center of the replacement deposit of Vulcano appear to indicate isotopic equilibrium. In such a case, evaluation of the hydrothermal environment may be done, and as it will be shown, equilibration of $SO_4^=$ and H_2S at Vulcano may well explain such "depleted" sulfur.

The $\delta^{34}S_{\Sigma S}$ of the hydrothermal solution can only be deduced from the $\delta^{34}S$ values of sulfur-bearing minerals in sulfur-systems where equilibrium was attained. Assuming local equilibration at Vulcano permits the calculation of this variable. The presence of magnetite-hematite associated with the sulfate-sulfide mineralization (see paragenetic diagram, figure III.5.) indicates that $m_{H_2S} << m_{SO_4}$, thus supporting the concept of an $SO_4^=$-dominated system. Under these conditions

$$\delta^{34}S_{\Sigma S} = \delta^{34}S_{sulfide} + \Delta_{SO4-H2S}$$

then at T= 250°C and using the average $\delta^{34}S$ of pyrite of samples 33-2, 33-3, and 33-5, $\delta^{34}S_{\Sigma S} \approx +13$ ‰.

From this and the $\delta^{34}S$ data for barite and sulfides, it is clear that the SO_4/H_2S ratio of the mineralizing system was very high. Thus it is not surprising that the relative volume of sulfides at La Minita is very small compared with that of barite: even if large amounts of metallic ions had been in solution, there was clearly insufficient H_2S present to precipitate any large quantities of sulfides.

The $\delta^{34}S$ of coexisting sulfates and sulfides can be used to place constraints on the postulated fO_2 and pH conditions of the solutions. Figure V.4 illustrates the stability fields of the mineral phases observed in the Vulcano replacement body, at T=250°C. It also shows several contours for $\delta^{34}S$ of pyrite and barite at $\delta^{34}S_{\Sigma S} = +13$ ‰ as a function of fO_2 and pH,
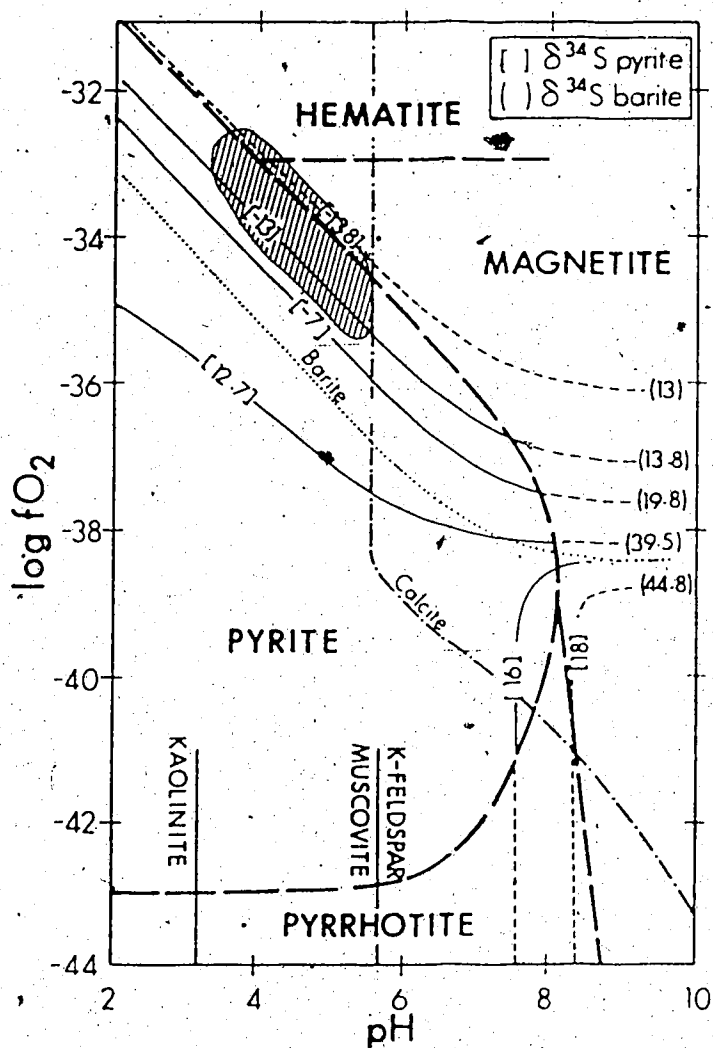
Figure V.4. Range of fO_2 and pH, at T=250°C, I =1, ΣS=0.1 m/kg $_{H2O}$, and K=0.05 m/kgH2O, of the ore-forming solutions at Vulcano. $\delta^{34}S$ of barite and pyrite is given for $\delta^{34}S_{\Sigma S}$ =13‰. The calcite solubility line is given for ΣC = 0.1 m/kg $_{H2O}$. The barite soluble/insoluble boundary is given at m_{Ba^+} =10^{-2}.

assuming equilibrium exchange conditions, according to Ohmoto (972). From the $\delta^{34}S$ values of barite and pyrite and the stability fields of hematite-magnetite-pyrite, the range of fO_2 and pH of the mineralizing fluid can be estimated to have lain in the upper sector of the diagram. The fact that calcite was mainly dissolved and replaced, seldom being preserved or redeposited, suggests that the solution was acidic to neutral. From the solubility curve of calcite (at $\Sigma C = 0.01$ m/kg $H_2O)^6$, it is clear that the fO_2 - pH of the fluid could be further restrained to the left (acid) sector of the upper half of the diagram. In fact, the pH range can be further restrained by the kaolinite <====> sericite and by the sericite <====> k-feldspar phase boundaries to have lain between 3 and less than 6.[7]

On the basis of the previous discussion, the field which represents the possible conditions during the sulfate-sulfide deposition has been indicated in figure V.4. Additionally, the approximated lower limit of the Ba^{++} concentration in the ore solution is also illustrated. Thus under the assumptions already made, the fluid would have had pH between 3 and 5, fO_2 between 10^{-34} and 10^{-32}, and a Ba^{++} concentration of at least $10^{-2}m/kg_{H2O}$. In fact, even if equilibrium in the sulfur isotope system was not attained, the calculated pH and fO_2 would remain valid on the basis of the stability conditions of the mineral association.

A vertical evolution of the fluid system can also be inferred. Figure V.5 illustrates the decrease in $\delta^{34}S$ of pyrite in the upper sector of the

---

[6] $\Sigma C=0.01$ m/kg is in agreement with the presence of zeolite-clinozoisite in the propylitically altered rocks, as was commented upon in the "hydrothermal alteration" section.

[7] K^+ has a large effect upon the pH, the lower activities shifting the reaction boundaries towards less acid pH. From fluid inclusions data of Kuroko deposits (Pisutha and Ohmoto, 1983) and from the K^+/H^+ ratio for the stability range of sericite mentioned in Chapter III, it seems that $K^+ - 0.05$ m/kg H_2O is a reasonable value.

replacement body at Vulcano. If pyrites from samples 33-2, 33-3, and 33-5 were formed under circumstances similar to those previously inferred, an increase in fO_2 has to be assumed to explain the decrease in $\delta^{34}S$. However, a drop in temperature would also contribute to such a decrease.

The Nature of the Parent Fluid

In submarine volcanogenic deposits it is generally assumed that seawater was the main ore fluid (Margaritz and Taylor, 1976; Spooner *et al.*, 1974; Ohmoto and Rye, 1974). At La Minita there is plenty of geologic evidence in favor of the predominance of marine water in the environment. No hydrogen isotope data were obtained, however a characterization of the ore fluid will be made with the available oxygen isotope information.

In figure V.6 the $\delta^{34}S$ and $\delta^{18}O$ of barites from La Minita have been plotted. The marine sulfate of Albian-Cenomanian age, adopted from Faure's curves (which has been adapted from the work of Claypool *et al.*, 1980), is also plotted. It is noted that most of the data for the barites cluster closely around the composition of such seawater sulfate, a few samples being slightly displaced towards larger $\delta^{18}O$.

The isotopic composition of Kuroko barites and of Miocene sulfate have also been plotted in figure V.6 for comparison. The Kuroko barites have a wider range of $\delta^{34}S$ than those of La Minita. Ohmoto *et al.*, (1983) explained the composition of the Kuroko barites as the result of the mixing of fluids from two sulfate sources: Miocene seawater sulfate and hydrothermal sulfate.
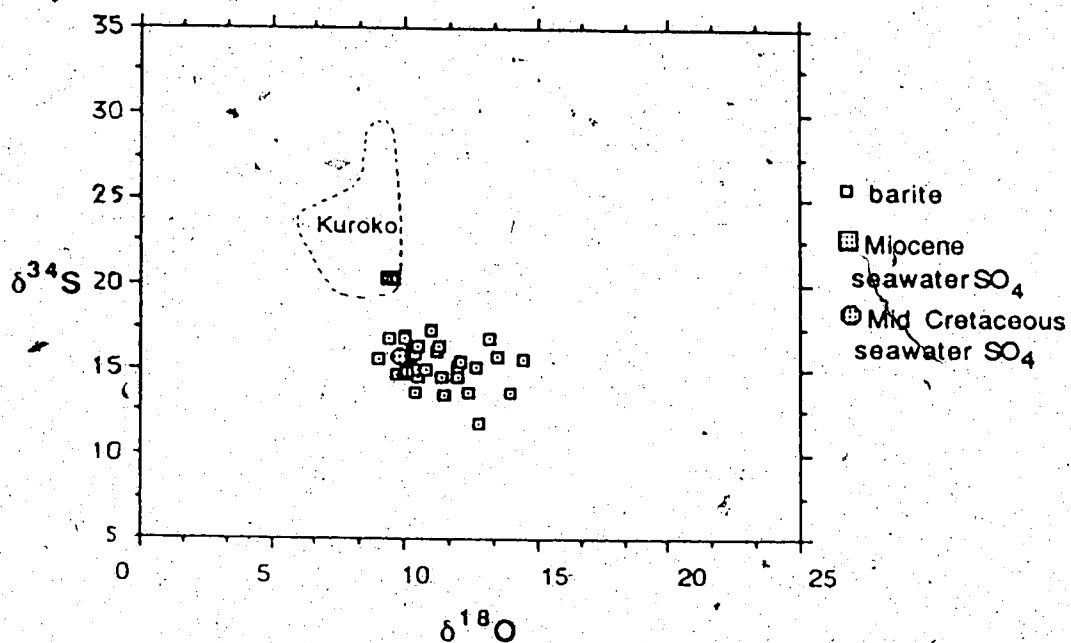
Figure V.6. Comparison of the isotopic composition of barites from la Minita with that of the Mid Cretaceous seawater sulfate, of Miocene seawater sulfate, and of Kuroko barite's sulfate. An apparent shift towards larger $\delta^{18}O$ with respect to the Cretaceous seawater is displayed by the samples from La Minita.

The seawater origin of the sulfur in the barites of La Minita has been already commented upon. Oxygen isotope isotope data reinforce this argument. The $\delta^{18}O$ versus time curve of evaporitic sulfate minerals, indicates a $\delta^{18}O$ - +13.5 ‰ for the oxygen of such sulfate minerals during Middle Cretaceous time. This value is 3.5 ‰ higher than that of the sulfate ion (Lloyd, 1968); thus, seawater sulfate must have had $\delta^{18}O$ +10 ‰ at that time, which is close to the values for La Minita's barites. However, it is known that the $SO_4^=$ ion is not in isotopic equilibrium with the seawater oxygen: for modern, marine sulfate the $\delta^{18}O_{SO4}$ is +9.6 ‰ instead of the +38 ‰ expected for an equilibrium situation (Lloyd, 1968). This may be due to the kinetic oxidation of sulfide ($\delta^{18}O$ -+4.6 ‰) with further ^{18}O-enrichment of the sulfate by bacterial reduction, and to the very slow rates of isotopic exchange between the sulfate ion and the dissolved oxygen at marine temperatures (Lloyd, 1968; O'Neil, 1987). Therefore, a direct comparison between the $\delta^{18}O$ of hydrothermally-produced sulfate minerals and that of evaporitic sulfates is invalid, since at higher temperatures isotopic equilibration is more likely.

There is no evidence to support oxygen isotope equilibrium between the barite and the ore fluid at La Minita. The sulfur isotope data generally indicate disequilibrium conditions. Nonetheless, by comparing the lengths of time required to equilibrate oxygen and sulfur, it can be concluded that equilibration of the former is more readily and rapidly attained (Kusakabe and Robinson, 1977; Ohmoto and Lasaga, 1982; Ohmoto, 1986). If this was the case at La Minita, the nature of the ore fluid could be better defined.

Instead of a direct comparision between the isotopic compositon of marine sulfate and barite, a more realistic comparison may be made by considering the $\delta^{18}O$ of seawater and the equilibrium fractionation of

barite and water at hydrothermal temperatures. The $\delta^{18}O$ of seawater can reasonably be assumed to have been 0 ‰ through Phanerozoic times (Muehlenbachs and Clayton, 1976; Taylor, 1979). Then, barite precipitated in equilibrium with heated seawater (200 - 250°C) would acquire $\delta^{18}O$ values -+3.6 to +6 ‰ (using the equation of Kusakabe and Robinson, 1977). On the other hand, the $\delta^{18}O$ of the hydrothermal water in equilibrium with barite whose $\delta^{18}O$ was +11.2 ‰ (average of barites) would have had a value of +5.1 to +7.5 ‰ at the indicated temperatures. The hydrothermal sulfate would have clearly been more ^{18}O-enriched than normal seawater sulfate. Thus, it is clear that the ore fluid was some form of modified seawater (^{18}O-enriched).

Table VII summarizes the calculated $\delta^{18}O$ composition of the ore fluid in equilibrium with the analyzed O-bearing minerals at their respective temperatures of formation. From this, it can be concluded that the ore fluid, through the different paragenetic stages, was ^{18}O-enriched, with a possible evolution from the most enriched fluid during the pre-ore stage to the less-enriched fluid during the post-ore stage (see table VII).

A slight ^{18}O-enrichment of the seawater may be related to the shallow nature of the marine paleoenvironment at La Minita. Since the mineralization took place in a tropical-sub-tropical region, partial evaporation of the seawater must have occurred. Under these circumstances, the seawater would have retained the heavy oxygen isotope, thus becoming a potential ore solution with a higher ^{18}O-content. However, it is known that evaporation of seawater produces only minor increases in the $\delta^{18}O$ of the seawater, which would be insufficient to explain the larger $\delta^{18}O$ of the mineralizing fluids at La Minita (Ohmoto et al., 1983; Faure, 1986; Longstaffe, 1986).

TABLE VII. CALCULATION OF THE PARENT ORE FLUID $\delta^{18}O$

SAMPLE	MINERAL	∂18O	TEMPERATURE	PARENT FLUID ∂18O
3 1 - 7	MAGNETITE	1.3	226	9.5
3 1 - 7	CALCITE	19.1	226	10.8
3 1 - 7	DOLOMITE	21.7	226	10.2
3 1 - 9	MAGNETITE	5.8	327	12.8
3 1 - 9	CALCITE	18.4	327	13.6
3 1 - 9	DOLOMITE	25.1	327	17.6
3 5	MAGNETITE	5.9	262	16.3
78D	MAGNETITE	8.3	262	6.2
78D	QUARTZ	16.2	262	15
78C	MAGNETITE	3.1	262	11.1
9 2 - 1	MAGNETITE	6	234	14.2
9 2 - 1	QUARTZ	25	234	13.9
			pre-ore stage average	12.6
	CALCITE	19.4	204	10.1
	CALCITE	19	204	9.7
	MAGNETITE	-1.3	241	6.8
	BARITE	12	241	7.9
1 9	MAGNETITE	-1.6	271	6.4
1 9	QUARTZ	15	271	7
2 7	MAGNETITE	-4.2	224	4
2 7	QUARTZ	15.6	224	5.4
1 1 B	BARITE	10	215 ^	4.7
1 1 D	"	9.7	215 ^	4.4
1 1 I	"	9.4	209 ß	3.8
1 2	"	10	204 "	4.1
1 4 A	"	10.1	204 "	4.2
1 8 A	"	10.9	204 "	5
1 8 B	"	10.3	204 "	4.4
3 2 C	"	9	196 ß	2.6
3 4	"	10.4	196 ^	4
3 5	"	10.5	196 ^	4.1
1 0 7	"	11.2	196 ^	4.8
T - 1 1 - 7	"	10.8	196 ^	4.4
3 1 - 6	"	11.4	254 ß	7.8
3 3 - 5	"	13.9	224 ^	9
3 3 - 7	"	10	224 ß	5.1
6 1	"	14.4	204 "	8.5
6 2 B	"	11.5	204 "	5.6
6 7 C	"	11.3	204 "	5.4
6 8 A	"	12	204 "	6.1
7 3	"	11.4	243 ^	7.4
7 5 B	"	10.2	190 ß	3.5
7 7 A	"	13.4	190 ^	6.7
7 8 C	"	10.5	204 "	4.6
7 9 B	"	13.1	204 "	7.2

8 2	"	12.1	204 "	6:2
			ore-stage average 5.8	
58A	"	10.5	124 ^	-1.3
112-3	"	12.4	154 ^	3.3
113-1	"	12.7	154 ^	3.6
113-2	"	12.6	154 ᵃ	3.5
			post-ore stage average 2.7	
* oxygen isotope temperature .				
' average oxygen isotope temperature of the pre-ore stage				
ᵃ Th of inclusions in the sample				
^ Th of inclusions in related sample				
" average Th for barites (without CO2)				

On the other hand, it is well known that a $\delta^{18}O$ shift towards higher values is experienced by fluids interacting with carbonate and/or silicate rocks (Taylor, 1979). Depending upon the initial oxygen isotope composition of the fluid and of the rock, the temperature, and the water/rock ratio of the hydrothermal system, a fluid with a particular $\delta^{18}O$ will be produced and, consequently, this will be reflected in the $\delta^{18}O$ composition of the altered rock and of the hydrothermal minerals. Therefore, if the isotopic composition of the altered rock and of the hydrothermal minerals is known, the origin of the parent fluid may be deduced.

At La Minita, the oxygen isotope information permits some important deductions to be drawn. Firstly, since the oxygen isotope composition of unaltered limestone, and of recrystallized limestone are similar, with a possible shift towards lower $\delta^{18}O$ produced by the hydrothermal fluid, one must infer that either very low water/rock ratios existed or that a parent fluid with a $\delta^{18}O$ composition similar to that of the limestone formed the deposits. Secondly, the observed decrease in $\delta^{18}O$ from one mineralizing stage to the other could have been produced by increasing volumes of water with respect of the volume of rock involved, and by a decrese in temperature as deduced from the modeling of Taylor (1976) and of Ohmoto (1986). Thirdly, since igneous rocks (basalts-andesites) generally have a $\delta^{18}O - 6.5\pm1$ ‰ (Taylor, *ibid*), a more ^{18}O-enriched rock must have contributed large amounts of such an isotope; this clearly suggests a large ^{18}O-contribution by the limestone. Therefore, the oxygen isotope data are well explained by a model in which heated oceanic water interacted with both marine limestone and igneous rocks, increasing its $\delta^{18}O$. Minerals deposited at higher temperatures (pre-ore stage) were formed during a

lower water/rock regime than for subsequent, somewhat cooler stages.

Although contribution of magmatic water to the hydrothermal system cannot be ruled out, the influence of meteoric water can. This is because meteoric water would have produced minerals with a larger ^{18}O-depletion than observed. Nonetheless, minor contributions of this kind of water are not possible to detect with oxygen isotopes alone.

E) Summary and Conclusions

The application of stable isotope geothermometry to samples from La Minita, has been complicated by their low temperatures of formation. On the basis of oxygen isotope studies, the pre-ore stage is deduced to have taken place at temperatures in the range from 327 to 226°C, which has some degree of overlap with the ore stage range of temperatures (272 to 224°C with oxygen isotopes; 240 to 181°C with fluid inclusions). Oxygen isotope temperatures of post-ore stage associations (~100°C) are much lower than the T_h of fluid inclusions, reflecting the longer times required for isotopic equilibration at low temperatures.

Sulfur isotopes, on the other hand, proved generally useless in the geothermometry study Only rarely did sulfate-sulfide pairs give temperatures (245 to 173°C) which agree with the T_h of fluid inclusions in barite. Consequently, isotopic disequilibrium in the sulfur system prevailed through most of the mineralization.

Carbon and sulfur isotope information suggests that at least two mechanisms were involved during sulfate-sulfide deposition. Firstly, disequilibrium deposition of minerals must have been the result of rapid precipitation, such that isotopic exchange between H_2S and $SO_4^=$ was minimal. Under these circumstances the isotopic composition of both sulfur-species remained identical to that of their respective sources. The sulfur of the barite was derived from sewater sulfate, whilst that of the sulfide minerals from inorganically-reduced sulfate (and/or igneous sulfide). Secondly, and less importantly, prolonged recirculation of the ore fluid permitted, at times, extensive exchange between the sulfate and the H_2S, such that near-equilibration occurred; this could have happened

during the formation of the impermeable cap on the ore zone. Exhalation of such a fluid might have provoked the deposition of the pyritic ore at Vulcano. The fact that the replacement body at this locality rarely shows evidence of equlibration in the sulfur isotope system, probably had to do with the more extended interaction of the fluids in that particular zone, which produced several episodes of replacement. Sulfur derived from organic reduction of marine sulfate, as the source for the pyritic ore, may be ruled out due to the extensive evidence of the oxydizing nature of the environment and to the "formal" carbon isotopic composition of the associated carbonates and limestone.

A general evolution of the hydrothermal system can be deduced in the light of the isotopic information. Firstly, the pre-ore stage took place at the highest temperatures, under rather oxidizing conditions, and at low water/rock ratios. Secondly, the ore stage occurred at lower temperatures under more reducing (or, rather, less-oxidizing) conditions, and at greater water/rock ratios than in the previous stage. And thirdly, the post-ore stage was characterized by the lowest temperatures, and probably the more reducing conditions an the largest water/rock ratios of the three stages.

It is apparent that the ore fluid was predominantly evolved seawater. The ^{18}O-enriched nature of such a fluid was the result of the replacement of the host limestone and of interaction with the igneous rocks. Replacement of the limestone was extensive during the pre-ore stage as indicated by the largest ^{18}O- enrichment of the inferred parent fluid.

VI. STRONTIUM- AND LEAD-ISOTOPE INVESTIGATION

A) Introduction

Isotopes of Sr and Pb are commonly applied in studies of geochronometry and petrogenesis. However, in hydrothermal ore deposits, geochronometry using the Rb-Sr and Pb-Pb methods is generally unsuccessful. Due to the inhomogeneity of the Sr isotope composition of hydrothermal systems, the isochron method of dating is unaplicable. Although model dates of Rb-Sr would theoretically yield adequate ages, rarely have they been applied. Dating of ore deposits by the Pb-Pb method. gives essentially model dates, which rarely agree with simple models of Pb growth. This may be due to multi-stages of Pb production under different U/Pb regimes, and to mixture of Pb of various provenances.

Conversely, isotopes of Sr and Pb have proven useful tracers in ore deposits. Since isotopic fractionation of these elements does not occur, they provide direct evidence of the composition of Sr and Pb in the ore solutions at the time of deposition. Sr, due to its strong geochemical similarities to Ba, may help infer the source of barium of barites. Thus, an insight into the provenance of some ore metals can be gained via the study of Sr and Pb isotopes.

B) Method and Results

Barite and whole rocks from several localities in the La Minita district were analyzed. Barite was dissolved by the sodium carbonate method. 100

mg of the mineral were fused with 1 g of sodium carbonate[8] in a platinum vessel. The resulting "cake" was dissolved in distilled water; the insoluble residue centrifuged, and the solution discarded. The residue was dissolved in HNO_3, and the Sr, Ba, and Pb precipitated as nitrates with an excess HNO_3, the solution being discarded and the precipitate dried. The nitrates were then dissolved in 2N HCl and the solution evaporated to dryness. Next, the Pb and Sr were extracted by ion-exchange chromatography.

For Pb extraction, 0.4 cm x 4 cm columns packed with BIORAD AG1-X8, 100 - 200 mesh anion exchange resin were employed. The sample was dissolved in 2 ml of 1.5N HCl, loaded in the columns, and eluted with 4 ml of 1.5N HCl. The eluted solution was collected and evaporated for further Sr separation. Pb was collected during final elution with 6 ml of distilled H_2O. For Sr two steps were followed: a) 1 cm x 18 cm columns, packed with DOWEX 50W-X12, 100 - 200 mesh cation exchange resin,were utilized. The sample was loaded in 2 ml 1.25N HCl, then sequentially eluted with 38 ml 1.25N HCl and 65 ml 2.5N HCl; then, the Sr was collected by elution with 25 ml 2.5N HCl. b) The sample collected in the previous step was evaporated and then dissolved in 0.5 ml 2.3N HCl and transferred to 0.4 cm x 8 cm columns packed with the same type of cation exchange resin. The sample was eluted with 7 ml 2.3N HCl and, next, the Sr collected by passing 5 ml of the same acid.

For the analysis of whole rocks, 200 to 300 mg of finely ground sample were dissolved in three steps, every step being carried out twice. 1) The samples were placed in teflon beakers and moistened with distilled water. A mixture of 2/3 HF + 1/3 HNO_3 was added, and the beaker covered with a lid,

---

[8] The Sr content of the carbonate was determined by spiking a solution containing 1g of Na_2CO_3. It was determined the ^{87}Sr and ^{86}Sr content of the carbonate is respectively 0.073 µg/g and 0.1025 µg/g. Such low contents do not affect the Sr isotope ratios of the barites, which generally have several thousand ppm Sr.

and left overnight at approximately 80°C. The lid was then removed and the solution taken to dryness. 2) HNO₃ was added to the fluoride salts, the resulting solution covered and left on the hot plate overnight. Next, the solution was taken to dryness. 3) The nitrates ,were converted to chlorides by adding 4N HCl. The covered solution was left on the hot plate overnight, and then taken to dryness.

Before spiking, the dissolved sample was split into two aliquots, one for Sr and the other for Rb analyses. The aliquots were weighted and an specific amount of spike added. Samples which had an insoluble residue were centrifuged to get rid of the solid material. The solution was evaporated, then transferred in 2ml 1.25N HCl to the Sr columns. Separation of Sr was as described above for barites. On the other hand, Rb was extracted in the same columns, although with different amounts of elutant: for the large columns, Rb was collected in the fraction between 25 and 40 ml of the elution phase with 2.5N HCl of the method described for Sr. In the small columns, Rb was purified by loading the sample in 2ml 2.3N HCl, eluting and discarding 2 ml 2.3N HCl, and finally collecting 3 ml of 2.3N HCl elutant.

Pb isotope ratios were measured in a MM30 solid source mass-spectrometer. Pb was loaded on single rhenium filaments using the standard silica gel technique. Mass-spectrometric measurement of $^{87}Sr/^{86}Sr$ were performed in MM30 and VG354 solid source mass spectrometers. Although more precise results are generally obtained in the VG354, similar precision may be attained in the MM30 (e.g. sample 68A barite). Sr was loaded on tantalum side-filaments of double filament beads; the center filament was made of rhenium. Rb mesurements were made in a home-built 12 inch, 90° magnet sector, solid source mass spectrometer.

Tables VIII and IX contain the Pb and Sr-Rb isotope data. The measuring error of the spectrometer, as determined by succesive runs of NBS standards, is indicated at the bottom of the tables. As can be seen in the tables, for individual runs some samples have a relatively large precision error (the error is given as 2 σ).

Sr isotope ratios have a wide range of variation. Nonetheless, groups of materials present a consistent range. Barites have $^{87}Sr/^{86}Sr$ ratios in the range from 0.70492 to 0.70535. The volcanics may be subdivided into two groups: a) mafic volcanics, with $^{87}Sr/^{86}Sr$ ratios between 0.70451 and 0.70557; b) felsic volcanics, with $^{87}Sr/^{86}Sr$ ratios between 0.70660 and 0.75709. The carbonate samples have a $^{87}Sr/^{86}Sr$ range from 0.70571 and 0.70685. The magnitude of the $^{87}Sr/^{86}Sr$ ratio of the volcanics correlates with the amount of Rb in the sample, the more radiogenic Sr occurring in the more Rb-enriched samples.

The Pb isotope ratios are rather peculiar. The galena has "normal" lead ratios, however, the barite contains extremely radiogenic lead, with $^{206}Pb/^{204}Pb$ ratios of up to 82 and $^{208}Pb/^{206}Pb$ ratios up to 70.

TABLE VIII. Sr-Rb DATA FOR BARITE AND WHOLE ROCK

SAMPLE	MINERAL/ROCK	87Sr/86Sr*		Sr ppm**	Rb ppm***	87Rb/86Sr	87Sr/86Sro
1l1 (T)	BARITE	0.704926±16	a	---	---	---	---
18B (T)	" "	0.70507±17	b	---	---	---	---
DD 33-5 (V)	" "	0.70524±8	a	3211	---	---	---
DD 33-7 (V)	" "	0.70491±2	b	---	---	---	---
DD 31-6 (V)	" "	0.70525±2	b	---	---	---	---
46 (O)	" "	0.705408±45	b	---	---	---	---
68A (V)	" "	0.705223±21	b	---	---	---	---
68A (V)	" "	0.705223±8	a	---	---	---	---
75B (V)	" "	0.70528±10	b	---	---	---	---
82 (V)	" "	0.705350±26	b	---	---	---	---
16C (T)	TRACHYTIC TUFF	0.75709±2	b	18	221.2	35.8616	0.70578
16D (T)	TRACHYTIC TUFF	0.75522±3	b	25	313.3	35.8745	0.70389
25 (T)	ANDESITIC SPILITE	0.70546±10	a	186	36.4	0.3256	0.70499
26A (T)	ANDESITIC SPILITE	0.70503±7	a	11	6.2	0.1574	0.70481
31-7 (V)	ALTERED LIMESTONE	0.70607±6	a	60	1	0.0674	0.705974
38 (V)	LIMESTONE	0.70685±7	b	755	5.6	0.0214	0.706819
65 (V)	SILICIFIED TUFF	0.706608±36	a	525	185.3	1.0292	0.70514
68A (V)	TRACHYTIC TUFF	0.721434±30	b	95	454.5	13.85	0.70162
78' (V)	RECRYSTALLIZED LIMESTONE	0.70571±3	b	386	0.45	0.0033	0.705705
78' (V)	" "	0.70573±6	a	*	*	*	0.705725
91 (S)	BASALTIC SPILITE	0.704517±26	a	792	18.6	0.06805	0.70442
94 (S)	BASALTIC SPILITE	0.70557±2	b	741	19.1	0.0735	0.70546

Notes:

Measuring error, as determined with succesive runs of the NBS SRM 987 standard is 0.1% for 86Sr/87Sr and 0.5% for 87Rb/86Sr.

(T) Tabaquito, (V) Vulcano, (O) Ojo de Agua, (S) Sapo Negro

* error is 2σ

a- measured in MM30 mass-spectrometer; b- mesured in VG. 354 mass-spectrometer

** Sr spike utilized: 4.865 ppm; 84Sr/86Sr=185.6; 87Sr/86Sr=0.417; 88Sr/86Sr=3.072

*** Rb spike utilized: 10.819 ppm; 85Rb spike: 85Rb=2%(atomic); 87Rb=98%

87Sr/86Sro calculated at 100 M.a. using λ=1.42x10⁻¹¹y⁻¹ (Steiger and Jäger, 1977)

TABLE IX. Pb ISOTOPE DATA FOR BARITE AND GALENA

SAMPLE			206Pb/204Pb	207Pb/204Pb	208Pb/204Pb
82	barite	(V)	55.1	17.89	57.06
11I	barite	(T)	59.22	18.21	59.04
18B	barite	(T)	82.32	19.51	70.13
46	barite	(O)	52.24	17.84	55.63
68A	barite	(V)	30.35	16.27	44.35
86	galena	(V)	18.45	15.56	38.23
Mass discrimination factor was: 206/204Pb=1.002664; 207/204Pb=1.004054					
208/204Pb=1.005959. Factor determined with the NBS SRM 981 standard					
Reproducibility: 206Pb/204Pb=0.24%; 207Pb/204Pb=0.31%; 208Pb/204Pb=					
0.36% determined with the same standard.					
(V) Vulcano; (T) Tabaquito; (O) Ojo de Agua					

C) Sr Isotope Systematics

The Sr isotope data from the barites and the various host rocks shed
some light on the origin of the mineralization. Barite being an abundant
mineral at La Minita, has an important bearing upon the genesis of the
deposits. In order to make a valid comparison between the $^{87}Sr/^{86}Sr$ ratios
of the different materials, the initial $^{87}Sr/^{86}Sr$ of the volcanics has to be
calculated. In table VIII this has been done, however a justification for the
chosen age must be advanced.

The presence of rudists (Caprinuloidea) in the limestone indicates an
Albian-Cenomanian age for the deposit (the boundary between these
epochs has been placed at 97.5 M.a. (Harland et al., 1982)). An attempt to
calculate the absolute age of the deposit was made, since coeval volcanic
rocks with varying Rb/Sr ratios were analyzed. Figure VI.1 is the $^{87}Sr/^{86}Sr$
versus $^{87}Rb/^{86}Sr$ plot of the volcanic rocks. The inset is an enlargment of
the points which lie close to the vertical axis. Calculation of the best fit
line, by the method of Cumming et al. (1972), gives a slope m=0.001427±17
and initial $^{87}Sr/^{86}Sr$ ratio of 0.704963±260, with M.S.W.D.[9] = 74.72. The age
calculated with such a slope is 100.4 M.a. The same information for the data
poits of the inset are m=0.001986±260, initial $^{87}Sr/^{86}Sr$ ratio of
0.704618±154, M.S.W.D.=10.83, the corresponding age being 139.7 M.a.
Although an isochron is not defined, 100 M.a. and 0.704963 might be close
to the actual age and initial $^{87}Sr/^{86}Sr$ ratio, since such an age is in

[9] M.S.W.D. stands for mean squared weighted deviates. It represents the error from an
imperfect fit of the data on a line. When MSWD=1 there is a perfect fit. Values <1
indicate that the points probably fit the line, but an overestimate of the analytical
error limits has been made. Values >1 indicate that the points do not fit the line,
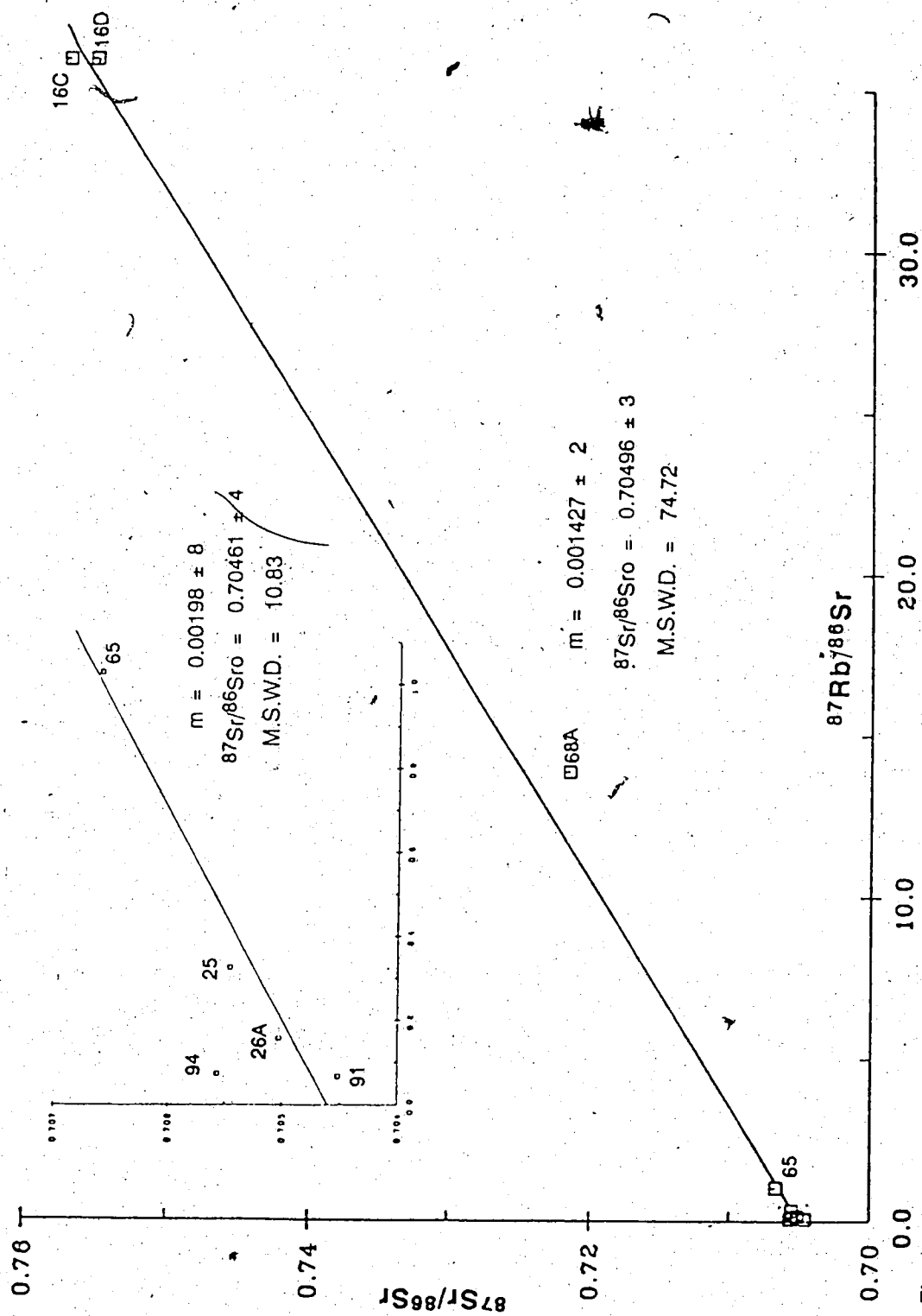provided that the analalycal error has not been underestimated (Krstic, 1981)

Figure VI.1. Rb-Sr plot of volcanic rocks from La Minita, Michoacán. The slop, intercept, and M.S.W.D. for all the data points and for those of the inset are given. Samples 68A and 94 were not included in the calculations

approximate agreement with the paleontologic age.Thus, not having a better estimate of the age of the deposit, 100 M.a. has been adopted.

Samples 94 and 68A were not included for the above calculations as they plot a considerable distance from the line, the former above while the latter below. It seems that sample 94 has gained radiogenic Sr, whilst sample 68A has lost it. Nonetheless, inclusion of these samples in the calculations did not considerably modify the results.

The range of initial $^{87}Sr/^{86}Sr$ ratios of the volcanics is rather wide. Two factors have contributed to this feature. First of all, the alteration of the rock has modified the original concentration of Sr and Rb in the samples. Second, the assigned age is , at best, approximated. Thus, from the sole Sr data it would not be possible to evaluate the Sr contribution to the barite by the various lithologies of the La Minita region. In fact, contribution of such an element by limestone would not be required to explain the Sr isotopic composition of such a mineral. In short, at this point the Sr data are ambiguous. Consideration of the behavior of Sr in hydrothermal systems may help clarify the origin of the $^{87}Sr/^{86}Sr$ in the barite.

Water-rock Interaction

In geothermal systems it has beeen noted that the composition of the fluid can be interpreted by mixing lines (Elderfield and Graves, 1981; Stetler and Allegre, 1978). For instance, it has been found that the composition of the Sr of the fluid lies between that of the host-rock and the original fluid (pure seawater or meteoric water), the proportion of the Sr contribution of both sources determining the final $^{87}Sr/^{86}Sr$ isotope ratio of the geothermal fluid. However, if more than one source was involved,

modelling of the fluid composition is hampered and, at the most, a comparison and a mere qualitative estimate of the possible contribution by the different sources may be made.

An additional limitation to the interpretation of the Sr composition of the fluid involves the process of leaching itself. A bias in the Sr composition of the fluid, due to selective leaching of the components of a rock, may occur. This is particularly important in environments where K-feldspar and quartz-rich rocks are present. These minerals appear to be more resistant to leaching, thus such rocks would contribute less Sr to the fluid. This is apparent when the temperature-dependence of the K/Ca ratio of the fluid is considered. Since Rb and Sr behave similarly to K and Ca respectively, a similar temperature-dependence of the Rb/Sr ratio with respect to the K/Ca ratio is expected (Stetler and Allegre, 1978).

In other instances, the amount of Sr contributed to the fluid is much less than expected. Formation of alteration minerals which take large amounts of Sr, limits the yield of this element. For instance, epidote and chlorite are alteration minerals whose Sr contents vary, respectively, between 215-220 ppm and 105-130 ppm (Elderfield and Graves, 1981). At first sight these figures are not significant, however if the average content of Sr in basalts (465 ppm (Turekian and Wedepohl, 1961)) is considered, they are. Elderfield and Graves (*ibid*) concluded that up to 75% of the Sr leached from a basalt may reprecipitate in alteration minerals as those above mentioned. Nonetheless, although the Sr contribution by the rock in these kind of situations is small, the rock plays an important role in controlling the $^{87}Sr/^{86}Sr$ ratio of the fluid system. Seyfried et al., (1979) experimentally demonstrated that the $^{87}Sr/^{86}Sr$ ratio of seawater is lowered by interaction with basalt, and that the magnitude of the shift is

dependent upon both, temperature and water/rock ratio. This has been long postulated for explaining the Sr isotope composition of the oceans (Dasch et al., 1973; Spooner, 1976; Elderfield and Graves 1981). Despite the fact that their Sr content appears normal, it has been observed that altered Mid-ocean basalts have a higher $^{87}Sr/^{86}Sr$ ratio than fresh basalts, which suggests the effect of seawater on the basalts.

From the previous discussion some aspects of the water-rock interaction may be summarized. Firstly, the temperature of the system may affect the Rb/Sr of the fluid. Secondly, the amount of Sr supplied to the hydrothermal fluid may not be equal to the Sr content of the host-rock (this is particularly important of rocks in which Sr-bearing alteration minerals are produced). Basalts, and mafic rocks in general, will yield lower amounts of Sr during alteration, whilst dissolution of limestone may yield rather large proportions of such an element. Thus, modelling of a mixing process in hydrothermal systems should take this process into account, in order to postulate adequate end members. Thirdly, the $^{87}Sr/^{86}Sr$ of the ore fluid is not necessarily controlled by the amounts of Sr contributed by the sources. Sr-isotope exchange between rock and water takes place, lowering or increasing the Sr ratio of the fluid. This implies that the Sr budget of a hydrothermal fluid is not influenced by certain lithologies, although they may control its $^{87}Sr/^{86}Sr$ ratio.

At this juncture it is apparent that the Sr isotope ratio cannot be certainly employed to identify the source of Sr and, hence, the source of Ba. In the following section the Sr composition of barites will be looked at more carefully in order to evaluate the origin of their $^{87}Sr/^{86}Sr$.

Origin of Sr in the Barites

Since the Rb content of the barites is negligible, they must retain the Sr isotope composition of the fluid at the time of deposition. At La Minita, the possible sources of Sr were the volcanics, the limestone, and the seawater (the last two having similar $^{87}Sr/^{86}Sr$ ratios). Taking 0.7049 as the best estimate of the initial ratio of the volcanics, it becomes apparent that they and the barites had a similar $^{87}Sr/^{86}Sr$ ratio, although that of barites being somewhat higher. On the other hand, the limestone has a considerably higher $^{87}Sr/^{86}Sr$ ratio which, on the whole, is lower than the average value for Albian-Cenomanian limestones (~ 0.7072 (Burke et al., 1982)). Even more, the recrystallized limestone shows both lower Sr isotope ratio and lower Sr contents than fresh limestone. All this strongly suggests a very large influence of the volcanics in controlling the Sr ratio of not only the hydrothermal fluid, but perhaps, of the local seawater environment as well. Localized, short-term fluctuation of the $^{87}Sr/^{86}Sr$ ratio of the sea has previously been reported by Faure (1978) and by Brookings (1976)

A clearer picture of the mixing of components from various sources in the ore fluid at La Minita is better shown in figure VI.2. The $^{87}Sr/^{86}Sr$ versus $\delta^{18}O$ plot points, again, to a mingling of elements from the limestone with those from the volcanics. The oxygen isotope composition of the volcanics from La Minita is unknown, thus the average composition of fresh volcanic rocks summarized by Taylor (1974) has been used. In the diagram, the seawater influence is clearly discarded, due to the opposite trend defined by the barite and the altered limestone.

In light of the previous discussion it is apparent that in this district the volcanics controlled the Sr ratio of the hydrothermal system. Although
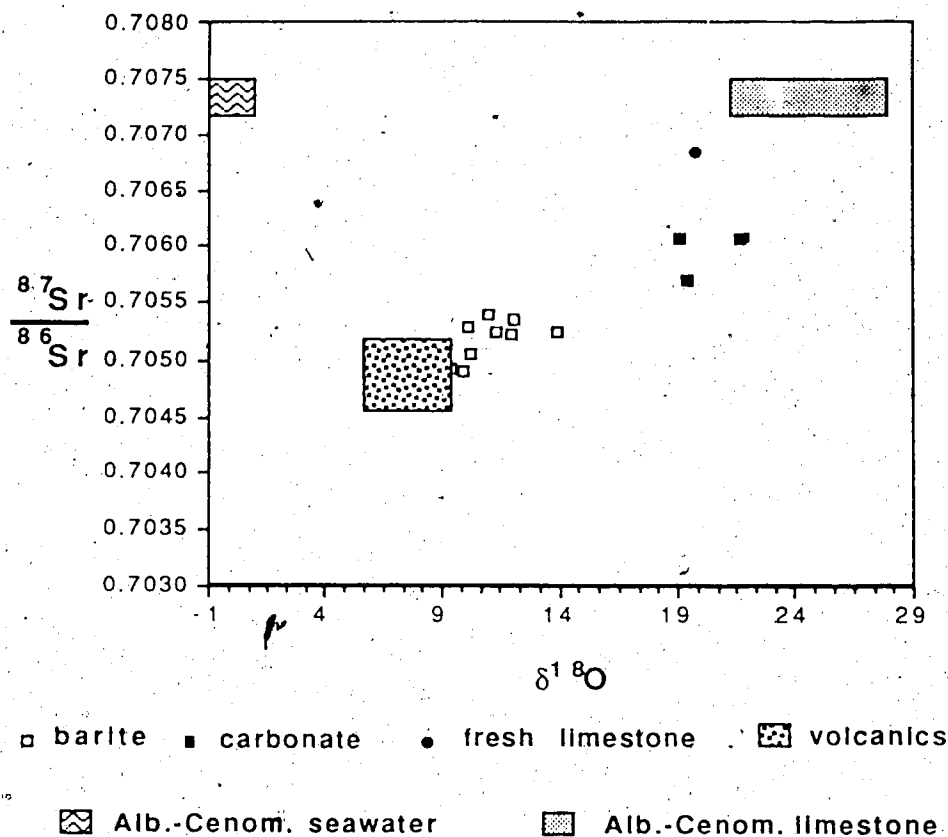
Figure VI.2. Comparison of the Sr- and O-isotope composition of La Minita's barites with that of carbonates and volcanic rocks of the district, and with that of marine limestone and seawater. The Sr composition of the volcanics is the average and variation obtained in this study, whilst the O-isotope composition was addopted from the summary of Taylor (1974). The composition of Sr of Albian-Cenomanian limestone is from Burke et al. (1982). The O composition of limestone was taken from Keith and Weber (1964)

they might not have supplied the large amounts of Sr required to explain the contents of this element in the barites. Probably a large Sr-contribution came from the limestone. Such an Sr suffered some exchange with the volcanic rocks, which thus lowered the $^{87}Sr/^{86}Sr$ ratio of the fluid. However, if large volumes of volcanic rock were involved, the limestone contribution is not required. The variability in the $^{87}Sr/^{86}Sr$ ratios of the barite may have resulted from temperature fluctuations and variations in the water/rock ratio of the hydrothermal system.

Origin of the Barium

Direct application of the previous conclusions may explain the origin of barium at La Minita. This would be a logical procedure, due to the geochemical similarities between Sr and Ba. However, it would be unlikely that all the different types of volcanic rocks contributed Ba in similar proportions. Farrel and Holland (1983) concluded that the Sr ratio of barites of the Kuroko deposits do not provide a categorical conclusion with regard to the source af Ba. They rather combined such ratios with Ba contents to identify the possible sources.

Average barium concentrations of such lithologies as are present at La Minita, as obtained from the literature, are: trachyte 1177 ppm; rhyolite 1127 ppm; andesite 703 ppm; basalt 300-600ppm; and limestone 92 ppm (Puchelet, 1978). The reason that trachytes and rhyolite contain large amounts of barium is the presence of K-feldspar, principally sanidine. This mineral exhibits barium contents averaging 3370 to 6850 ppm (Carmichael, 1965; Hewlet, 1959). On the other hand, the low barium content of basalts-andesites is due to the fact that plagioclase (andesine-oligoclase) usually has lower barium contents of up to 3480 ppm (Anderson, 1966). The larger

Ba content of the sanidine is due to the similar ionic radii of Ba and K, which enables more complete diadochy. During initial differentiation of basaltic magmas, barium is preferentially concentrated in the melt. With further crystallization, the melt becomes depleted in barium due to crystallization of sanidine and micas. Consequently, both the initial and final stages of crystallization may produce phases with comparatively low Ba contents (Puchelet, 1978).

This discussion leads to a more definitive identification of the source of barium. It is apparent from the Sr isotope information and from the average Ba contents of the rocks, that trachytes and rhyolites are the most viable sources of barium[10]. Contribution by andesite, basalt, and limestone must have been minor, its relative importance following the indicated order. Therefore, it is concluded that the $^{87}Sr/^{86}Sr$ isotope ratio cannot alone distinguished the source of barium, due to the complex numerous steps that intervene in the process of hydrothermal leaching and isotopic exchange.

To summarize, a series of events were involved during the evolution of the $^{87}Sr/^{86}Sr$ isotope ratio of the ore fluid. The process started with percolation of seawater into the substratum, through the volcanic pile. The Sr content of this fluid was low and its $^{87}Sr/^{86}Sr$ ratio comparatively high. As the temperature increased a larger rock-water exchange took place which decreased the Sr ratio of the fluid and probably increased, slightly, its Sr content. Interaction of the fluid was not only with the volcanics, but with the limestone as well. Leaching of Sr from the limestone considerably

---

[10] Formation of sericite (muscovite) by alteration of sanidine in trachytes and rhyolites may decrease the Ba content of the solution. Nonetheless, muscovite can only capture less than 1/3 of the Ba that sanidine can yield, thus sanidine (and then its containing rocks) is still the major supplier of this element.

increased the Sr content of the fluid. However this would have to suffer some exchange with the volcanics (or mixing with fluid alredy affected by such rocks) in order to lower the global $^{87}Sr/^{86}Sr$ ratio of the hydrothermal fluid. The process of isotopic exchange caused the Sr ratio of the volcanics to increase in variable proportions (the reason why the volcanics do not form an isochron at present). Mafic volcanics were probably more affected due to the formation of alteration minerals which consumed some of the Sr in the solution.

On the other hand the explanation of the barium seems to be more straightforward. Since the Ba concentration in the trachytes and rhyolites overwhelmed that of the other rocks, there was just one possible direction of movement of this element. That is, as soon as the solution leached it from the sanidine, the final destination of this element would be the barite. Probably the concentration of this element in the ore solution was augmented by minor contributions from the basalts and from the limestone.

D) Pb Isotopes: Discussion

Only a brief account of the Pb isotope data will be undertaken, due to the few analysis performed. Additionally, due to the lack of regional Pb isotope investigations in the study area, most of the interpretations are neccessarily speculative, although in accordance with conventional Pb systematics.

In figures VI.3 the $^{207}Pb/^{204}Pb$ vs $^{206}Pb/^{204}Pb$ and the $^{208}Pb/^{204}Pb$ vs $^{206}Pb/^{204}Pb$ compositions of the samples from La Minita have been plotted. The two-stage Pb growth-curve of Stacy and Kramers (1975) has been included for reference.* Two features of this plot are noted. Firstly, the galena sample plots well below such a growth-curve and, secondly, the Pb in barites is extremely radiogenic. Additionally, not only are the barites enriched in radiogenic ^{206}Pb, but also they are enriched in radiogenic ^{208}Pb. Thus it becomes apparent that the Pb of these deposits does not fit the typical models of Pb evolution and may be considered "anomalous".

The fact that the galena sample plots well below the two-stage growth-curve, indicates that its Pb evolved in a depleted reservoir (i.e. a reservoir with $\mu < 9.74$). In fact, it plots within the field of Pb of oceanic volcanics, which also contains the Kuroko field (from the summary of Doe and Zartman, 1979).

Mixing of leads is one of the possible explanations for the array depicted in figure VI.3. The slope of the line passing through the data points has generally been interpreted as being representative of the age of the source of the Pb contaminant. However, it is apparent that the data points do not fit a line. Under these conditions, the age of the contaminant
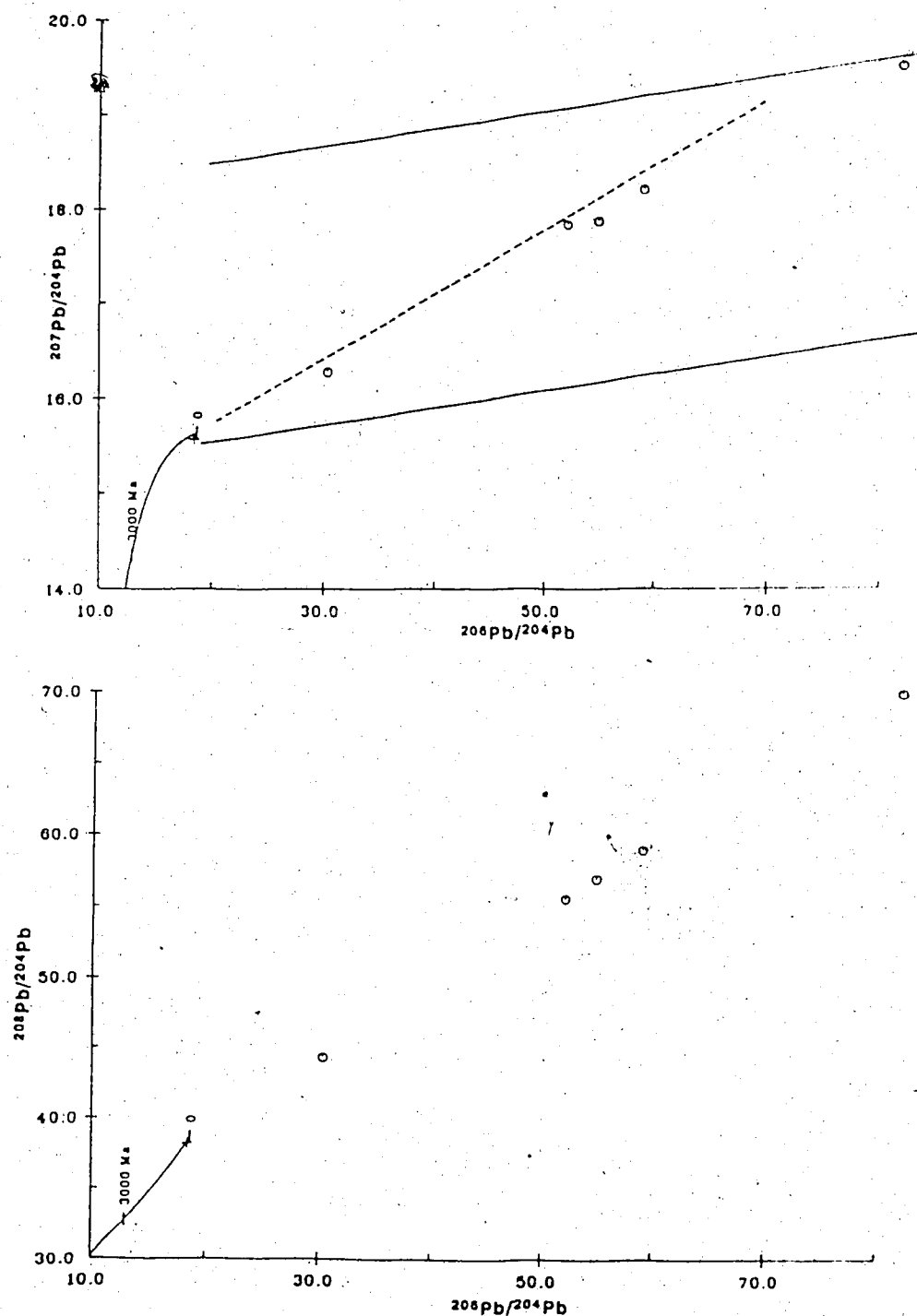
Figure VI.3. $^{207}Pb/^{204}Pb$-$^{206}Pb/^{204}Pb$ and $^{208}Pb/^{204}Pb$-$^{206}Pb/^{204}Pb$ plots of barites and galrna from La Minita, Michoacán. 100 M.a. reference isochrons have been drawn in the first diagram.

source cahnot be calculated. In any case, by the previous mode of interpretation, in order to explain the extremely radiogenic lead of the barites, an old, highly U- and Th-enriched source would have to be postulated. This kind of source is unacceptable, since the geologic and isotopic (Sr) evidence indicates that the area of. La Minita (and the Guerrero terrane in general) is not underlain by ancient continental crust.

Another possibility for the origin of the radiogenic Pb of the barites is the production of such Pb within the barites themselves. For this kind of explanation, it would be required that both U and Th were present in the mineral. In this way every barite would behave as an independent reservoir with particular $^{238}U/^{204}Pb$, $^{235}U/^{204}Pb$, $^{232}Th/^{204}Pb$ ratios. In order to produce such radiogenic Pb, these ratios must have been rather high. Now, since the age of the deposit is approximately known (100 M.a.) it would be expected that the data points would plot on a line with the respective slope equivalent to 100 M.a. 100 M.a. reference isochrons have been drawn in figure VI.3., and a clear departure from the expections from such a model is noted.

Several reasons can be advanced in order to explain the above described diversion. Firstly, the dissolution and rehealing displayed by the barites has been already commented upon. Evidently, these minerals have not behaved as totally closed systems and addition and/or removal of material has taken place. Secondly, it is unlikely that the ore solution had homogeneous Pb isotope compositions, as indicated by the inhomogeneous Sr ratios. Thus, since the barites did not have the same Pb initial ratio, they would not define an isochron at any time of their evolution. The best

approximation to the initial Pb ratio is given by the galena, however its range of variation cannot be revealed with the present cursory data.

Although there are no data available in the literature with regard of the U-Th contents of barites, the second model is the most appealing. An example of such a model has been reported for pyrite-chalcopyrite of the Copper Belt, Zaire (Richards et al., 1988). In fact, the U-Th content of the mineral is not the controlling factor in this model; rather, the U/Pb and Th/Pb ratios of the mineral determine its $^{207}Pb/^{206}Pb$ and $^{208}Pb/^{206}Pb$ evolution. In accordance with the inhomogeneous initial Pb ratios and the open-system behavior of the barites, evolution of Pb from radioactive decay within the mineral would produce a "fan" array instead of an isochron.

In short, the Pb of galena and that of barites at the time of mineralization was derived from a depleted source with U/Pb and Th/Pb ratios being considerably lower than for continental crust materials. The presence of extremely radiogenic lead in barites may be due to U- and Th-decay within such a mineral. The fact that the Pb data of the barites do not define linear arrays (isochrons) has to do with the inhomogeneous Pb composition of the fluid, and with the open-system behavior of the barites.

VII. CONCLUSIONS

The mineral deposits of the La Minita district were formed below the shallow, marine waters of the Cretaceous volcanic island arc of present-day southwestern Mexico. Emplacement of sulfate-sulfide mineralization was controlled both lithologically by carbonate facies and structurally by deep-seated fractures. The main orebody of the district was formed by replacement of a limestone reef which developed in the vicinity of one such fractures (namely, the replacement body at Vulcano). The occurrence of the mineral deposits within a restricted stratigraphic interval indicates a relatively short-lived mineralizing episode. The close relationship between mineralization and centres of volcanic activity is manifested by the presence of lavas and coarse-grained pyroclastics underlying and, sometimes, overlying the mineral bodies. This is indicative of periods of mineral deposition and reef growth during volcanic hiati. It is possible that mineralization and reef growth were somehow related: perhaps the rudists of the region could flourish in ecologic niches where nutrient-rich, warm water was issuing from low-toxicity submarine exhalative vents. Nonetheless, such a relationship might have been purely coincidental, since in nearby districts no mineralization has as yet been reported associated with such reefs. A detailed paleontologic/facies investigation is required in order to clarify this uncertainty.

A) Origin of the Fe-Ba-Sulfide Replacement Bodies

The mineralization of La Minita reflects a spectrum between proximal and distal depositional sites. Proximal mineralization in the form of Fe-Ba-

117

sulfide replacement bodies is seen at Vulcano and Tabaquito. Distal mineralization is present at the Sapo Negro locality in the form of Fe-Mn formations.

The most complicated evolutionary history is exhibited by the replacement bodies. A sequence of events from high- to low-temperature gave rise to such mineralization. The high temperature events took place at 327 to 224°C with the deposition, by replacement of carbonate reef, of hematite-magnetite-quartz. During this stage the ore fluid was largely ^{18}O-enriched, probably as a result of the dissolution of the limestone. The highly-oxidizing conditions of the mineralizing environment are compatible with an open-, shallow-water facies conductive to reefal development environment during reef formation. It is not entirely clear whether submarine exhalations produced the iron formation facies of the region during this episode. However, the jasper beds which overly the replacement bodies (Vulcano and Tabaquito) could have been formed during this stage. These beds well represent siliceous sinter caps analogous to the tetsusekiei of the classic Kuroko deposits.

The following mineralizing stage occured under less-oxidizing conditions and at lower temperatures. Barite and sulfides were predominantly deposited in the interval when the solutions cooled to between 240 and 181°C. The ore fluid was still ^{18}O-enriched and had salinities of between 9.2 and 6.2 wt% NaCl equivalent. The hydrothermal sulfur isotope system was generally under disequilibrium, probably due to mixing of seawater-derived sulphide with inorganically-reduced sulfur and/or igneous sulfur. The negative character of the $\delta^{34}S$ of some sulfides at Vulcano and its absence at Tabaquito is one of the main differences between the mineralized bodies of the two localities.

Bacterial reduction of seawater-derived sulfur could explain the ^{34}S-depleted sulfur of the Vulcano deposit. Nevertheless, neither the geologic evidence nor the carbon isotope data support such a contribution from a biologic reducing mechanism. The hypothesis of a system which approached equilibrium between oxidized and reduced sulfur-species, thus lowering the $\delta^{34}S$ of the H_2S in solution is preferred. Equilibration could have been effected during closed system recycling of the fluid below the seafloor, due to containment by the jasper sinter cap.

Another feature which distinguishes the Vulcano deposit from the Tabaquito deposit is the existence of exhalative pyrite at Vulcano. This body provides evidence of the attainment of local less-oxidizing conditions at Vulcano and of proximal exhalative sulfide deposition outside the replacement environment. Farther away from the vent, under more oxidizing regimes, jasper-hematite beds were deposited. Precisely this kind of underwater activity has been described from present-day sites in the Atlantis II Deep (Bignel et al., 1976), the East Pacific Rise (Francheteau et al., 1979), the Bauer Deep between the Galapagos and the East Pacific Rise (Sayles and Bischoff, 1973), etc. These are, however, deep-water examples. Modern shallow subsea hydrothermal systems occur at Santorini, Italy (Smith and Cronan, 1975; Puchelet (1972), Baia di Levante, Vulcano (Honorez et al., 1971), Matupi Harbor, New Britain (Ferguson and Lambert, 1972), among others. All these shallow-water systems are comparatively similar among themselves. However, only at Baia di Levante are sulfides being precipitated (mainly pyrite-marcasite). Although the sulfides are not being actually exhaled onto the seabed as particulates (they accumulate within the pore spaces of trachytic tuffaceous sediments) they provide evidence of the deposition of sulfides in a shallow, oxygenated marine

setting. In many of the shallow susbsea springs the segregation of Fe from Mn has been documented, supporting the aforementioned concept of "distal" and "proximal" mineralization. Cronan (1980) has compared the zoning of chemical sediments away from the submarine springs off Santorini with that of the Atlantis II Deep. A clear similarity was demonstrated for both regions, with sulfide deposition taking place at the vent, iron-bearing sediments being deposited further away, and manganese-bearing sediments being deposited more distally. In cases where only iron- and manganese-bearing sediments are being produced, it was considered reasonable to anticipate that sulfide segregation had taken place at depth.

Thus, at La Minita, similar processes must have operated. In order for sulfides to have been exhaled and precipitated to generate the pyritic body, the environment must have attained sufficiently reducing conditions right to the point of hydrothermal discharge. Otherwise Fe-Mn oxides would have precipitated as proximal deposits. Such a reducing environment (or rather less-oxidizing) could have been attained during the above-mentioned recyrculation of the hydrothermal fluid beneath the siliceous sinter cap. This would have isolated the sub-seafloor environment, preventing its oxygenization. Furthermore, boiling of the fluid would likely be generally prevented by such a cap. At times, during hydraulic fracturing, the fluid must have boiled, in addition to have exhaled sulfides.

If the above-described model is valid, the negative $\delta^{34}S$ of the Vulcano pyritic body could represent H_2S equilibrated with $SO_4^=$ at depth. Likewise, boiling of the solutions would help explain, in part, the large ^{18}O-enrichment of the ore fluid and the actual mineral deposition.

Finally, the origin of barium and lead in these deposits can e traced to the volcanics in the host sequence. Trachytes and rhyolites were the most likely source of barium, whilst the lead has less clear origin. It can only be deduced that it was derived from a source similar to oceanic volcanics, perhaps the whole submarine volcanic pile of the district.

B) Comparison of La Minita Deposits with the Classical Kuroko Model

In table X the principal features of La Minita's deposits and of the Kuroko ores are compared. Some similarities, but also major differences, are evident. The similar features are the salinity, the temperature and the pH of the ore-forming solutions, the mineralogy (with the exception of the presence of magnetite and the absence of anhydrite-gypsum at La Minita), and the close association with proximal felsic volcanics. The major differences are the age of the mineralization, the overall chemical character of the deposit, the depth of mineralization, the occurrence of replacement bodies after limestone at La Minita, and the isotopic composition of S, O, and Sr.

The noted differences with regard to the isotopic compositions of sulfur and strontium in barites may be in part due to the evolution of the composition of the seawater reservoir. Nonetheless, the presence of negative $\delta^{34}S$ in the sulfides of Vulcano is another major difference. As far as oxygen is concerned, the isotopic composition of barites is heavier in samples from La Minita than in kuroko deposits. This difference cannot be explain by such an evolution of the seawater for it has been noted

TABLE VIII. Sr-Rb DATA FOR BARITE AND WHOLE ROCK

	LA MINITA	KUROKO
Lithologic setting	mafic to felsic lavas and pyroclastics, and patch reefs	basaltic to rhyolitic (bimodal) volcanics produced in submarine calderas
Age	Albian-Cenomanian (~ 100 M.a.)	Miocene (16 - 11 M.a.)
Formation depth	< 350 m, frequent boiling	> 2000 m, no boiling (Pisutha et al., 1983)
Mineralogy	hematite, magnetite, barite, pyrite, sphalerite, galena, chalcopyrite, tetrahedrite, quartz	sphalerite, pyrite, galena, tetrahedrite, chalcopyrite, barite, anhydrite, quartz (Eldridge et al., 1983)
Temperature	327 - 134°C	350 - 150°C (Pisutha et al., 1983)
Salinity of ore fluids	6.2 (reaching 9.2) to 2.4 wt% NaCl equiv.	6 to 3.5 wt% NaCl equiv. (Pisutha et al., 1983)
Log(aO2)	-34 to -32	-33.4 to -35.5 (Yoshida et al., 1977; Shikazano and Kohuda, 1979)
pH at 250°C	6 to 3	5 to 4.2 (from the summary of Pottorf and Barnes, 1983)
Range of ∂18O in barite	+9 to +14 ‰	+6.4 to +10.9 ‰ (Watanabe and Sakai, 1983)
Range of ∂34S in barite	+14 to +18 ‰	+19.5 to +25.5 ‰ (Watanabe and Sakai, 1983)
Range of ∂34S in sulfides	+7 to -14.4 ‰	< +8 to > -7 ‰ (from the summary of Rye and Ohmoto, 1974)
Sr isotope ratio in barite	0.7049 to 0.7053	0.7068 to 0.7083 (Farrel and Holland, 1983)

(Claypool *et al.*, 1980) that the isotopic composition of seawater-sulfate has remained almost constant since Jurassic times.

In short, it appears that the two types of vulcanosedimentary deposits share many basic characters, but that they do differ in a number of aspects. Global concepts may be applied for regional prospecting for this kind of deposits, but is clear that unique criteria must be utilized according to the targets.

C) Exploration Criteria for Future Discoveries in the District

From the results of this study a list of general criteria for further exploration for Fe-Ba-sulphide deposits of the "La Minita" type can be generated. These include:

a) Lithologic: (i) Rudist reef patches within broad areas of volcanic rocks, particularly reefs related to felsic vulcanic domains; such felsic domains should also be revealed by scintillometric or gamma-spectrometric surveys. (ii) Alteration of the limestone to assemblages of magnetite and quartz; clearly detectable with a magnetometer; (iii) The presence of iron formations in the vicinity of reefal lithologies is very important.

b) Structural: The presence of major fracture zones beneath the reef, predating reef growth; possibly visible via VLF-EM surveys.

c) Isotopic: (i) Sulfur. The most sulphide-rich deposits may exhibit a "light" sulfur isotope composition in sulfide minerals found in outcrop or core; (ii) Sr and O. These may be significant indicators of mineralization in limestone. Both the Sr isotope ratio and the $\delta^{18}O$ of the limestone would be lower than their "normal" values.

It is at this point interesting to speculate that if limestone was being deposited during underwater spring activity, lower Sr ratios would be acquired not only by the altered limestone but by the fresh limestone as well. This statement must be further tested, for in this investigation it could not be done.

REFERENCES

ALONSO-DAVILA, V. and JIMENEZ-ROLDAN, A., Inventario de Mineral 1987. Servicios Industriales Peñoles, Unpublished Internal Report.

AMSTUTZ, G.C. and PATWARDHAN, A.M., 1974; A reapraisal of the textures and composition of the spilites in the Permo-Carboniferous Verrucano of Glarus, Switzerland: in Amstutz editor, Spilites and Spilitic Rocks, IUGS, Series A, No. 4, Springer Verlag, Berlin, pp. 71-81.

AMSTUTZ, G.C., 1968; Spilites and spilitic rocks: in Hess and Poldervaart editors, Basalts: The Poldervaart Treatise on Rocks of Basaltic Composition. Interscience (Wiley), New York, pp.737-753.

ANDERSON, A.T. Jr., 1966; Mineralogy of the Labrieville anorthosite, Quebec: Am. Mineralogist, 51, pp. 1671-1711.

BARTON, P.B.Jr., 1978; Some ore textures involving sphalerite from the Furutobe Mine, Akita Prefecture, Japan: Mining Geology, 28, pp. 293-300.

BEARTSCHI, P., 1976; Absolute ^{18}O content of Standard Mean Ocean Water: Earth Planet. Sci. Lett., 31, pp. 341.

BECKER, R.H., 1971; Carbon and oxygen isotope ratios in iron formations and associated rocks from the Hamerley Range of Western Australia, and their implications: Unpublished Ph D. thesis, University of Chicago (in Friedman and O'Neil, 1977)

BERGQUIST, H.R. and COBBAN, W.A., 1957; Molluscs of the Cretaceous: Geol. Soc. America, Memoir 67, pp. 871-884.

BIGNELL, R.D., CRONAN, D.S., and TOOMS, J.S., 1976; Red Sea metalliferous brine precipitates: in D.S. Strong (ed), Metallogeny and Plate Tectonics, Geol. Assoc. Canada Spec. Papers, 14, pp. 147-184.

BLATTNER, P., BRAITHWAITE, W.R., and GLOVER, R.B., 1983; New evidence on magnetite isotope geothermometers at 175°C and 112°C in Wairakei steam pipelines (New Zealand): Isot. Geosci., 1, pp. 195-204.

BODNAR, R.J., REYNOLDS, T.J., and KUEHN, A.C., 1985; Fluid inclusion systematics in epithermal systems: in Reviews in Economic Geology, Vol. 2, Geology and Geochemistry of Epithermal Systems, pp. 73-97.

BOTH, R, CROOK, K., TAYLOR, B., CHAPPEL, B., FRANK, E., LIU, L., SINTON, J., and TIFFIN, D., 1986; Hydrothermal chimneys and associated fauna in the Manus back-arc basin, Papua New Guinea: EOS, 67, No. 21, pp.489-490.

BOTTINGA, Y. and JAVOY, M., 1973; Comments on oxygen isotope geothermometry: Earth and Planet. Sci. Lett., 20, pp. 250-265.

BÖSE, E. and CAVINS, O.A., 1927; The Cretaceous and Tertiary of southern Texas and Northern Mexico: Texas Univ. Bull. 2748, pp. 7-142.

BROOKINGS, D.G., CHAUDURI, S., and DOWLING, P.L., 1960; The isotopic composition of strontium in Permian limestones, eastern Kansas: Chem. Geol., 4, pp. 439-444.

CAMPA, M. F., 1978; La evolucion tectonica de Tierra Caliente, Guerrero: Bol. Geol. Soc. of Mexico, XXXIX, pp. 52-64.

CAMPA, M.F. and CONEY, P.J., 1983; Tectonostratigraphic terranes and mineral resources distribution in Mexico: Can. J. Earth Sci., 26, pp. 1040-1051.

CAMPA, M.F., and RAMIREZ, J., 1979; La evolucion geologica y la metalogenesis del noroccidente de Guerrero. Serie Tecnico-Cientifica de la Universidad Autonoma de Guerrero, No. 1, 102 p.

CARMICHAEL, J.S.E., 1965; Trachytes and their feldspar phenocrysts: Mineral. Mag., 34, pp. 107-125.

CASTILLO-MADRID, A., 1986; Informe final de evaluacion geologico-minera del proyecto "El Sapo Negro", Municipio de Coalcoman, Michoacan: Servicios Industriales Peñoles, Unpublished Internal Report.

CETENAL-INSTITUTO DE GEOGRAFIA,1970; Carta de climas: Mexico, D.F., Comision de Estudios del Territorio Nacional e Instituto de Geografia, Hoja Colima 13Q-VI, 1:500000.

CLAYPOOL, G.E., HOLSER, W.T., KAPLAN, I.R., SAKAI, H., AND ZAK, I., 1980; The age curves of sulfur and oxygen isotopes in marine sulfate and their mutual interpretation: Chem. Geol., 28, pp. 199-260.

CLAYTON, R.N., O'NEIL, J.R., and MAYEDA, T.K., 1972; Oxygen isotope exchange between quartz and water: Jour. Geophys. Research, 77, pp. 3057-3067.

CONDIE, K.C., 1977; Effects of alteration on element distribution in Archean tholeiites from the Barberton greenstone belt, South Africa: Contrib. Mineral. Petrol., 64, pp. 75-89.

CONEY, P.J., 1983; Un modelo tectonico de Mexico y sus relaciones con America del Norte, America del Sur y el Caribe. Rev. Inst. Mex. Petrol., 15, pp. 6-16.

COOMER, P. G. and ROBINSON B. W., 1976; Sulphur and sulphate-oxygen isotopes and the origin of the Silvermines deposits, Ireland: Mineral Deposita, 11, pp. 155-169

COX, L. R., 1933; The evolutionary history of the rudists: Geologists' Assoc. London Proc., vol. 44, pt. 4, pp. 379-388.

CRAIGH, H., 1957; Isotopic standards for carbon and oxygen and correction factors for mass-spectrometric analysis of carbon dioxide: Geochim. Cosmochim. Acta, 12, pp. 133-149.

CRONAN, D.S., 1980; Underwater Minerals. Academic Press, New York, 362 p.

CSERNA, Z., ARMSTRONG, R., YANES, C., and SOLORIO, J., 1978; Rocas metavolcanicas e intrusivos relacionados paleozoicos de la region de Petatlan, Estado de Guerrero. Instituto de Geologia, UNAM, 2, No. 1, pp. 1-7.

CUMMING, G.L., ROLLET, J.S., ROSSOTTI, E.J.L., and WHEWELL, R.J., 1972; Statistical methods for the computation of stability constants PartI. Straight line fitting of points with the correlated errors: Jour. Chem. Soc., Dalton Trans., pp. 2652-2658.

DAMON, P. E., SHAFIQUILLAH, M. and CLARK, K. F., 1983; Geochronology of the porphyry copper deposits and related mineralization of Mexico: Can. J. Earth Sci., 26, pp. 1052-1071.

DASCH, E.J., HEDGE, C.E., and DYMOND, J., 1973; Effect of seawater interaction on strontium isotope composition of deep-sea basalt: Earth Planet. Sci. Lett., 19, pp. 177-183.

DECHASEAUX, C. and PERKINS, B.F., 1969; Family CAPRINIDAE d'Orbigny, 1850; in Moore, R.C. and Teichert, C. (eds): Treatise on Invertebrate Paleontology, Mollusca 6, Bivalvia, part N, vol. 2, pp. 787-799.

DEINES, P. and GOLD, D.P., 1973; The isotopic composition of carbonatite and kimberlite carbonates and their bearing on the isotopic composition of deep-seated carbon: Geochim. Cosmochim. Acta, 37, pp. 1709-1164.

DELGADO, L.A. and MORALES, J.E., 1984; Rasgos geologicos y economicos del complejo basico-ultrabasico de El Tamarindo, Guerrero: Geomimet, 128, pp. 81-96.

DOE, B.R. and ZARTMAN, R.E., 1979; Plumbotectonics, the Phanerozoic: in Barnes, H. L., ed.: Geochemistry of Hydrothermal Ore Deposits, John Wiley & Sons, New York, pp.22-70.

DRUMMOND, S.E. and OHMOTO, H., 1980; Chemical modelling of hydrothermal fluid mixing [abstract]: Geol. Soc. Am. Abstracts with Programs, 12, pp. 417.

ELDERFIELD, H. and GRAVES, M.J., 1981; Strontium isotope geochemistry of Icelandic geothermal systems and implications for seawater chemistry: Geochim. Cosmochim. Acta, 45, pp. 2201-2212.

ELDRIDGE, C.S., BARTON, P.B.Jr., and OHMOTO, H., 1983; Mineral textures and their bearing on formation of the Kuroko orebodies: in Ohmoto, H. and Skiner, B.J. (eds), Kuroko and Related Volcanogenic Massive Sulphide Deposits. Economic Geology Monograph 5, pp. 241-281.

ENOS, P., 1974; Reef, platforms and basins of Middle Cretaceous in Northeast Mexico: Amer. Assoc. Petrol. Geol. Bull., 58, pp. 800-809.

FABRE, S., 1940; Le Crétacé Superieur de la Basse Provence Occidentale 1 Cenomanien et Turonien: Faculté Sci Marseille Annales, 2nd ser., 14, 355 p.

FARREL, C.W. and HOLLAND, H.D., 1983; Strontium isotope geochemistry of the Kuroko deposits: in Ohmoto, H. and Skiner, B.J. (eds), Kuroko and Related Volcanogenic Massive Sulphide Deposits. Economic Geology Monograph 5, pp. 302-319.

FAURE, G., 1986; Principles of Isotope Geology. 2nd. ed., John wiley & Sons, New York 589p.

FAURE, G., ASSERETO, R., and TRUMBA, E.L., 1978; Strontium isotope composition of marine carbonates of Middle Triassic to Early Jurassic age, Lombardic Alps, Italy: Sedimentology, 25, pp. 523-543.

FERRUSQUIA-VILLAFRANCA I., APPLEGATE S. P. and ESPINOSA-ARREBURENA, L.,1978; Rocas volcanosedimentarias mesozoicas y huellas de dinosaurios en la region suroccidental pacifica de Mexico: Univ. Nal. Auton. de Mex., Inst. Geol., 2, pp. 150-162.

FLUET, D.W., 1986; Genesis of the Deer Trail Zn-Pb-Ag Vein Deposit, Washinton, U.S.A. Unpublished MSc thesis, University of Alberta.

FRANCHETEAU, J., NEEDHAM, H.D., CHOUKROUNE, P., JUTEAU, T., SEGURET, M., BALLARD, R.D., FOX, P.J., NORMAN, W., CARRANZA, A., CORDOBA, D., GUERRERO, J., RANGIN, C., BUGAULT, H., CAMBON, D., and HEKINIAN, R., 1979; Marine deep-sea sulfide deposits discovered on the East Pacific Rise: Nature 277, pp. 523-528.

FRIEDMAN, I. and O'NEIL, J.R., 1977; Compilation of stable isotope fractionation factors of geochemical interest: in Fleischer, M. (ed), Data

of Geochemistry, 6th ed., U.S. Geological Survey, Profesional Paper 440KK.

FRIES, C.Jr., 1960; Geologia del Estado de Morelos y de partes adyacentes de Mexico y Guerrero, region central meridional de Mexico: Bol. del Instituto de Geologia, UNAM, No. 60, 236 p.

GASTIL, G. and KRUMMENACHER, D., 1979; Reconnaissance geologic map of central part of the State of Nayarit, Mexico: Geol. Soc. Amer. Map and Short Series, MC_24, scale 1:200 000, Geol. Soc. Am. Bull., 80, pp. 15-18.

GAYTAN-RUEDA, J. E., DE LA GARZA, V., AREVALO, E., ROSAS, A., 1979; Descubrimiento, geologia y genesis del Yacimiento Vulcano, La Minita, Michoacan: Memoria de la XIII Convencion Nal. de la Asoc. de Ings. de Minas, Met. y Geol. de Mexico. Acapulco, Gro., pp. 58-113.

GOLDFARB, M.S., CONVERSE, D.R., HOLLAND, H.D., and EDMOND, J.M., 1983; The genesis of hot-spring deposits on the East Pacific Rise, 21°N: in Ohmoto, H. and Skiner, B.J. (eds), Kuroko and Related Volcanogenic Massive Sulphide Deposits. Economic Geology Monograph 5, pp.184-197.

GUILBERT, J.M. AND PARK, F.C., 1986; The Geology of Ore Deposits. 4th ed., W.H. Freemand & Co., New York, 985 p.

HAAS, J.L., 1971; The effects of salinity on the maximum thermal gradient of a hydrothermal system at hydrostatic pressure: Econ. Geol., 66, pp. 940-946.

HARLAND, W.B., COX, A.V., LLEWELLYN, P.G., PICTON, C.A., SMITH, A.G. and WALTERS, R., 1982; A Geological Time Scale: Cambridge, Cambridge University Press, 128 p.

HARRIS, G.D. and HODSON, F., 1922; The rudistids of Trinidad: Paleont. Americana, 1, no. 3, pp. 119-162.

HAYMON, R.H. and KASTNER, M., 1981; Hot spring deposits on the East Pacific Rise at 21°N: preliminary description of mineralogy and genesis: Earth Planet. Sci. Lett., 53, 363-381.

HEKINIAN, R., FRANCHETEAU, J., RENARD, V., BALLARD, R.D., CHOUKROUNE, P., CHEMINEE, J.L., ALBAREDE, F., MINSTER, J.F., CHARLOU, J.L., MARTY, J.C., and BOULEGUE, J., 1983; Intense hydrothermal activity at the axis of the East Pacific Rise near 13°N: submersible witnesses the growth of chimney: Marine Geophysical Research, 6, pp. 1-14.

HEWLET, C.G., 1959; Optical properties of potassic feldspars. Bull. Geol. Soc. Am., 70, pp. 511-.

HIGGINS, N.C., 1980; Fluid inclusion evidence for the transport of tugsten by carbonate complexes in hydrothermal solutions: Can. J. Earth Sci., 17, pp. 823-830.

HOEFS, J., MULLER, G., SCHUSTERS, K.A., and WALDE, D., 1978; The Fe-Mn ore deposits of Urucum, Brazil: an oxygen isotope study: Isot. Geosci., 65, pp. 311-319.

HONNOREZ, J., HONNOREZ-GUERSTEIN, J., and WAUSCHKUHN, S., 1971; Present day formation of an exhalative sulfide deposit at Vulcano (Thyrrhenian Sea), Part II: active crystallization of fumarolic sulfides in the volcanic sediments of the Baia di Levante: in G.C. Amstutz and A.J. Bernard (eds.), Ores in Sediments, International Union of Geological Sciences, Series A, No. 3, Springer Verlag, pp.139-166.

HYNDMAN, D.W., 1985; Petrology of igneous and metamorphic rocks. 2nd ed., Mac Graw Hill, New York, 785 p.

KAJIWARA, Y. and KROUSE, H.R., 1971, Sulfur isotope partitioning in metallic sulfide systems: Can. Jour. Earth Sci., 8, pp. 1397-1408.

KEITH, M.L. and WEBER, J.N., 1964; Carbon and oxygen isotope composition of selected limestones and fossils: Geochim. Cosmochim. Acta, 28, pp. 1787-1816.

KEPPIE, J.D., 1977; Plate tectonic interpretation of Paleozoic world maps: Nova Scotia Dept. Mines, Paper 77-3, 45 p.

KERRICK, D.M., 1974; Review of metamorphic mixed volatiles (H_2O-CO_2) equilibria: Am. Mineral., 59, pp. 729-762.

KRSTIC, D., 1981; Geochronology of the Charlebois Lake area, Northeastern Saskatchewan. Unpublished MSc thesis, University of Alberta.

KUSAKABE, M. and ROBINSON B.W., 1977; Oxygen and sulfur isotope equilibria in the $BaSO_4$-HSO_4-H_2O system from 110 to 350°C and applications: Geochim. Cosmochim. Acta, 41, pp. 1033-1040.

LLOYD, R.M., 1968; Oxygen isotope behavior in the sulfate-water system: J. Geophys. Res., 73, pp. 6099-6109.

LONGSTAFFE, F. J., 1987; Stable isotope studies of diagenetic processes: Mineralogical Association of Canada, Short Course in Stable Isotope Geochemistry of Low Temperature Fluids, 13, pp. 187-257.

LOPEZ-RAMOS, E., 1981; Geologia de Mexico, Vol. III, pp. 43-139.

LYNDON, G.W., 1988; Ore deposit models #14. Volcanogenic massive sulfide deposits. Part 2: Genetic models: Geoscience Canada, 15, pp. 43-65.

MaC GILLAVRY, H. J., 1937; Geology of the Province of Camaguey Cuba with revisioned studies in rudist paleontology, Utrecht, (referred to in Mapes, 1959).

MAPES, E., 1959; Los yacimientos ferriferos de La Truchas: Cons. de Recur. Nat. No Renov., 46 p.

MARGARITZ, M. and TAYLOR, H.P.Jr., 1976; Oxygen, hydrogen and carbon isotope studies of the Franciscan formation, Coast Ranges, California: Geochim. Cosmochim. Acta, 40, pp. 215-234.

MATTHEWS, A. and KATZ, A., 1977; Oxygen isotope fractionation during dolomitization of calcium carbonate. Geochim. Cosmochim. Acta, 41, pp. 1431-1438.

MATTHEWS, W.H., 1951; Some aspects of reef paleontology and lithology in the Edwards formation of Texas: Texas Jour. Sci., no. 2, pp. 217-226.

McCREA, J.M., 1950; On the isotopic chemistry of carbonates and a paleotemperature scale: J. Chem. Phys., 18, no. 6, pp. 849-857.

MONTOYA, J.W. and HEMLEY, J.J., 1975; Activity relations and stabilities in alkali feldspar and mica alteration reactions: Econ. Geol., 70, pp. 577-594.

MOODY, J. B., 1979; Serpentinites, spilites, and ophiolite metamorphism: Can. Mineral., pp. 871-887.

MORAN-ZENTENO, D. J., 1986; Breve revision sobre la evolucion tectonica de Mexico: Geof. Int., 25, pp. 9-38.

MUEHLENBACHS, K. and CLAYTON, R.N., 1976; Oxygen isotope composition of the oceanic crust and its bearing on seawater: J. Geophys. Res., 81, pp. 4365-4369.

MULLERIED, F.K., 1934; Sobre el hallazgo de paquiodontos gigantescos en el cretácico de Chiapas: Inst. Biología Anales, tomo 5, pp. 81-82.

NIELSEN, H., 1979; Sulfur isotopes: in E. Jager and J.C. Hunt (eds), Lectures in Isotope Geology, Springer Verlag, Berlin, pp. 283-312,

NORTHROP, D.A. and CLAYTON, R.N., 1966; Oxygen isotope fractionation in systems containing dolomite. J. Geol., 74, pp. 174-195.

O'NEIL, J. R., 1987; Preservation of H, C, and O isotopic ratios in the low temperature environments: Mineralogical Association of Canada, Short Course in Stable Isotope Geochemistry of Low Temperature Fluids, 13, pp. 85-128.

O'NEIL, J.R., CLAYTON, R.N., AND MAYEDA, T., 1969; Oxygen isotope fractionation in divalent metal carbonates: J. Chem. Phys., 51, pp. 5547-5558.

OHMOTO, H. and LASAGA, A. C., 1982; Kinetics of reactions between aqueous sulfates and sulfides in hydrothermal systems: Geochim. Cosmochim. Acta, 46, pp. 1727-1746.

OHMOTO, H. and RYE R., 1979; Isotopes of sulfur and carbon; in Barnes, H. L., ed.: Geochemistry of Hydrothermal Ore Deposits, John Wiley & Sons, New York, pp. 509-567.

OHMOTO, H. and RYE, R.O., 1974; Hydrogen and oxygen isotopic composition of fluid inclusions in the Kuroko deposits, Japan: Econ. Geol., 69, pp. 947-953.

OHMOTO, H., 1972; Systematics of sulfur and carbon isotopes in hydrothermal ore deposits: Econ. Geol., 67, pp. 551-578.

OHMOTO, H., 1986; Stable isotope geochemistry of ore deposits: in Valley, J.W., Taylor, H.P., Jr., and O'Neil, J.R. (eds), Stable Isotopes in High Temperature Geological Processes, Mineral Assoc. America. Reviews in Mineralogy, 16, pp. 491-559.

OHMOTO, H., COLE, D.R. and MOTTL, M.J., 1976; Experimental basalt-seawater interaction: sulfur and oxygen isotope studies: EOS, 57, pp. 342.

OHMOTO, H., MIZUKAMI, S.E., DRUMMOND, C.S., ELDRIDGE,V., PISUTHA-ARNOND, V., and LENAGH, T.C., 1983; Chemical processes of Kuroko formation: in Ohmoto, H. and Skiner, B.J. (eds), Kuroko and Related Volcanogenic Massive Sulphide Deposits. Economic Geology Monograph 5, pp.:570-604.

ORTEGA-GUTIERREZ, F., 1981; Metamorphic belts of Southern Mexico and their tectonic significance. Geof. Int., 20, pp. 177-202.

PALMER, R. H., 1928; The rudistids of Southern Mexico: California Acad. Sci. Occ. Paper 14, pp. 1-137.

PANTOJA-ALOR, J. and ESTRADA, S., 1986; Estratigrafia de los alrededores de la mina El Encino, Jalisco: Bull. Geol. Soc. of Mexico, Tomo XLVII, pp. 1-15.

PANTOJA-ALOR, J., 1959; Esdtudio geologico de reconocimiento de la Region de Huetamo, Estado de Michoacan: Cons. Recursos Nat. No Renovables, 50, 44 pp.

PERRY, E.C., TAN, F.C., and MOREY, G.B., 1973; Geology and stable isotope geochemistry of the Biwabik iron formations: Econ. Geol., 68, pp. 1110-1125.

PISUTHA, V. and OHMOTO, H., 1983; Thermal hystory, and chemical and isotopic composition of ore forming fluids responsible for the Kuroko massive sulfide deposits in the Hokuroku district of Japan: in Ohmoto, H. and Skiner, B.J. (eds), Kuroko and Related Volcanogenic Massive Sulphide Deposits. Economic Geology Monograph 5, pp. 523-558.

POTTER, R.W. II, CLYNE, M.A., and BROWN, D.L., 1978; Freezing point depression of aqueous sodium chloride solutions: Econ. Geol., 73, pp. 284-285.

POTTORF, R.J. and BARNES, H.L., 1983; Mineralogy, geochemistry, and ore genesis of hydrothermal sediments from the Atlantis II Deep, Red Sea: in Ohmoto, H. and Skiner, B.J. (eds), Kuroko and Related Volcanogenic Massive Sulphide Deposits. Economic Geology Monograph 5, pp.198-223.

PUCHELET, H., 1971; Recent iron sediment formation at the Kameni islands, Santorini (Greece): in G.C. Amstutz and A.J. Bernard (eds), Ores in Sediments, International Union of Geological Sciences, Series A, No. 3, Springer Verlag, pp. 227-245.

PUCHELET, H., 1978; Barium: in K.H. Wedepohl (ed) Handbook of Geochemistry, 5th ed., Vol. II/4, Springer Verlag, New York, pp. 56-A-1 - 56-O-2.

RAMDOHR, P., 1980; The Ore Minerals and Their Intergrowths, Vol. 2, 2nd. ed., International Series in Earh Sciences, Pergamon Prees, pp. 441-1205.

RICHARDS, J.D., CUMMING, C.L., KRSTIC, D., WAGNER, P., and SPOONER, E.T.C., 1988; Pb isotopic constraints on the age of sulfide ore deposition and U-Pb age of late uraninite veining at the Musoshi stratiform copper deposit Central African Copper Belt, Zaire: Econ. Geol., in press.

ROEDDER, E, 1979; Fluid inclusions as samples of ore fluids. in Barnes, H. L., ed.: Geochemistry of Hydrothermal Ore Deposits, John Wiley & Sons, New York, pp. 684-737.

ROEDDER, E, 1984; Fluid Inclusions. Reviews In Mineralogy, 12. Mineralogic Society of America. Edited by Paul Ribbe, 594 p.

ROEDDER, E., 1971; Fluid inclusion studies on the porphyry type ore deposits at Bringham, Utah, Montana, and Climax, Colorado: Econ. Geol., 66, pp. 98-120.

ROSE, A.W. and BURT, M.D., 1979; Hydrothermal alteration: in Barnes, H. L., ed.; Geochemistry of Hydrothermal Ore Deposits, John Wiley & Sons, New York, pp. 173-236.

ROSS, C.A. and OANA, S., 1961; Late Pensilvanian and Early Permian limestone petrology and carbon isotope distribution, Glass Mountains, Texas: J. Sed. Petrol., 31, 231-244

RYE, R. and OHMOTO, H., 1974; Sulfur and carbon isotopes and ore genesis: a review: Econ. Geol., 69, pp. 826-842.

SAKAI and MATSUBAYA, 1974; Isotope geochemistry of the thermal waters of Japan and its bearing on the Kuroko ore solutions: Econ. Geol., 69, pp. 974-991.

SAKAI, H. and KROUSE, H.R., 1971; Elimination of memory effects in $^{18}O/^{16}O$ determinations in sulfates: Earth Planet. Sci. Lett., 11, pp. 369-373.

SAYLES, F.L. and BISCHOFF, J.L., 1973; Ferromanganoan sediments in the Equatorial East Pacific Rise: Earth Planet. Sci. Lett., 19, pp. 330-336.

SHATSKIY, N.S., 1966; On manganiferous formations and the metallogeny of manganese, Paper I. Volcanogenic-sedimentary manganiferous formations: Intern. Geol. Rev., 6, pp. 1030-1056.

SHELTON, K.L. and RYE, D.M., 1982; Sulphur isotope composition of ores from Mines Gaspe, Quebec: An example of sulphate-sulfide disequilibria in ore-forming fluids with applications to other porphyry type deposits: Econ. Geol., 77, pp. 1688-1709.

SHEPHERD, T.J., RANKIN, A.H., and ALDERTON, D.H.M., 1985; A Practical Guide to Fluid Inclusion Studies. Blackie & Son Ltd., London, 239 p.

SHIKAZANO, N. and KOUDA, R., 1979; Chemical composition of tetrahedrite-tennanite minerals and the chemical environments of some japanese ore deposits: Mining Geology, 29, pp. 33-41.

SMITH, P.A. and CRONAN, D.S., 1975; The dispersion of metals associated with an active submarine exhalative deposit: Oceanology International 1975, pp. 111-114.

SPOONER, E.T.C., 1976; The strontium isotopic composition of seawater, and seawater-oceanic crust interaction: Earth Planet. Sci. Lett., 31, pp. 167-174.

SPOONER, E.T.C., BECKINSALE, R.D., FYFE, W.S., and SMEWINGS, J.D., 1974; ^{18}O-enriched ophiolite metabasic rocks from E. Liguria (Italy), Pindos (Greece) and Troodos (Cyprus): Contrib. Min. Petrol., 47, pp. 41-67.

STACEY, J.S. and KRAMERS, J.D., 1975; Approximation of terrestrial lead isotope evolution by a two-stage model: Earth and Planet. Sci. Lett., 26, pp. 207-221.

STEIGER, R.H. and JÄGER, E.; 1977; Subcommission on geochronology: Convention on the use of decay constants in geo- and cosmochronology: Earth Planet. Sci, Lett., 36, pp. 359-362.

STETTLER, A. and ALLEGRE, C.J., 1978; ^{87}Rb - ^{87}Sr studies of waters in a geothermal area: The Cantal, France: Earth Planet. Sci. Lett., 38, pp. 364-372.

STETTLER, A., 1977; ^{87}Rb - ^{87}Sr systematics of a geothermal water-rock association in the Massif Central, France: Earth Planet. Sci. Lett., 34, pp. 432-438.

STYRT, M. M., BRACKMAN, A. J., HOLLAND, H. D., CLARK, B. C., PISUTHA-ARNOND, V., ELDRIDGE, C. S. and OHMOTO, H., 1981; The mineralogy and isotopic composition of sulfur in hydrothermal sulfide/sulfate deposits on the East Pacific Rise, 21°N latitude: Earth and Planet. Sci. Lett., 53, pp. 382-390.

TANIMURA, S., DATE, J., TAKAHASHI, T., and OHMOTO, H., 1983; Geologic setting of the Kuroko deposits, Japan. Part II: Stratigraphy. and structure of the Hokuroko district: in Ohmoto, H. and Skiner, B.J. (eds), Kuroko and Related Volcanogenic Massive Sulphide Deposits. Economic Geology Monograph 5, pp. 24-38.

TAYLOR, H.P. Jr., 1979; Oxygen and hydrogen isotope relationships in hydrothermal deposits: in Barnes, H. L., ed.: Geochemistry of Hydrothermal Ore Deposits, John Wiley & Sons, New York, pp. 236-277.

TAYLOR, H.P., 1974; The application of oxygen and hydrogen isotope studies to problems of hydrothermal alteration and ore deposition: Econ. Geol., 69, pp. 843-883.

THODE, H.J., MONSTER, J., and DUNFORD, H.B., 1961; Sulfur isotope geochemistry: Geochim. Cosmochim. Acta, 25, pp. 150-174.

THOMPSON, A.B., 1971; P_{CO_2} in low-grade metamorphism; zeolite, carbonate, prehnite relations in the system $CaO-Al_2O_3-SiO_2-CO_2-H_2O$: Contrib. Min. Petrol., 33, pp. 145-161.

TUREKIAN, K.K. and WEDEPOHL, K.H., 1961; Distribution of elements in some major units of the Earth's crust: Geol. Soc. Am. Bull., 72, pp. 175-182.

UEDA, A. and KROUSE, R., 1986; Direct conversion of sulphide and sulphate minerals to SO_2 for isotopic analyses: Report submitted to the Geochemical Journal in April, 1986.

URRUTIA-FUCCUGACHI, J., 1981; Preliminary paleomagnetic study of Lower Tertiary volcanic rocks from Morelos and Guerrero state: Geof. Int., 22, pp. 81-110.

VALLANCE, T.G., 1974; Pyroxenes and the basalts spilite relation: in Amstutz editor, Spilites and Spilitic Rocks, IUGS, Series A, No. 4, Springer Verlag, Berlin, pp. 59-68.

VIDAL, R., CAMPA, M.F., BUITRON, B., and ALANCASTER, G., 1980; El conjunto petrotectonico de Zihuatanejo, Guerrero-Coalcoman, Michoacan: Soc. Geol. Mexicana, Resumenes de la V Convencion Geologica Nacional, pp. 111-112.

VON DAMM, K.L., EDMON, J.M., GRANT, B., and MEASURES, C.I., 1985; Chemistry of submarine hydrothermal solutions at 21°N, East Pacific Rise: Geochim. Cosmochim. Acta, 49, pp. 2197-2220.

WATANABE, M. and SAKAI, H., 1983; Stable isotope geochemistry of of sulfates from Neogene ore deposits in the Green Tuff region, Japan: in Ohmoto, H. and Skiner, B.J. (eds), Kuroko and Related Volcanogenic Massive Sulphide Deposits. Economic Geology Monograph 5, pp. 282-291.

YOSHIDA, T., IZAWA, E., and MARIMOTO, M., 1977; The hydrothermal alteration in the Kuroko type stockwork deposit at the Iwami mine, Shiwane prefecture, Japan: Mining Geology, 27, pp. 181-189.

ZHANG, R., 1986; Sulfur isotopes and pyrite-anhydrite equilibria in a volcanic basin hydrothermal system of the middle to lower Yangtze River Valley: Econ. Geol., 81, pp. 32-45.